Review

Hybrid Maximum Power Extraction Methods for Photovoltaic Systems: A Comprehensive Review

Haoming Liu [ID], Muhammad Yasir Ali Khan *[ID] and Xiaoling Yuan

College of Energy and Electrical Engineering, Hohai University, Nanjing 211100, China;
liuhaom@hhu.edu.cn (H.L.); lingx@hhu.edu.cn (X.Y.)
* Correspondence: m.yasir_alikhan@yahoo.com

Abstract: To efficiently and accurately track the Global Maximum Power Point (GMPP) of the PV system under Varying Environmental Conditions (VECs), numerous hybrid Maximum Power Point Tracking (MPPT) techniques were developed. In this research work, different hybrid MPPT techniques are categorized into three types: a combination of conventional algorithms, a combination of soft computing algorithms, and a combination of conventional and soft computing algorithms are discussed in detail. Particularly, about 90 hybrid MPPT techniques are presented, and their key specifications, such as accuracy, speed, cost, complexity, etc., are summarized. Along with these specifications, numerous other parameters, such as the PV panel's location, season, tilt, orientation, etc., are also discussed, which makes its selection easier according to the requirements. This research work is organized in such a manner that it provides a valuable path for energy engineers and researchers to select an appropriate MPPT technique based on the projects' limitations and objectives.

Keywords: hybrid MPPT; photovoltaic (PV); partial shading condition; GMPP; renewable energy

1. Introduction

Due to the depletion of fossil fuels, economic aspects, and environmental concerns, the integration of Renewable Energy Resources (RES) in power networks has increased globally. Among the RES, solar energy (Photovoltaic (PV)) has become more popular due to its zero-emission, universal availability, better return on investment, and low operational cost [1].

According to the global status report (REN21), globally, for the last six consecutive years, the installation of RES has been more than the combined fossil fuels and nuclear power. At the end of 2021, globally, the total installed capacity of RES was about 3146 GW, of which the share of hydropower is 1195 GW, PV is 942 GW, wind is 845 GW, bio-power is 143 GW, geothermal is 14.5 GW, concentrating solar thermal power is 6 GW, and ocean power is 0.5 GW. Although the largest contribution to generate electricity is from hydropower, but in the last few years (2016–2021), PV showed the fastest growth rate among all RES. As a result, the total installed capacity of a PV system increased from 305 GW in 2016 to 942 GW in 2021 [2]. This fast expansion and growth in the PV market are mainly due to the rising demand for electricity, the increase in the emission of harmful gases, the desire to control the energy generation from fossil fuels, government support, reduction in material prices, technological improvements, and advancements in PV integration technologies [3]. The total installed capacity of PV along with an annual increment from 2011 to 2021 is presented in Figure 1 [2].
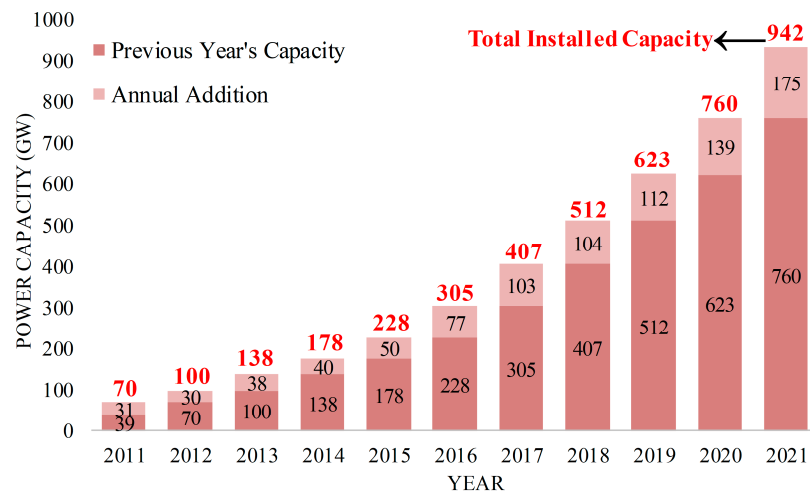
Figure 1. Total installed capacity of PV (2011–2021) [2].

Although the integration of PV into the power system has increased significantly due to the dependency of a PV module on atmospheric conditions such as Temperature (T) and Irradiance (G), its generated power fluctuates significantly. Under Uniform Environmental Conditions (UECs), there exists only one point on the Current-Voltage (I-V) and Power-Voltage (P-V) characteristics of a PV module called a Maximum Power Point (MPP), where the PV module produces Maximum Power (MP). However, when the PV module is subjected to VEC (irregular G and T or under PSC), then the I-V and P-V characteristics have numerous multiple peaks (multiple local and one global) [4]. Therefore, to accurately and precisely track the MPP and increase the lifetime and efficiency of PV system, different MPPT techniques are designed. These MPPT techniques can be categorized into six different groups based on their features and characteristics, as presented in Figure 2.
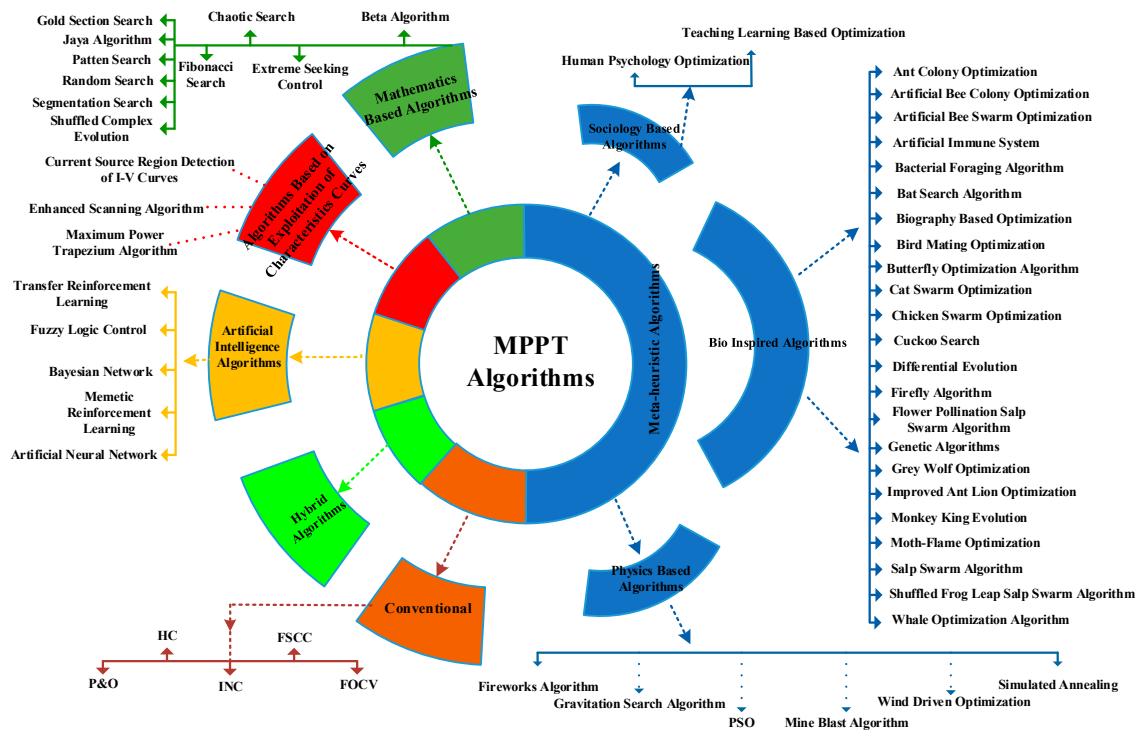

Figure 2. Classification of MPPT techniques.

A 1st group of MPPT techniques are the conventional techniques, as shown in Figure 1. The conventional MPPT techniques include Perturb and Observe (P and O) [5], Hill Climb (HC) [6], Fractional Open Circuit Voltage (FOCV) [7], etc. These techniques show high performance and accurately track the MPP under UEC. However, steady-state oscillations are observed when these conventional techniques are employed. Moreover, in the case of VEC, they cannot track the Global Maximum Power Point (GMPP) and trap the Local Maximum Power Point (LMPP). Therefore, numerous improvements have been made to enhance their performance, as follows: In [8], an improved P and O algorithm is presented in which the reference voltage is defined as a function of G and T. Similarly, in [9], a variable step size Incremental Conductance (IC) is proposed. Although these improvements have increased the system's tracking accuracy and efficiency, performance degradation is observed under PSC.

To accurately track the GMPP under VEC or PSC, a group of meta-heuristic algorithms that include Particle Swarm Optimization (PSO) [10], Gravitational Search Algorithm (GSA) [11], Differential Evolution (DE) [12], Artificial Bee Colony (ABC) [13], Human Psychology Optimization [14], etc., are designed. Similarly, mathematics-based algorithms such as the Jaya algorithm [15], segmentation search [16], Beta (β) algorithm [17], etc., ensure high tracking accuracy and fast convergence. The Artificial Intelligence (AI)-based algorithms such as Fuzzy Logic Controller (FLC) [18] and Artificial Neural Network (ANN) [19], etc., and algorithms based on the exploitation phenomena effectively improve the calculation accuracy, reduce the computation burden, and track the GMPP with a fast dynamic response.

Although these advanced MPPT algorithms show high performance under PSC compared with conventional algorithms, there are some limitations associated with them. For example, in the PSO algorithm, the diversity of the particles increases with the increment in the iteration number; as a result, an MPP cannot be tracked precisely, and steady-state oscillations are observed near the MPP [10]. The DE algorithm is unable to efficiently locate the GMPP, but it has high accuracy in tracking the LMPP within its search area [12]. The Firefly Algorithm (FA) is unable to accurately locate the GMPP in rapid PSC [20]. The Cuckoo Search Algorithm (CSA) can guarantee a fast convergence, but high oscillations are observed at steady state, and the algorithm has a high failure rate to accurately locate the GMPP [21]. Similarly, the Grasshopper Optimization Algorithm (GOA) shows good steady-state and dynamic responses, accuracy to track the MPP under PSC, but it has a high tracking time that needs to be enhanced [22]. The Salp Swarm Algorithm (SSA) has the advantage of simple upgrading functionality but has the risk of falling into the local optimum solution in the case of PSC. Moreover, due to a lack of exploration and exploitation, it creates large oscillations at the output and is unable to perform fast tracking [23]. The ABC technique has a high computational cost and convergence time, and it also produces oscillations in the converter variables [13]. A main disadvantage of FLC is its high dependency on the user's knowledge. A user must have enough knowledge about the system so that the outputs can be determined based on the inputs [18]. The ANN technique surpasses an FLC due to its user's independence characteristic, but it needs to be trained specifically for PV application through a time-consuming training process [19]. The GSA has a high ability to search GMPP while having a poor local search ability [11]. the Chaotic Search (CS) technique has slow convergence speed [24]. The Grey Wolf Optimization (GWO) method suffers from oscillations around GMPP under PSC [25].

From the literature review discussed above, it is concluded that these MPPT techniques pose many disadvantages. Therefore, to cope with these challenges, two or more algorithms are integrated together such that they eliminate the cons and enhance the pros of each other. The resultant hybridized algorithm enhances the tracking accuracy, speed, and efficiency under PSC. Many comprehensive studies about the hybrid MPPT algorithms are conducted, for example, the authors in [26] discussed 20 different hybrid algorithms. These algorithms are divided into sequential and simultaneous hybrid MPPT techniques based on their operation. The operation, advantages, and disadvantages of these algorithms are elaborated.

Moreover, a criterion for selecting a suitable MPPT technique based on operation, cost, implementation, complexity, etc., is also explained. A detailed review of different MPPT techniques feasible for PSC is presented in [27]. In this review, a primary is focus on the non-hybrid MPPT techniques and a least consideration is provided to the hybrid MPPT techniques. To be exact, a total of 12 hybrid techniques is discussed and their performance is compared based on some basic indicators. The authors in [28] categorize different MPPT techniques for uniform irradiance and non-uniform irradiance. In this manuscript, non-hybrid MPPT techniques are discussed in context of uniform irradiance condition, whereas for non-uniform irradiance condition, different hybrid techniques are presented. However, only a limited consideration is provided to the hybrid techniques; moreover, few key specifications for selecting an appropriate MPPT technique are discussed.

The authors in [29] presented a comprehensive review of different meta-heuristic MPPT techniques. A detailed comparative analysis of swarm-based MPPT techniques with other meta-heuristic MPPT techniques such as GOA, GWO, PSO, etc., is presented. However, in this paper, no consideration is provided to the hybrid MPTT techniques. The authors in [30] presented a detailed review of the MPPT techniques used to track the MPP under non-uniform irradiance. The authors classified the MPPT techniques into online and soft computing-based methods. The authors also presented a comparative analysis in table form and discussed the selection criteria considering four indicators, i.e., tracking capability, convergence speed, sensitivity, and design complexity. In this review, the authors only focus on the non-hybrid techniques and no consideration is provided to hybrid techniques. In [31] different PV cell models are presented, and to extract the maximum power from the PV system, some conventional and non-conventional MPPTs are discussed. To extract the maximum power from the PV system, the authors in [32] presented a comprehensive review of different MPPT techniques. The MPPT techniques are divided in four different categories, i.e., based on calculation, measurement, online schemes, and intelligent schemes. However, these review papers [31,32] did not discuss any hybrid MPPT technique. Similarly, the authors in [33–40] also discussed different MPPT algorithms, where the focus was on the non-hybrid MPPT techniques. The authors in [34] presented a review of different non-hybrid techniques, but presented only the hybrid algorithms based on P and O and firefly algorithms. Similarly, the authors in [36] presented a review of different conventional, bio-inspired, and intelligent MPPT techniques. However, no consideration was provided to the hybrid MPPT techniques; moreover, the criteria for selecting appropriate MPPT techniques are also not discussed.

A comparative analysis of these state-of-the-art research works [26–40] with the work presented in this manuscript is presented in Table 1. From Table 1, it can be concluded that these review papers do not discuss the global status of PV. Moreover, in these recent review papers, the authors mainly focus on the non-hybrid MPPT algorithms, while only a limited amount of attention is provided to the hybrid algorithms. Most of the authors present a comparative analysis of different MPPT algorithms, but the criteria to select a suitable MPPT technique are very limited. Therefore, based on these points, it is essential to conduct a review on hybrid MPPT techniques.

The main contributions of this research work can be summarized as:

- This research work presents a review of more than 90 different MPPT techniques present in the literature and categorizes them into three types. The 1st type is the combination of two or more conventional MPPT techniques; the 2nd type is the combination of two or more soft computing techniques; and the 3rd type is the combination of conventional and soft computing methods;
- This manuscript summarizes numerous MPPT techniques and provides a comprehensive comparison considering different characteristics such as DC–DC converter topology, complexity level, tracking speed, steady-state oscillation, tracking accuracy, cost, etc.;

- Besides the MPPT technique, there are many other factors, e.g., the location and season of a PV system, PV panel tilts and orientations, conversion efficiency, the selection of a DC-DC converter, etc., that should be considered while installing a PV system. This work provides a comprehensive review of these factors;
- This manuscript provides a valuable path for future research in the field of hybrid MPPT techniques and will help the energy engineers to select an appropriate technique according to the project's requirements.

Table 1. Comparative analysis of state-of-art literature review.

Ref.	PV Global Status	Primary Focus on Hybrid MPPT Methods	Secondary Focus on Hybrid MPPT Methods	Primary Focus on Non-Hybrid MPPT Methods	MPPT Selection Criteria	Comparative Analysis of MPPT Methods
[26]	x	✓	x	x	✓	✓
[27]	x	x	x	✓	x	✓
[28]	x	x	✓	✓	✓	✓
[29]	x	x	✓	✓	x	✓
[30]	x	x	x	✓	✓	✓
[31]	x	x	x	✓	x	x
[32]	x	x	✓	✓	x	✓
[33]	x	x	✓	✓	✓	✓
[34]	x	x	x	✓	x	x
[35]	✓	x	✓	✓	✓	✓
[36]	✓	x	x	✓	x	✓
[37]	✓	x	✓	✓	x	✓
[38]	x	x	✓	✓	x	✓
[39]	x	x	x	✓	x	✓
[40]	✓	x	x	✓	x	✓
Proposed	✓	✓	x	x	✓	✓

Following the introduction, in Section 2, different hybrid MPPT techniques are discussed that are categorized into three main types, i.e., combination of conventional algorithms, combination of soft computing, and combination of conventional and soft computing methods. The criteria for selecting an appropriate MPPT technique and comparative analysis are presented in Section 3. Finally, the concluding remarks and future directions are presented in Section 4.

2. Hybrid MPPT Algorithms

A main task of the MPPT technique is to extract the maximum power from the PV system. For this purpose, different MPPT techniques were developed that perform very well in UEC. However, in the case of VEC, it is very difficult to extract the maximum power from the PV system due to multiple peaks in the I-V and P-V characteristic curve. In other words, under VEC numerous LMPPs emerge while there is only GMPP. Due to numerous peaks, many MPPT algorithms fail to track the GMPP and become stuck in the LMPP that cause a hotspot effect, reduction in output efficiency, as well as reliability issues of the PV system. To handle such problems and accurately track the GMPP, the hybrid MPPT techniques were developed. As discussed above, hybrid algorithms are the combination of two or more MPPT techniques that are combined in such a way that they enhance the advantageous features of each other and cancel the disadvantageous features of each other. In other words, the main purpose of designing the hybrid algorithm is to optimally track the MPP in terms of accuracy and speed under VEC. In the literature, different hybrid MPPT techniques are presented that can be categorized into three groups based on their characteristics and features. A group of the 1st type of hybrid techniques are those that are formed by combining two or more conventional MPPT techniques. The hybrid MPPT techniques that are placed in the 2nd type are those that are formed by the combination of two or more soft computing methods (meta-heuristic algorithms, artificial

intelligence algorithms, etc.). The hybrid MPPT techniques that are formed by combining the conventional algorithms with soft computing algorithms are grouped in the 3rd type. This broad categorization of hybrid MPPT techniques are sketched in Figure 3 and are discussed below in detail.
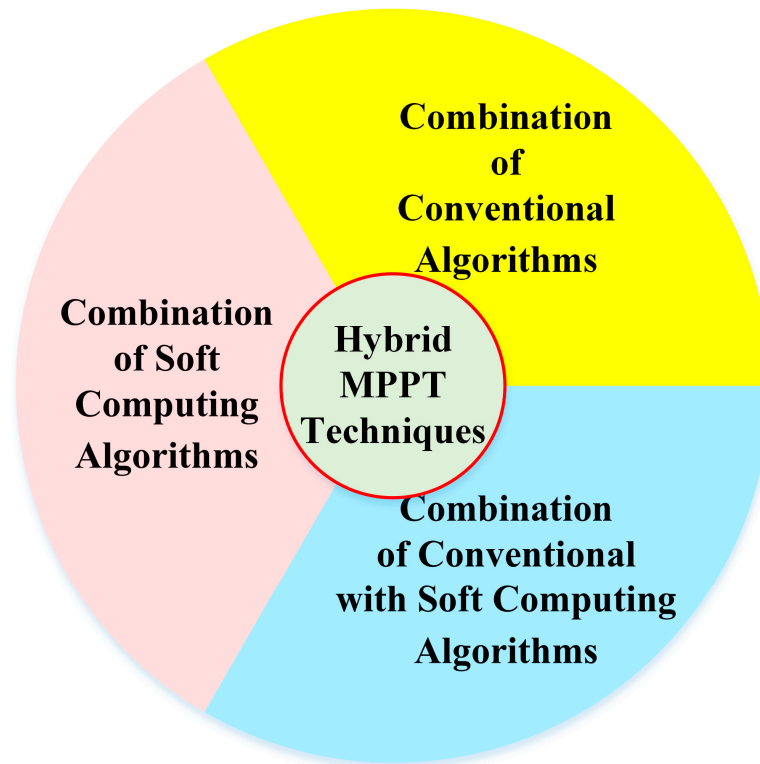

Figure 3. Types of hybrid MPPT techniques.

2.1. Combination of Conventional Algorithms

The MPPT techniques that are categorized in this type are the combination of two or more conventional algorithms. These hybrid techniques are shown in Figure 4 and are discussed below in detail.
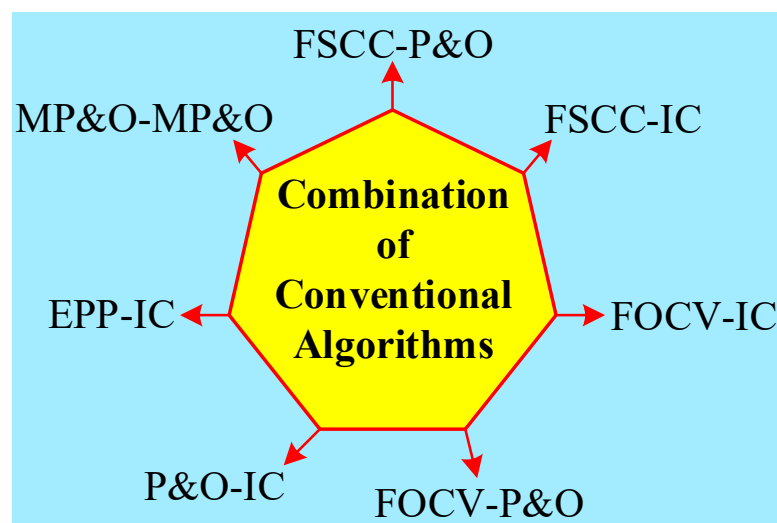

Figure 4. Types of combination of conventional hybrid MPPT techniques.

2.1.1. P and O with Fractional Short Circuit Current (FSCC)

The prominent feature of FSCC is its fast convergence speed, but it lacks MPP tracking accuracy under PSC [41]. Therefore, the authors in [42] combined the FSCC method with P and O technique to increase tracking accuracy and convergence speed of the individual technique. The operation of this technique is divided into two stages, as presented in Figure 5. In the 1st stage, the FSCC method is used to measure a short circuit current (I_{SC}), and then the maximum current (I_{MPP}) of the PV panel is estimated by (1).

$$I_{MPP} = k \cdot I_{SC} \tag{1}$$

where *k* is a constant, which depends on the weather conditions, utilized material, and fabrication technology [43]. After estimating the PV panel parameters, the system moves towards the 2nd stage. In a 2nd stage, a P and O is employed for efficient tracking of MPP and to operate the system near MPP with low oscillations. This technique enables a P and O algorithm to select a small step size, and the perturbation direction is determined by comparing the difference between present and previous perturbations as in (2) or (3).

$$\Delta P \cdot \Delta V < 0 \ decrease \ voltage \tag{2}$$

$$\Delta P \cdot \Delta V > 0 \ increase \ voltage \tag{3}$$

The system evaluates the power difference after every perturbation. If a difference is greater than a set threshold, that is a change in environmental parameter; as a result, a new measurement of the I_{SC} is initiated and the process continues again. The main advantages of this technique include good convergence speed, high MPP tracking accuracy, and simple implementation. Besides these advantages, there are some disadvantages to this method, as it is not very reliable under PSC, oscillations are observed around the MPP, and it has a low tracking speed.

2.1.2. FSCC with IC

Similarly, the authors in [44] combined FSCC with the IC algorithm to achieve accurate and fast tracking of MPP. In this method, FSCC provides a high tracking speed while IC provides high tracking accuracy [45]. The operation of this technique is implemented in two stages. In the 1st stage, an FSCC method is used to operate the system near MPP. It is performed by measuring I_{SC}, and then the I_{MPP} of the PV panel is estimated using (1). However, the FSCC method is unable to accurately track the actual MPP; therefore, the tracking process is switched to the 2nd stage, where an IC technique is used due to its high tracking accuracy. The tracking principle of an IC method is the same as the P and O method, but with low steady-state oscillations around the MPP as it stops the perturbation process once it locates the MPP. It measures both the conductance and change in conductance of the PV panel by comparing the instantaneous conductance with the incremented one and is provided by (4)–(6).

$$\Delta I / \Delta V > -I/V \ left \ of \ MPP \tag{4}$$

$$\Delta I / \Delta V < -I/V \ right \ of \ MPP \tag{5}$$

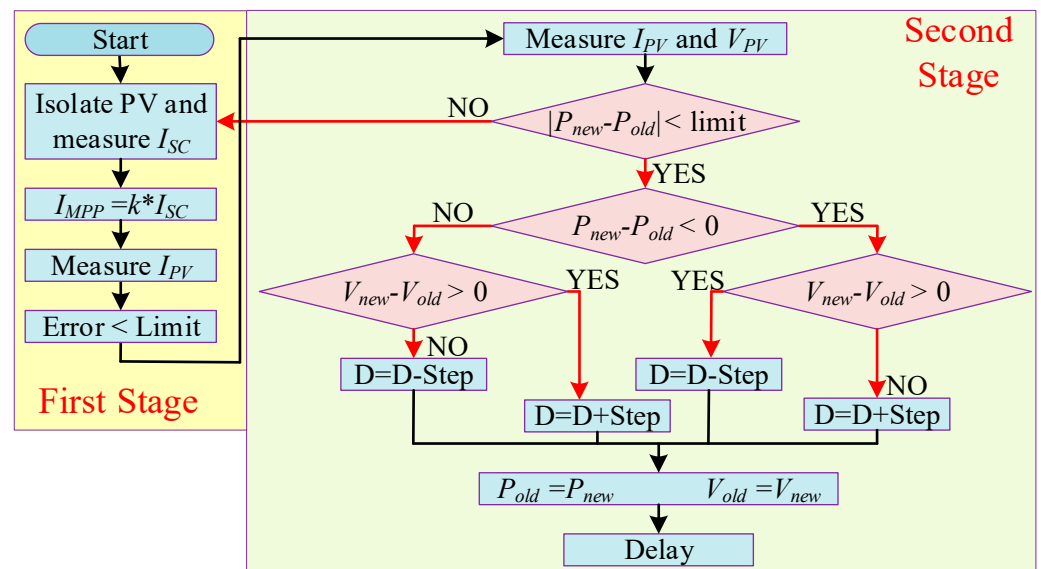$$\Delta I / \Delta V = -I/V \ at \ MPP \tag{6}$$

Figure 5. Flowchart of P and O-FSCC technique [42].

2.1.3. FOCV with P and O

To extract the MP from the PV panel under PSCs, the authors in [46] proposed a hybrid algorithm in which the FOCV technique is combined with the P and O technique. The operation of the proposed algorithm is divided into two stages. In the 1st stage, a FOCV algorithm is used to approximate the system operating point close to the MPP. Moreover, a system is detached from the load to measure the open circuit voltage (V_{OC}), and then V_{MPP} is estimated by putting the value of V_{OC} in (7).

$$V_{MPP} = k_v \cdot V_{OC} \tag{7}$$

where k_v is a constant generally found to be in the range of 0.71–0.78, and it depends on the weather conditions, fabrication technology, and utilized material [43]. As in the 1st stage, the system operating point becomes very close to MPP but not very accurate; therefore, a P and O algorithm is used in the 2nd stage to improve the system's accuracy. A P and O technique uses a small step size, which reduces the oscillations around the MPP and improves accuracy by driving the system's operating point as close as possible to the MPP. This is performed by multiplying the present sensed current and voltage to obtain power, and then this power is compared with the previous one. If there is a positive change in the power, i.e., the new operating point has more power than the old one, then the controller takes its next step in the same direction. If there is a negative change in the power, then the controller takes the next perturbation in the opposite direction.

2.1.4. FOCV with IC

Similarly, to improve the tracking accuracy and convergence speed of the conventional MPPT technique, the author in [47] combined FOCV with IC as shown in Figure 6. Just like the other two-stage operation, in this technique, a FOCV is used to estimate the system operating point close to the MPP by using (1) in the 1st stage, while in the 2nd stage, an IC is initiated to calculate the conductance and variation in conductance of the PV panel. An IC uses a variable step length of the duty cycle (to drive the converter switch) that can be calculated according to (8).

$$D(t) = D(t-1) \pm N * |dP/dV| \tag{8}$$

where $D(t)$ presents the current duty cycle, $D(t-1)$ is the previous duty cycle, N is number of series cells, and $|dP/dV|$ present the slope of power-voltage curve such that $|dP/dV| = 0$ at MPP.
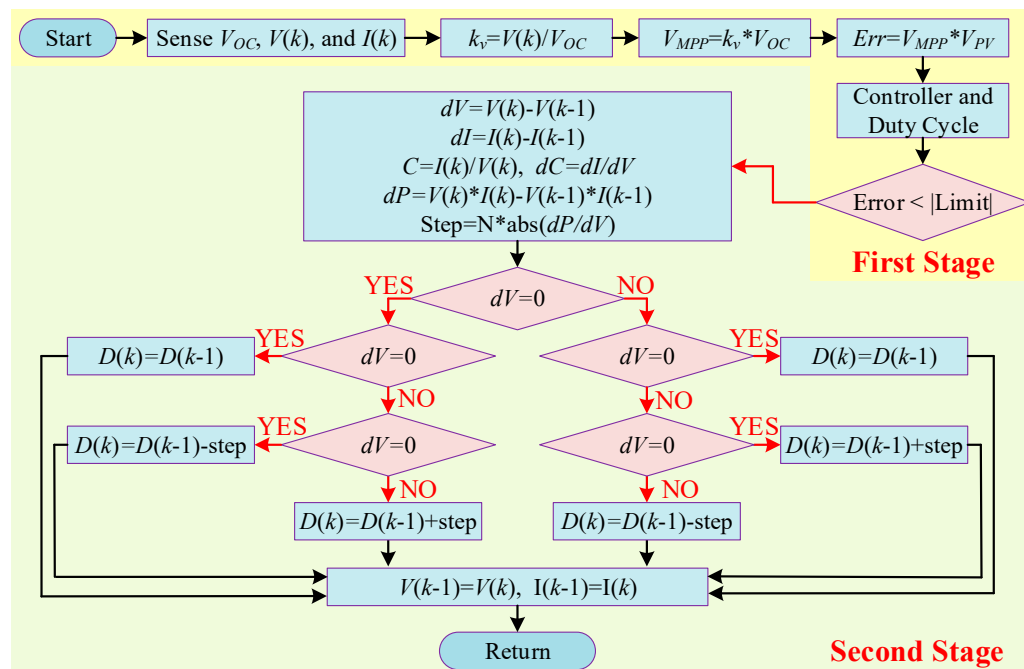

Figure 6. Flowchart of FOCV-IC algorithm [47].

When irradiance level changes, the algorithm goes back to its initial point (FOCV stage) and the system is disconnected again from the load to measure the V_{OC}, current, and voltage to estimate the V_{MPP}.

2.1.5. P and O with IC

A P and O technique is unable to track the GMPP under PSC and particularly to trap the LMPP. Therefore, the authors in [48] combine P and O with IC to eliminate the disadvantages of both algorithms and enhance the MPPT tracking capability. A core idea of this technique is based on variable step sizes that are taken automatically according to the MPP. When a power is climbing, the algorithm takes high and large steps; on the contrary, the step size is significantly reduced when the power is close to MPP. As a result, the proposed algorithm provides fast convergence and low oscillations around MPP compared with the traditional P and O technique.

2.1.6. Modified Perturb and Observe (MP and O)

The authors in [49] proposed an MP and O method that consists of two parts, i.e., the main program and a Global Point (GP) track subroutine. In this technique, based on the PV panel voltage (V_{min} and V_{max}), the upper and lower limits of GMPP are adjusted to avoid scanning the entire system repetitively while tracking GMMP. This algorithm starts from the "main program", where initially the reference voltage is set as V_{OC}, i.e., $V_{OC} = V_{ref} = 85\%$. The algorithm continuously searches for the GMPP by applying the P and O technique until any unpredicted disturbance, such as a PSC or timer interruption, occurs. If any of these uncertainties occur, the "main program" calls the "GP track subroutine". A "GP track subroutine" part then starts to track a new GMPP, and once the GMPP is accurately tracked, it passes the operation back to the "main program" part. A "main program" continuous to perform its operation at this new GMPP until the next disturbance is observed. Furthermore, a feed-forward controller to regulate the duty cycle of the converter is also used that results in fast tracking speed with low steady-state oscillations.

Compared with the conventional P and O algorithm, in this technique the tracking time is reduced about ten times.

2.1.7. Estimation-Perturb-Perturb (EPP) with IC

The authors in [50] proposed a modified P and O technique in which a conventional P and O method is modified by adding an estimation process that records the irradiance variation after two perturbations. This improved technique is referred to as an EPP method. Hence, the author in [51] proposed a hybrid MPPT technique in which an EPP and a variable step IC algorithm are used simultaneously to efficiently track the GMPP. Both algorithms adjust the duty cycle of the converter switch consequently. Then the power obtained from both algorithms is compared, and the algorithm with the higher power is selected.

2.2. Combination of Soft Computing Algorithms

The hybrid MPPT techniques that are categorized in this type are the combination of two or more soft computing-based MPPT algorithms. Numerous MPPT techniques that fall into this category are presented in Figure 7 and are discussed in detail below.
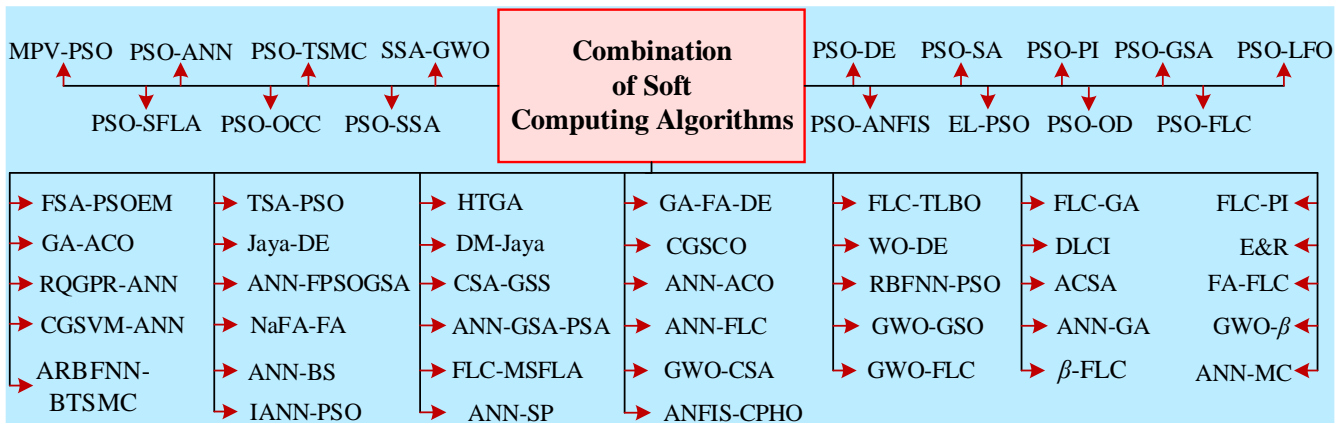

Figure 7. Types of combination of soft computing-based hybrid MPPT techniques.

2.2.1. PSO with DE

A PSO is a population-based search algorithm that seeks the global optimum value of the entire population. PSO has the advantage of high tracking speed, but at the same time, high steady-state oscillations, and a lack of accuracy in tracking the GMPP is observed under PSCs. Moreover, in PSO, the diversity of the particles increases with an increase in the iteration number, which results in an increment in the computational burden. Therefore, it is combined with many other MPPT techniques, such as in [52], it is also combined with the DE algorithm to overcome the above-mentioned limitation. As DE is a population-based random search algorithm, its main limitation is that it is unable to efficiently locate the GMPP, but it has a high accuracy in tracking the LMPP within its search area [53]. Therefore, both DE and PSO are combined in such a manner that they avoid the weaknesses of both algorithms and take benefits from their advantageous features. In this technique, a DE algorithm operates during the even iterations while a PSO technique operates during the odd iterations. This methodology results in the accurate, precise, and fast tracking of MPP under PSCs and even in PSC. A flowchart of this proposed technique is presented in Figure 8.
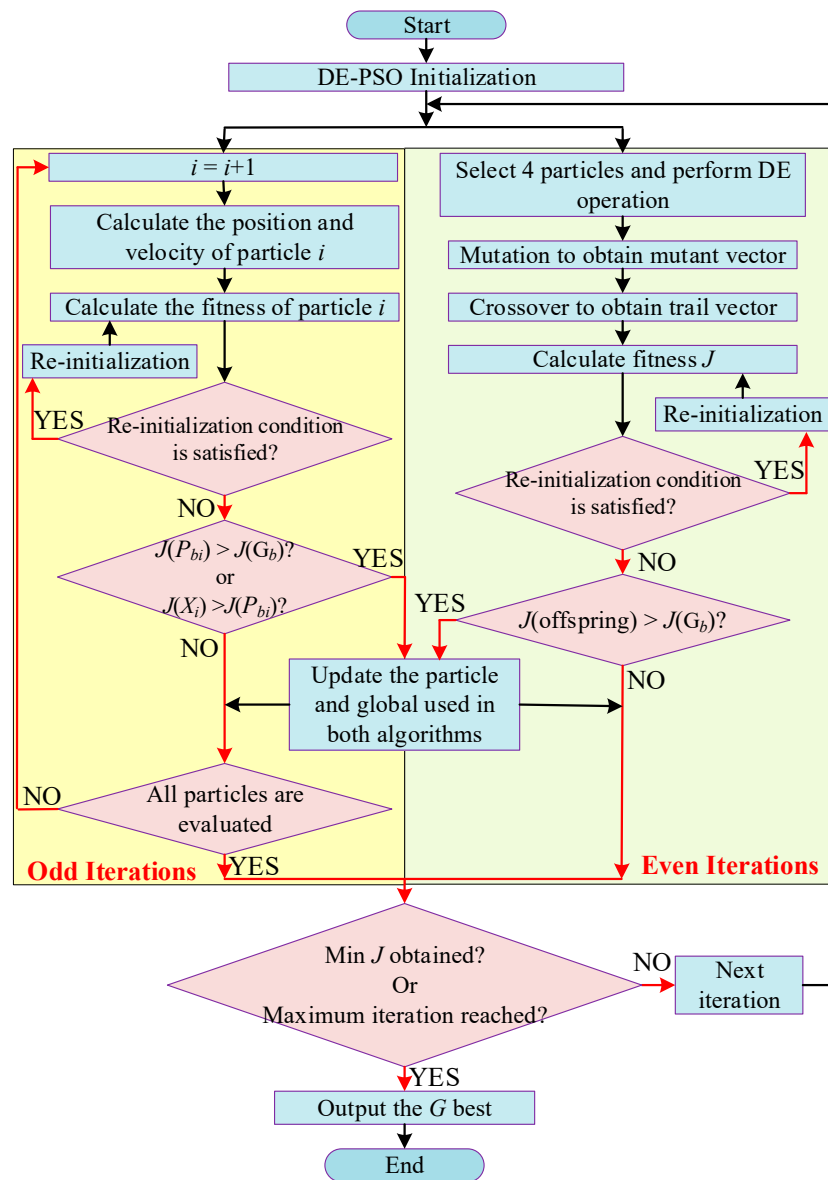
Figure 8. Flowchart of PSO-DE algorithm [52].

2.2.2. PSO with Proportional Integral (PI) Controller

The authors in [54] proposed a two-stage hybrid technique in which PSO is combined with Proportional Integral (PI) controller. Initially, PSO is used to locate the neighborhood area around the MPP where the operating point exists, and then in a 2nd stage, a PI controller is used to accurately locate the GMPP. The derivative of power with respect to voltage is zero, i.e., $dP(t)/dV(t) = 0$ at MPP; hence, a PI-based feedback controller uses this approach to find the exact MPP. Based on this, the control variable is provided as:

$$e(t) = dP(t)/dV(t) \tag{9}$$

When the irradiance level changes, it has a significant impact on the output power of the PV system; therefore, the variation in power must be limited and a threshold value must be allotted as provided in (10):

$$\left| \frac{P_{i+1} - P_i}{P_i} \right| > 10\% \tag{10}$$

where P_{i+1} represents the power at the present iteration and P_i represents the power at the previous iteration. Upon the detection of the inequality presented in (10), a command is sent to re-initialize the proposed algorithm.

2.2.3. PSO with Overall Distribution (OD)

In [55], an OD algorithm is integrated with PSO that can explore and discover the GMPP precisely and quickly under PSC. In this technique, initially, an OD algorithm is used to quickly explore the area near the GMPP and facilitate the initial values that are transferred to the PSO algorithm to perform its control actions. Once the initial values are obtained, a PSO algorithm only needs to search the GMPP within a predefined limited area. Due to these advantages, this algorithm can accurately and precisely identify the GMPP in case of PSC.

2.2.4. PSO with Adaptive Neuro Fuzzy Inference System (ANFIS)

In [56], an ANFIS is integrated with PSO to track the MPP under PSC. The schematic of the proposed MPPT technique is presented in Figure 9. In this method, the fuzzy data are collected with trained learning rules for the appropriate adjustment of membership function values before minimizing the error to the least value. The learned system is prepared to work as a hybrid technique whenever the parameters of the membership function are adapted. During the process of defuzzification, a centroid method is used for adapting the duty ratio of the converter, which is determined in accordance with the flowchart presented in Figure 9. Moreover, in this technique, both consequent and antecedent parameters are trained simultaneously to curtail the error. The proposed method does not require extra sensors for temperature and irradiance measurements to obtain the MP from the PV panel with zero oscillations. It provides fast tracking speed and tracking accuracy under PSC with high efficiency and low steady-state error.
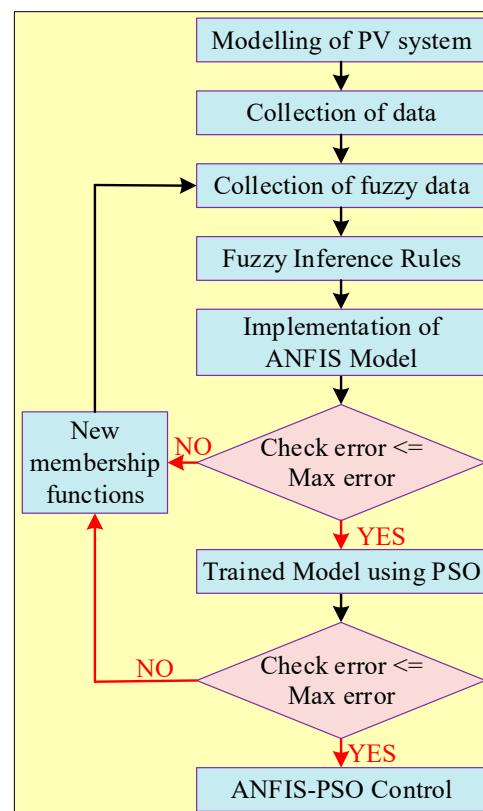

Figure 9. Flowchart of PSO-ANFIS MPPT algorithm [56].

2.2.5. PSO with One Cycle Control (OCC)

In [57], PSO is combined with OCC to extract the MP from the PV panel. The operation of this algorithm can be divided into two stages. In the 1st stage, the PSO algorithm is used to find the optimal current in accordance with the MP derived from the PV panel. In the 2nd stage, the current references generated by PSO are sent to the OCC, where the OCC enables the converter to track these references efficiently and quickly [58]. Compared with the traditional PSO or OCC method, in this hybrid technique, the tracking accuracy and the convergence speed to precisely locate the GMPP under PSC are significantly improved.

2.2.6. Enhanced Leader PSO (EL-PSO)

A conventional PSO algorithm has all the capabilities needed to reach global convergence under PSC, but it is found to be less desirable due to inappropriate initialization and velocity update limitations [59]. Hence, to enhance the performance of conventional PSO, the authors in [60] proposed a customized version of PSO known as EL-PSO. To strengthen and improve the search capability of a conventional PSO, it is modified by introducing mutations on the global best (G_{best}) particle. These mutations add a high value to particle updating, ensuring a quick convergence of the EL-PSO at GMPP. Moreover, EL-PSO shows better dynamic performance, fast convergence, precision in tracking MPP, and efficiency in comparison with the conventional PSO method.

2.2.7. PSO with Simulated Annealing (SA)

The authors in [61] combine the advantageous features of SA and PSO algorithms to precisely track the GMPP of the PV module under PSCs. A proposed technique increases the tracking accuracy, reduces the tracking speed, and efficiently tracks the GMPP. The operation of PSO-SA is discussed in seven different steps, as presented in Figure 10. In the 1st step, initial parameters such as step size, ending temperature T_{min}, temperature decrement rate α, and starting temperature T_o are set. In the 2nd step, the voltage operating point (V_i) from zero to V_{OC} is chosen. In the 3rd step, a power (P_i) is calculated in accordance with the operating point on the P-V curve. In 4th step, the step is calculated according to (11) as provided as:

$$step = step \times w + r_i c_i \left(U_{\max} - U_{ref\_out} \right) \tag{11}$$

where w is the weight of inertia and c_i is the acceleration speed of an individual particle.

In the 5th step, the random voltage is calculated (V_k) such that $V_k = V_i$ + step and the P_k in is calculated in accordance with V_k. In the 6th step, when T_o is greater than T_{min}, then the procedure from (a) to (e) should be followed as: (a) generate V_k, (b) calculate P_k according to the operating point on the *P-V* curve, (c) continuously update the P_k in every perturbation, and when $P_k > P_i$, it means that $V_i = V_k$ and $P_i = P_k$. If $P_k > P_{max}$, then update $V_{max} = V_k$ and $P_{max} = P_k$. (d) when $P_k < P_i$, then update the operating point according to (12) as:

$$P_r = \exp\left(\frac{P_k - P_i}{T_k} \right) \tag{12}$$

where T_k current temperature of the PV system, and (e) after N_T step changes, cool down the temperature. The "step" is restarted and set $V_i = V_{max}$. In a 7th step, when the stop criteria are satisfied, the current voltage perturbation also stops, and the command is sent to start a new perturbation.

2.2.8. PSO with Levy Flight Optimization (LFO)

In [62], PSO and LFO are combined to track the GMPP under PSCs. In this technique, a PSO algorithm is initially used to detect the GMPP, and then an LFO algorithm is used to enhance the extraction of the GMPP. During its operational process, initially, a PSO is used to check all the particles present in a search space. The fitness of every duty cycle is assessed, and then based on the fitness function, and the algorithm evaluates the values of

P_{best} and G_{best}. A duty cycle constraint is also added for every duty cycle before updating the position and velocity. Once the constraint is satisfied, i.e., if the current duty cycle exceeds the constraint value, then the position and velocity are updated. Once the duty cycle is updated, then in the next step, its fitness value is evaluated. Compared with the P_{best}, if the new fitness value is improved, then the P_{best} is updated, or else the value is increased by +1 and the process continues until the maximum iteration. The schematic flowchart of this MPPT technique is presented in Figure 11.
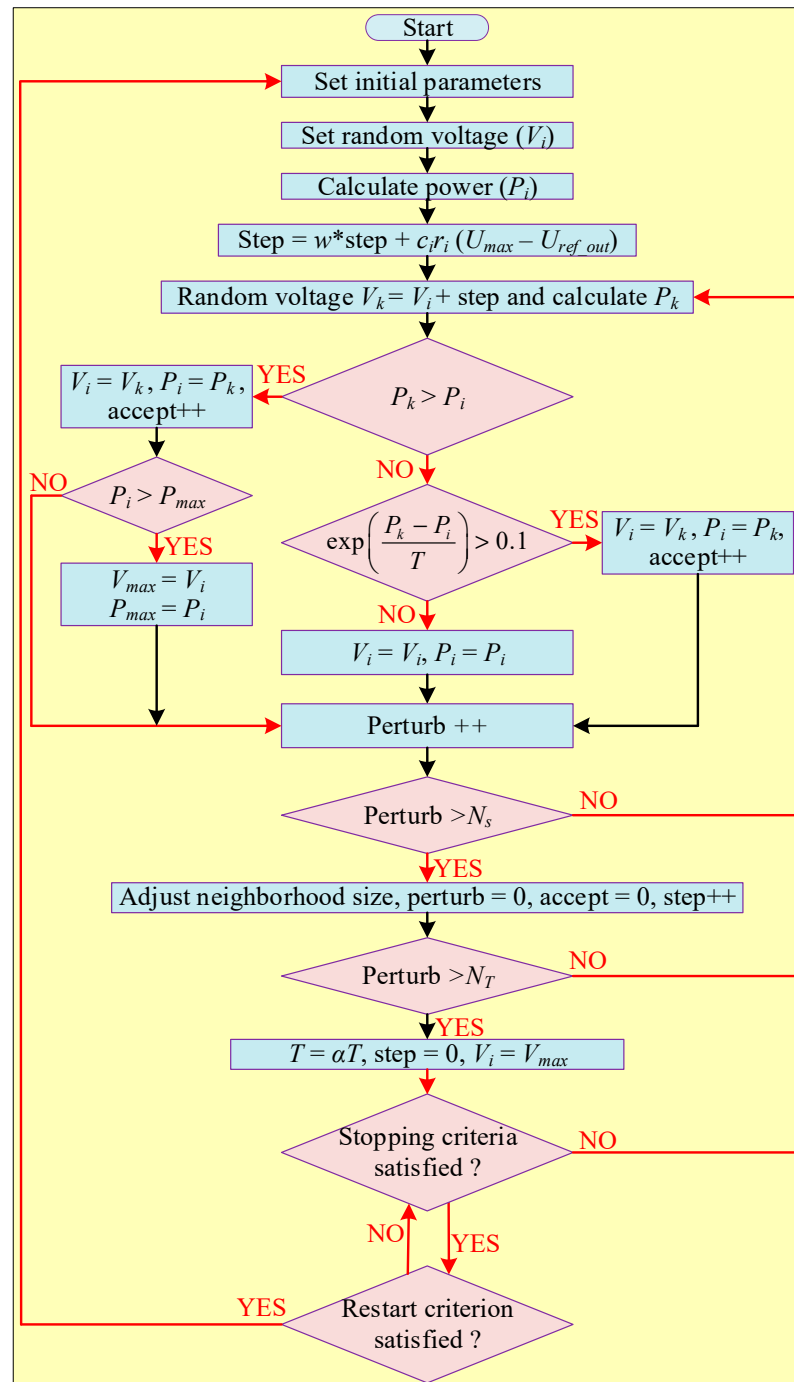

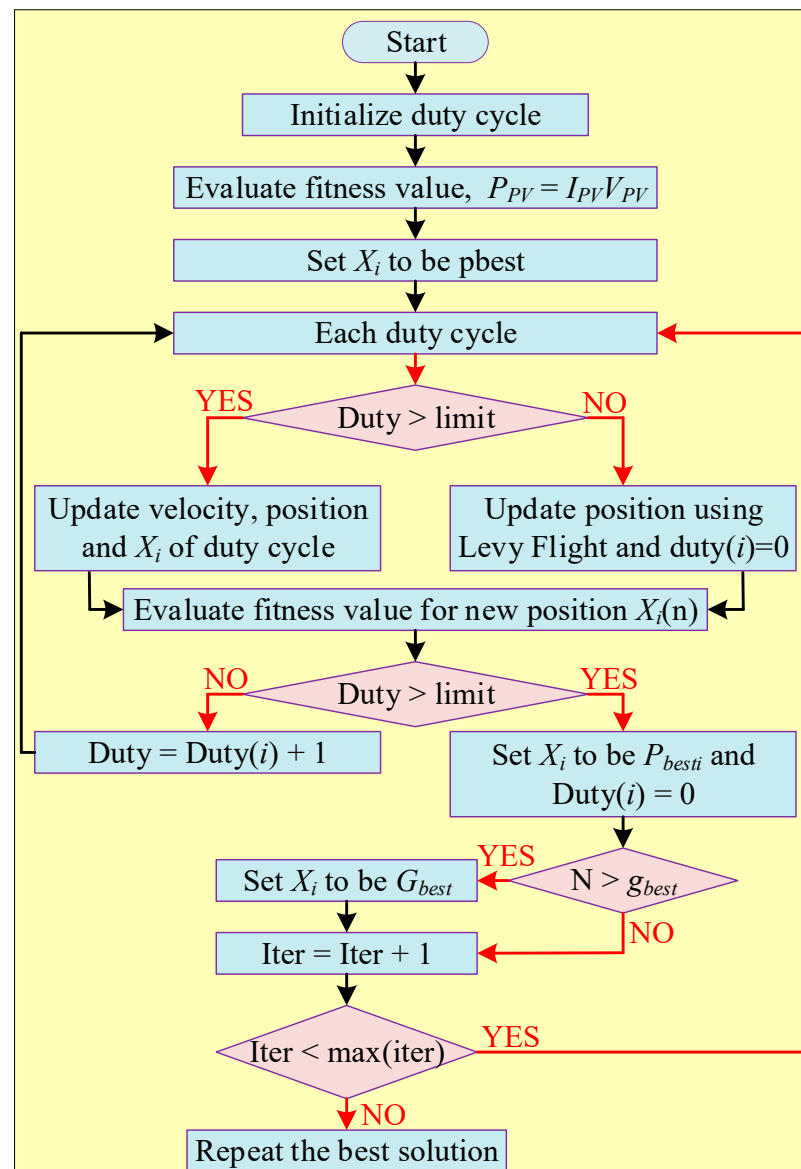**Figure 10.** Flowchart of PSO-SA MPPT algorithm [61].

Figure 11. Flowchart of PSO–LFO MPPT algorithm [62].

2.2.9. PSO with FLC

Another hybrid MPPT technique presented in [63] uses two different methodologies to optimize the input MF of the asymmetrical FLC. In the 1st method, the P-V curve of solar cells under Standard Test Conditions (STCs) (i.e., G = 1000 W/m^2 and T = 25 °C) is used to set the values of the input MF. This technique uses a simple methodology that is easy to adopt and can improve the performance of FLC. In the 2nd method, the values of input MF are optimized using the PSO algorithm. The PSO algorithm uses a cost function for its operation; therefore, a cost function is designed that meets the requirements of the PV system. After obtaining the optimized input MF values, in the next step, a proposed hybrid technique is implemented by using a digital controller, as presented in Figure 12. From the results, it can be concluded that the proposed algorithm has a high fitness value and enhances tracking accuracy, speed, and precision compared with the P and O and conventional FLC methods.
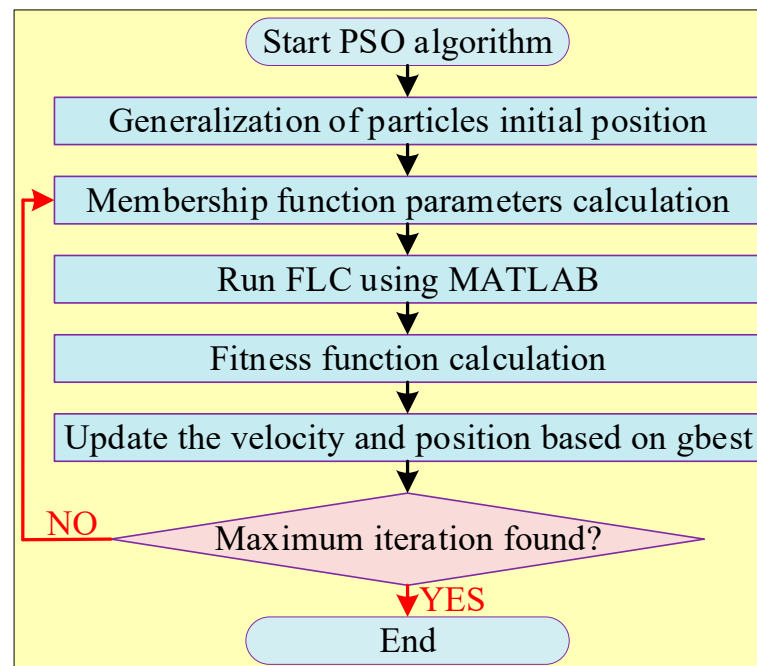
Figure 12. Flowchart of PSO-FLC MPPT method [63].

2.2.10. PSO with Terminal Sliding Mode Controller (TSMC)

In [64], a TSMC is integrated with the PSO to extract the MP from the PV panel under variable environmental circumstances. In a proposed method, to regulate the duty cycle of the converter's switch, a TSMC is used that keeps the PV system performing at the required reference regardless of variation in environmental circumstances. Furthermore, a PSO algorithm is applied to determine the optimal or ideal parameter values of the TSMC such that the proper trajectory of the system is guaranteed for varying environmental circumstances.

2.2.11. PSO with GSA

A hybrid MPPT technique presented in [65] combines a PSO with GSA due to its high local searching capability. In this method, a PSO is initially applied to rapidly scan all the search space for the GMPP, while the GSA is used for the local search only. Hence, this technique eliminates the steady-state oscillations once the GMPP is tracked by using its local search ability and social thinking. Moreover, from the simulation results, it can be concluded that this hybrid technique has a better ability to avoid the LMPP traps and has high tracking accuracy and efficiency compared with the conventional PSO and GSA.

2.2.12. PSO with ANN

In [66], PSO is combined with ANN to detect the GMPP under PSCs in order to extract the MP from the PV panel. A schematic flowchart of the proposed technique is shown in Figure 13. In this method, initially, an ANN algorithm is trained (100 data samples obtained by a trial-and-error process) for different values of power variation (ΔP) and the initial value of PV current (I_C) according to the different combinations of irradiance. Hence, in case of any variation in irradiance level, an ANN algorithm generates I_C and ΔP according to the trained data. A PSO in turn generates the PV current at MPP, corresponding to the change in solar isolation. As a result, the MP is always extracted from the PV panel due to the detection of PV current at MPP, even under PSCs.
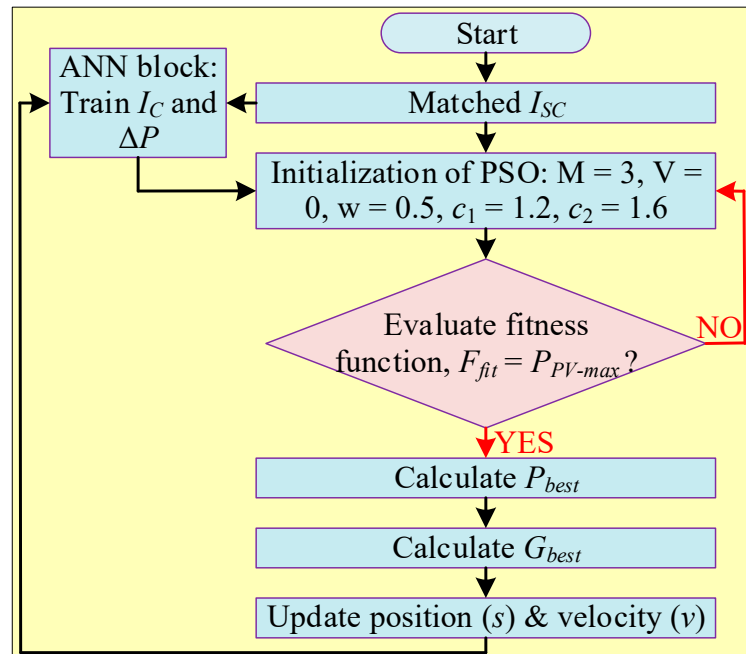
Figure 13. Flowchart of PSO-ANN MPPT technique [66].

2.2.13. PSO with Shuffled Frog Leaping Algorithm

In [67], PSO is combined with SFLA for MPPT applications. A schematic flowchart of PSO-SFLA is depicted in Figure 14. In this MPPT technique, the PSO population of particles is divided into many swarms/groups to enhance the optimization accuracy and convergence speed. Moreover, to further improve the convergence speed, an adaptive speed factor is also applied to the PSO algorithm. Compared with the individual usage of PSO or SFLA, the proposed method shows high performance and conversion efficiency under the same PSCs.

Figure 14. Flowchart of PSO-SFLA Hybrid MPPT technique [67].

2.2.14. Modified Particle Velocity (MPV)-Based PSO

In [68], an MPV-based PSO algorithm referred to as (MPV-PSO) is proposed to accurately track the GMPP under PSCs. This method eliminates the inherent randomness in PSO by eliminating the use of random numbers in the velocity equ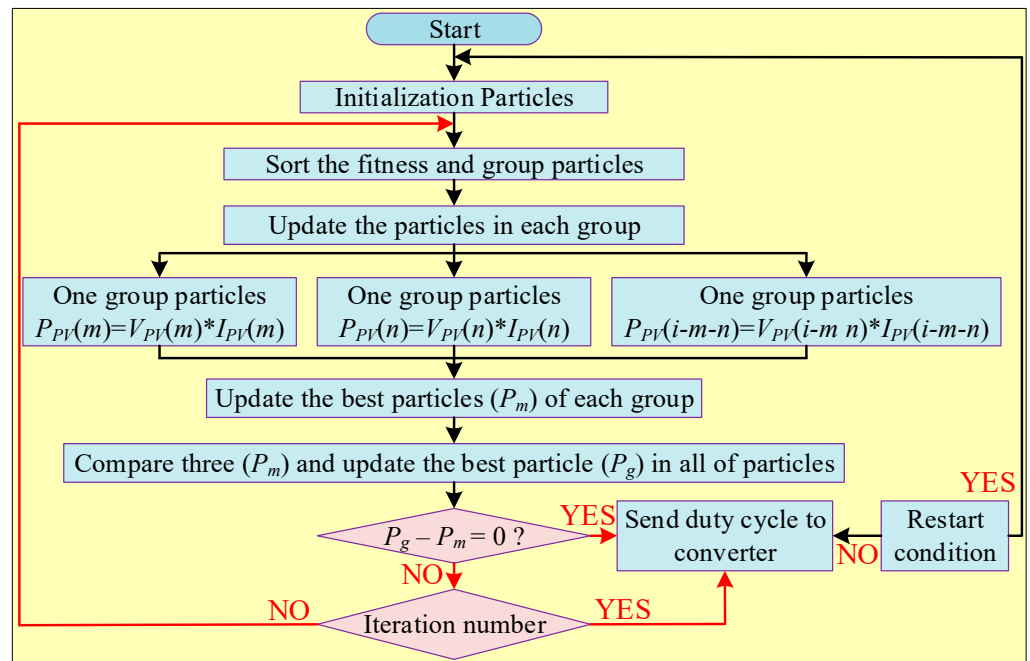ation. Moreover, this method is adaptive in nature by introducing the social acceleration and cognitive coefficients that adapt themselves according to the position of particles, the requirement for tuning the weight factor is also eliminated. These adaptive coefficients also avoid the trapping of algorithm in local minima and result in no steady-state oscillation around MPP. The position of the particle is updated as:

$$y_i^{k+1} = y_i^k + V_i^{k+1} \tag{13}$$

where y_i^k and y_i^{k+1} are the current and updated particle positions in the current and next cycle, respectively; and V_i^{k+1} presents the particle's updated velocity in the current cycle. The updated magnitude and velocity of the particle are determined as follows:

$$V_i^{k+1} = w \cdot V_i^k + c_2 \gamma_1 \left(y_{lb\_i} - y_i^k \right) + c_1 \gamma_2 \left(y_{gb\_i} - y_i^k \right) \tag{14}$$

where c_1 and c_2 are the social acceleration and cognitive coefficients, respectively; γ_1 and γ_2 are the random numbers ranging from 0 to 1; w is the weight factor and is used to ensure that the particles direction is the same as the direction in the previous cycle; $c_2 \gamma_1 \left(y_{lb\_i} - y_i^k \right)$ is a cognitive factor, y_{lb_i} is the particle's best position moving towards the best solution; $c_1 \gamma_2 \left(y_{gb\_i} - y_i^k \right)$ is the social factor that enables the movement of particles to the G_{best} position; and y_{gb_i} presents the best position among all particles from the start to the current cycle.

2.2.15. PSO with SSA

An SSA, like other meta-heuristic algorithms, has slow convergence and poor exploitation capability. Therefore, to overcome this limitation, the authors in [69] proposed a hybrid MPPT technique in which SSA is combined with PSO. In this technique, the basic structure of SSA is also modified to allow the merging of the update mechanism of PSO into the structure of SSA. This combination adds more flexibility and diversity to SSA during population exploration, resulting in fast convergence. The schematic flowchart of this method is presented in Figure 15. From Figure 15, it can be observed that in the 1st stage of this technique, the parameters are defined, and a population is generated that represents a set of solutions for the problem. Then the fitness function of every solution is evaluated, and the best solution is found among them. In the next step, the current population is updated by utilizing either SSA or PSO based on the quality of the fitness function. If the probability of the fitness function is greater than 0.5, then SSA is used, and if the probability is less than 0.5, then PSO is used. After that, the solution to every fitness function is evaluated to determine the best solution after updating the population. In the next step, it is checked whether the stopping criteria have been satisfied or not. If the stopping criteria is satisfied, then the algorithm returns the best solution. On the contrary, if the stopping criteria is not satisfied, then the algorithm repeats the previous steps (from computing the probability) until the stopping condition is met.

2.2.16. SSA with GWO

The authors in [70] proposed a hybrid MPPT technique in which GWO and SSA are combined to improve the GMPP tracking accuracy and speed of SSA under PSC. In this method, the leader structure of SSA is optimized by using GWO while maintaining the adaptive mechanism of SSA to avoid the LMPP traps. Hence, different from conventional SSA that consists of only one leader, in the proposed method, half of the salps are selected for the leader group while the remaining are the followers. Moreover, a special hierarchy

of GWO is also introduced in this method that enhances the global search capability of the population and enables fast convergence. A schematic flowchart of the SSA-GWO MPPT technique is presented in Figure 16.
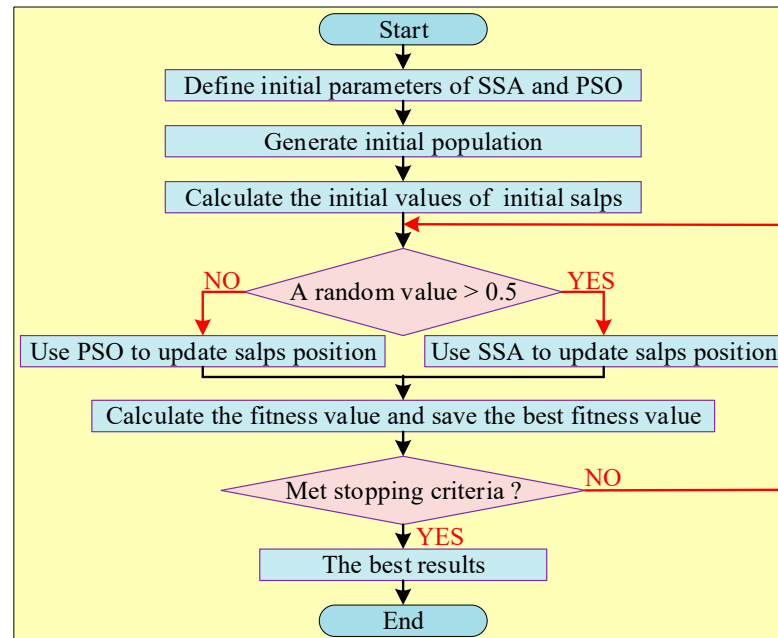

Figure 15. Flowchart of SSA-PSO MPPT technique [69].

2.2.17. Tunicate Swarm Algorithm (TSA) with PSO

A hybrid technique in which a TSA is combined with the PSO algorithm for MP extraction from the PV system is presented in [71]. A flowchart of the proposed method is presented in Figure 17. The performance of the proposed method is improved by integrating a PSO algorithm that enhances the exploitation ability of TSA. The performance of TSA-PSO is verified through simulation results under different PSCs. From the results, it can be observed that the proposed method tracks the GMPP accurately with a fast convergence speed and reduced steady-state oscillations than the TSA and PSO when they are used individually.

2.2.18. Artificial Fish Swarm Algorithm (FSA) with PSO

In [72], the authors combine FSA and Particle Swarm Optimization with Extended Memory (PSOEM) for a PV MPPT application. In this method, the velocity (inertia factor and memory) and learning capability of PSOEM are incorporated into FSA. Hence, such a controller is applied to efficiently and optimally predict the output voltage values for PV panels. Hence, this method efficiently tracks the GMPP with low oscillations around MPP under different PSCs. A flowchart of this technique is presented in Figure 18.

2.2.19. Fusion Firefly Algorithms

The operation of the FA is based on the behaviour of a firefly. Hence, its basic principle is based on the attraction phenomenon of a firefly, which usually attracts a firefly from a dim light to a bright light [20]. In FA, to maximize the objective function, its value is compared with the illumination of a firefly. Moreover, the illumination of a firefly represents the output power, and the location of a firefly denotes a duty cycle. FA has fewer regulatory parameters, converge on maximum value with low fluctuations, high tracking speed, and high accuracy. However, in rapid VEC, it is sometimes unable to accurately locate the GMPP [73]. Numerous improvements have been made to address this issue, such as the Fusion Firefly Algorithm (FFA) proposed by the authors in [74]. A schematic of this is

presented in Figure 19. In FFA, a Neighbourhood Attraction Firefly Algorithm (NaFA) is integrated with the conventional firefly algorithm to stop pinning down at LMPPs. This hybrid method outdoes P and O, PSO, Genetic Algorithm (GA), and NaFA in terms of accuracy, tracking speed, and efficiency.
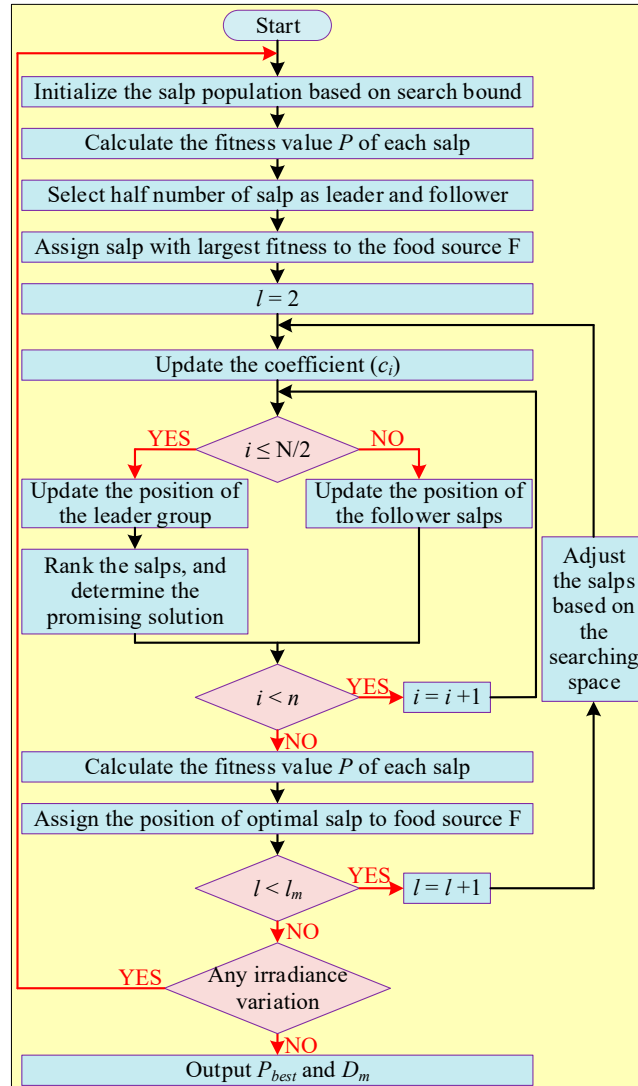

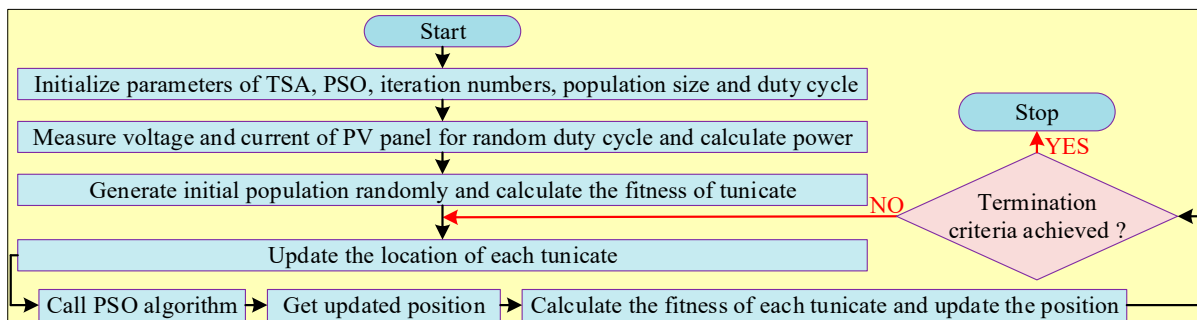**Figure 16.** Flowchart of SSA-GWO MPPT technique [70].

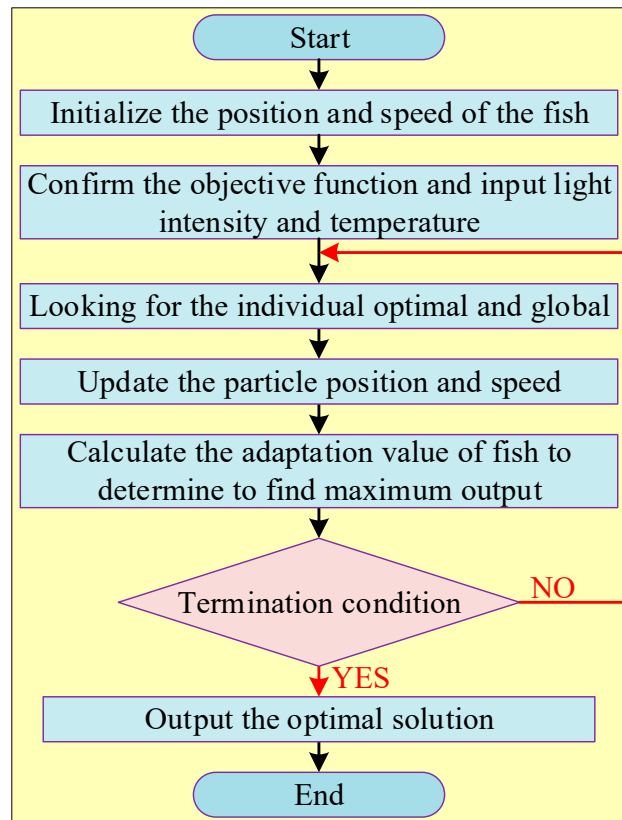**Figure 17.** Flowchart of TSA-PSO MPPT technique [71].

Figure 18. Flowchart of FSA-PSOEM MPPT technique [72].
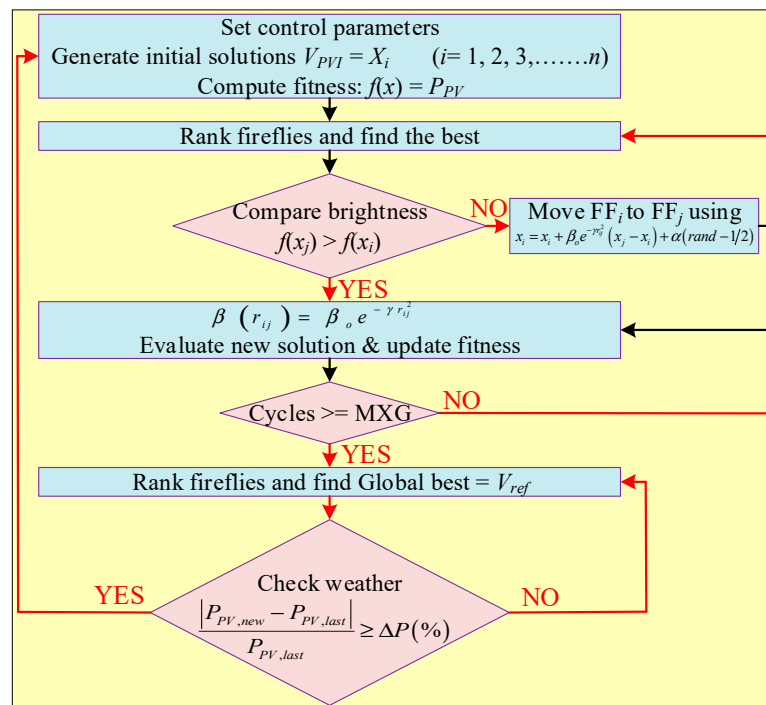

Figure 19. Flowchart for MFA [74].

2.2.20. FA with FLC

A hybrid MPPT technique that combines FA with FLC is proposed in [75]. In this technique, the FA algorithm is used to tune the Membership Function (MF) of the FLC to extract the MP from the PV panel. The coefficient of FA enables quick convergence in every iteration. The basic movements of FA can be provided as follows:

$$X_{i+1} = x_i + \beta_0 e^{-\lambda r_{ij}^2}(x_j - x_i) + \alpha \in_i \tag{15}$$

where r represents the distance between two fireflies; α is the randomization parameter; β_0 shows the attractiveness; x_i and x_j are the spatial coordination to i and j, respectively; and $\in_i$ is a constant ranging from 0 to 1. The MF of the FLC is tuned by the FA and the inputs of the FLC are provided as:

$$\Delta P = P(k) - P(k-1) \tag{16}$$

$$\Delta I = I(k) - I(k-1) \tag{17}$$

where ΔP and ΔI represent the change in the PV panel's output power and current, respectively. The output of the FLC is provided as:

$$\Delta D = D(k) - D(k-1) \tag{18}$$

where ΔD is the change in the duty cycle of the boost converter. Moreover, different rules for the FLC are set based on the FA in order to reach GMPP. This hybrid algorithm outperforms P and O and FLC methods in terms of tracking accuracy and speed and attains the highest efficiency of 99.98%.

2.2.21. Adaptive Cuckoo Search Algorithm (ACSA)

The fixed or constant switching parameters in the CSA engage in long random jumps at irregular intervals that result in power losses near MPP at a steady state. As the position of every particle of CSA symbolizes a value allocated to the gate of the switch (duty cycle) of the converter, any abrupt or unwanted change in the duty cycle causes unwanted glitches and oscillations in output power. Moreover, when using a CSA, high oscillations are observed at a steady state and has a high failure rate to accurately locate the GMPP [21]. Hence, to overcome these limitations and enhance the tracking accuracy and convergence efficiency of CSA, the authors in [76] proposed an ACSA. In this approach, the fixed parameters of the CSA are continuously updated at every sampling time to eliminate the undesirable glitches in voltage and power output waveforms. The efficiency of CSA can be enhanced by updating the switching parameters as follows:

$$P_{aci} = P_{a\_\max}\left(\frac{C_i}{T_i}\right) \tag{19}$$

where C_i and T_i represent the current and total number of iterations, respectively. As the switching parameters are increased exponentially along with iterations and is presented as:

$$P_{aci} = (P_{a\_\max})\exp\left(\frac{C_i}{T_i}\right) \tag{20}$$

Taking cube of switching parameter would yield (20) as:

$$P_{aci} = (P_{a\_\max})\left(\frac{C_i}{T_i}\right)^3 \tag{21}$$

During the search process in ACSA, appropriate samples must be selected for a smooth operation. The samples are defined as the duty cycle, i.e., D_i (i = 1, 2, 3, ..., n), where n is

the total number of samples. The value of power at MPP is defined as the fitness function (*J*). The voltage samples produced according to Levy's distribution are provided as follows:

$$D_i^{t+1} = D_i^t + \alpha \oplus Levy(\lambda) \tag{22}$$

$$\alpha = \alpha_0(d_{best} - d_i) \tag{23}$$

where α is the step size and λ denotes a variance.

In the proposed method, fast convergence is achieved due to the high initial population, while the large steps yield better GMPP and avoid the LMPP traps. Furthermore, this technique minimizes the computational time, improves the PV system's performance, and significantly minimizes the oscillation around GMPP.

2.2.22. CSA with Golden Section Search (GSS)

Similarly, the author in [77] proposed a hybrid method that combines the advantages of both CSA and GSS in one algorithm. In this method, CSA is responsible for accurately locating the tracking area where GMPP lies, whereas GSS is responsible for locating the exact GMPP. This method has the advantage of high tracking accuracy by limiting the MPP inside a specified tracking area. The tracking area is continuously shrunk by using a golden ratio until the GMPP is accurately located. Although the tracking speed to locate the GMPP is increased but it makes the algorithm complex and expensive.

2.2.23. ANN with Rational Quadratic Gaussian Process Regression (RQGPR) and Coarse Gaussian Support Vector Machine (CGSVM)

An ANN is very flexible in terms of input and output variables. Therefore, when it is used to extract the MP from the PV, the input variables can be non-electrical (irradiance, temperature) or electrical (power, current, voltage). Similarly, the output can be current or voltage at MPP or the duty cycle of the converter. Moreover, ANN shows very efficient performance, having a fast dynamic response and low steady-state oscillations. Besides all these advantages, a major challenge in designing an ANN-based MPPT technique is that it requires large and accurate data sets to train the ANN for efficient tracking [78].

To accurately train the ANN that efficiently and precisely tracks the MPP under PSC, different hybrid techniques have been developed. The authors in [79] proposed a RQGPR. A RQGPR method uses real-time samples to effectively create large, accurate, and acceptable training data sets that are required to train an ANN for proper tracking of GMPPT under PSCs. Similarly, the same authors use a CGSVM to train ANN for the MPPT task [79]. In this method, a few data sets (19 instances) were collected from the PSIM software, and based on these data sets, a CGSVM method is used to predict and generate a new training data set for ANN. The schematic of a CGSVM-trained ANN is presented in Figure 20. From this research, it can be observed that the regression error and mean square error statistics of the RQGPR and CGSVM-based ANN methods are better compared with the conventional ANN-based MPPT technique.
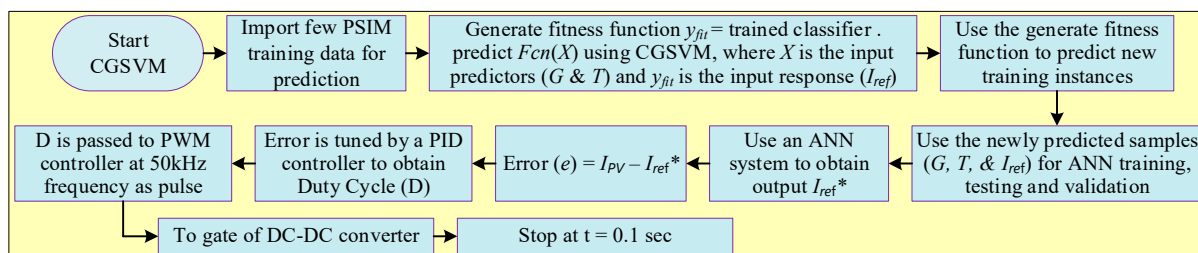

Figure 20. Schematic of CGSVM-trained ANN MPPT algorithm [79].

2.2.24. ANN with Fuzzy Particle Swarm Optimization Gravitational Search Algorithm (FPSOGSA)

To improve the tracking performance of the ANN-based MPPT technique, it is combined with the FPSOGSA [80]. In this hybrid technique, FPSOGSA is used to train and optimize an ANN algorithm. Hence, by using FPSOGSA, an appropriate initiation function for all the layers of the ANN structure is determined that results in fast and accurate tracking efficiency with low steady state. However, the implementation cost and complexity of this algorithm are very high. A schematic of an FPSOGSA-trained ANN is shown in Figure 21.
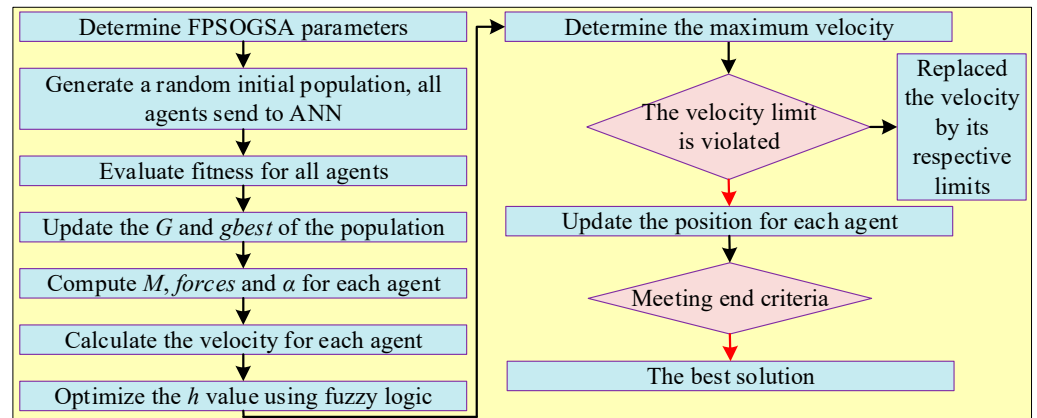
Figure 21. Schematic of FPSOGSA-trained ANN MPPT algorithm [80].

2.2.25. ANN with GSA and Pattern Search Algorithm (PSA)

The author in [81] proposed a hybrid algorithm in which GSA and PSA are combined together to train an ANN algorithm for MPPT applications. A schematic flowchart of this MPPT technique is presented in Figure 22. In this method, temperature and irradiance are considered input variables, while the optimal voltage is taken as the output variable of GSA-PSA. The optimal output voltage of GSA-PSA is used to regulate the ANN, which in turn has the responsibility to track the MPP accurately. Moreover, a P and O algorithm is also used in this technique that considers the sampled current, voltage, and output of ANN as input variables and starts to operate when ANN is unable to accurately locate the MPP. Hence, by using this hybrid technique, the number of samples required for ANN training is considerably reduced, resulting in a low computational burden.
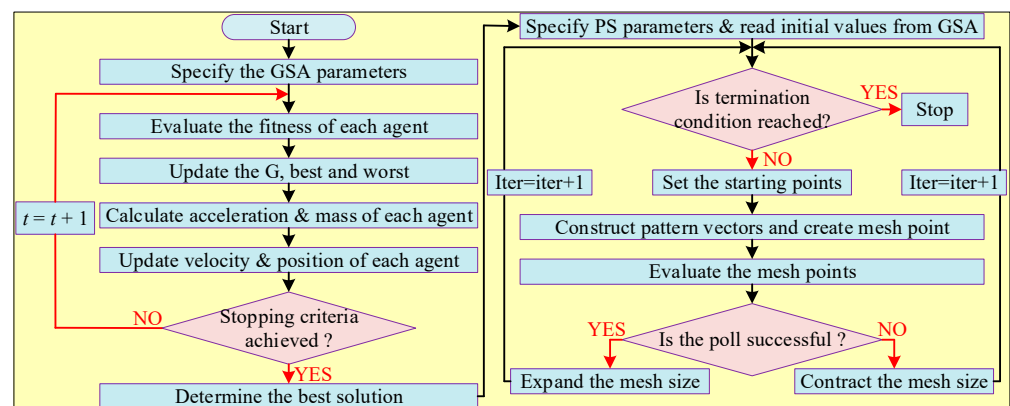

Figure 22. Schematic of GSA-PSA-trained ANN MPPT algorithm [81].

2.2.26. ANN with GA

The author in [82] proposed a hybrid technique in which a GA is used to optimize the ANN algorithm to accurately find the GMPP under PSC. In this method, the optimized

data from the GA is used to train the ANN by using a Bayesian regulation technique that predicts the MPP at given irradiance and temperature. Hence, the performance of the proposed technique to track the MPP is considerably improved compared with the conventional ANN algorithm.

2.2.27. ANN with FLC

In [83], the authors proposed an ANFIS technique that combines the advantages of ANN with FLC while discarding the disadvantages. An ANFIS is flexible, optimal, and adaptable to any new configuration of PV system. The system under consideration in [83] uses a Battery Energy Storage System (BESS) in a PV system. Therefore, initially, the amount of PV-generated energy is forecasted to set the output trends by utilizing an ANFIS algorithm, and then the capacity of BESS is calculated based on the forecasted output data. The load power is then calculated and categorized into two sections by using a Cartesian plan, i.e., left plane and right plane, from the peak load, for the purpose of seeking BESS equal capacity. Moreover, FLC provides network-switching sequence over consumption to choose the best BESS utilization for power peak curtailment. A schematic flowchart of the proposed method is presented in Figure 23.
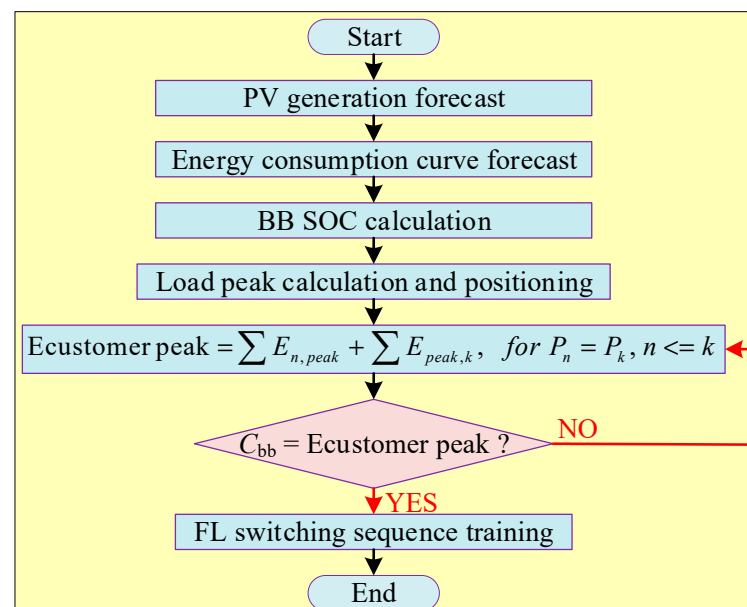
Figure 23. Schematic of ANN-FLC MPPT technique [83].

2.2.28. ANN with Scanning Procedure (SP) Technique

A hybrid MPPT technique proposed in [84] combines an ANN algorithm with the SP technique. In this method, initially, SP is activated to compare the value of actual power with the previous power and store the value that is highest among them, referred to as the MP value ($P_M(k)$). To obtain the GMPP, every $P_M(k)$ is compared with the previous MP value ($P_M(k-1)$) such that GMPP = $P_M(k)$. ($P_M(k-1)$). Once the GMPP is detected, in the next step, an ANN is activated to generate a suitable duty cycle that is used to control the switch of the converter.

2.2.29. ANN with Ant Colony Optimization (ACO)

In [85], an ACO technique and an ANN algorithm are integrated together to form the ACO-ANN technique. In this hybrid technique, an ACO is used to train the multi-layer ANN, develop the connection weights, and generate the optimal duty cycle for the converter. Hence, ANN acts as a podium to generate the optimal duty cycle for the switch to reach the MPP with a fast dynamic response and enable the PV generator to operate near the MPP.

2.2.30. ANN with Monte Carlo (MC) Filtering

The authors in [86] proposed a hybrid MPPT technique where ANN is combined with sequential MC filtering. In this method, ANN is used for forecasting the MPP, whereas MC filtering is used for state estimation. Moreover, IC is used as a state-space model for the sequential estimation of MPP, whereas ANN is used to predict the GMPP based on observed data (irradiance, current, voltage, etc.) in order to improve the estimation made by MC. Furthermore, in a proposed method, a detection technique is used to detect a rapid variation in irradiance. Upon detection of rapidly varying irradiance, the MC-based MPPT technique uses ANN support for MP extraction.

2.2.31. ANN with Back Stepping (BS) Controller

In [87], an ANN vision-based MPPT technique is combined with BS controller to accurately locate the GMPP under PSCs. In this method, real-time changes in solar irradiance and PSCs are identified by an ANN-based webcam to provide MP and a reference voltage. A BS controller is used to control the DC–DC converter by controlling the time varying error between the actual PV output voltage and the ANN-generated maximum reference voltage. However, the proposed method efficiently extracts the MP from the PV panel, but in the case of large power plants, the applicability, complexity, computational process, and computational burden are not taken into consideration.

2.2.32. Improved ANN with PSO

The authors in [88] proposed a hybrid MPPT technique in which an Improved ANN (IANN) is combined with the PSO algorithm, where the primary focus is to improve the conversion efficiency and tracking capability. Generally, IANN executes a mapping among the input and output patterns rather than a problem statement. Therefore, it is very beneficial in forecasting the non-linear behaviour of varying solar irradiance and temperature. The tracking efficiency (η_{MPP}) of IANN-PSO is provided as:

$$\eta_{MPP} = \frac{avg(P_{ss})}{\max(P_{EC})} \tag{24}$$

where $avg(P_{ss})$ in the average output power and $\max(P_{EC})$ is the maximum available power. The output equation of IANN is provided as:

$$\theta_{IANN} = \sum e_i w_i + \theta \tag{25}$$

where e_i denotes an input error, w_i presents the weight function of related input, and θ denotes the minimum number of neurons required for activation.

All the weight values for IANN are placed in a space having n dimensions; therefore, the weights should be optimized in such a manner that they track the position of the particles in PSO. During the evaluation of particle fitness, the optimal weights are allocated to IANN, and thus its predicted accuracy is determined as the fitness for particles. The fitness function of the particles in PSO is provided as:

$$fitness\ function = \max[\eta_{MPP}]_T \tag{26}$$

If the fitness is best for the particles, it would be considered as a personal best (P_{best}), and if it is best for the swarm, it would be taken as a G_{best}. The position of G_{best} after some iterations yields to optimized weights for IANN. Moreover, the position of each particle is provided as:

$$v_i(t) = v_i(t-1) + c_1 r_1[P_{best}(t) - x_i(t-1)] + c_2 r_2[g_{best}(t) - x_i(t-1)] \tag{27}$$

where $x_i(t)$ is the position of the particle, $v_i(t)$ is the velocity, and c_1 and c_2 present the irradiance and temperature, respectively. A flowchart of the IANN-PSO is presented in Figure 24.
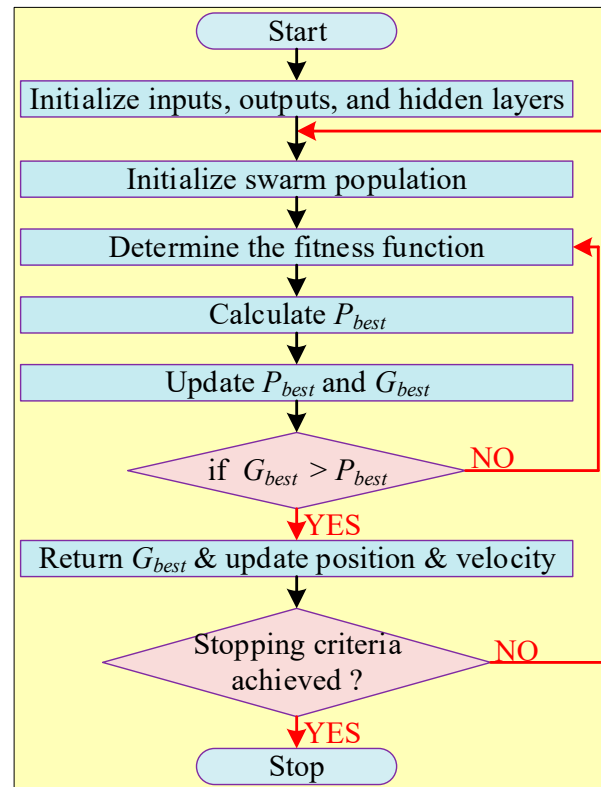
Figure 24. Flowchart of IANN-PSO MPPT technique [88].

2.2.33. Radial Basis Function Neural Network (RBFNN) with PSO

An estimation mechanism based on automatic learning methods such as the RBFNN creates a model for an unknown function to find a relation among the input and output data. In RBFNN, the weight, centre, and variance of the radial base function must be selected appropriately. If these variables are not selected appropriately, then it can affect the accuracy and validity of the model. Moreover, the unwanted growth in the size of hidden layers of RBFNN increases the computational time, which is another disadvantage [19]. Therefore, to cope with these issues, the authors in [89] proposed a novel hybrid MPPT technique in which RBFNN is combined with PSO to extract the MP under PSCs. In this method, an adaptive control strategy based on PSO is used to optimize the RBFNN parameters. The adaptive PSO dynamically adjusts the new velocity vector and inertia weight factors at every sampling time. The adaptive PSO also determines the connection weights, widths, and centres of RBFNN to ensure a good follow-up of MPPT. Moreover, FLC is also used in this system to generate the controlled signals for the switch of the boost converter.

2.2.34. RBFNN with Back-Stepping Terminal Sliding Mode Controller (BTSMC)

Similarly, another RBFNN-based MPPT technique in which it is combined with a nonlinear BTSMC is presented in [90]. In this method, RBFNN uses a relation between PSC, i.e., irradiance, temperature, and maximum PV voltage, to generate a reference voltage. The BTSMC tracks the reference voltage and generates the control signal for the switch of the non-inverting buck-boost converter. The proposed method improves the transient response, extracts the MP from the PV panel due to less chattering, and increases tracking

accuracy compared with individual usage of RBFNN and SMC. Moreover, a Lyapunov function is used to validate the finite time stability of the system.

2.2.35. GWO with β-Algorithm

A GWO technique a prominent MPPT techniques that ensures fast tracking and rapid convergence under PSC. However, high oscillations are observed around MPP at steady-state conditions [91]. Therefore, to cope with this challenge, the researchers in [92] proposed a hybrid technique in which GWO is combined with the *β*-algorithm for PV MPPT application. In this method, a disadvantageous feature of GWO (high steady-state oscillations) and *β*-algorithm (variables dependency on PV array characteristics) is active while their advantageous features are enhanced. The main objective of the proposed GWO-*β* technique is to reduce the power oscillations around GMPP and enhance the convergence speed that results in high efficiency. In this method, a GWO method is used to attain a GMPP, meanwhile a *β* technique is applied to calculate the MPPT reference according to PV current and voltage at GMPP. A flowchart of this proposed MPPT technique is presented in Figure 25.
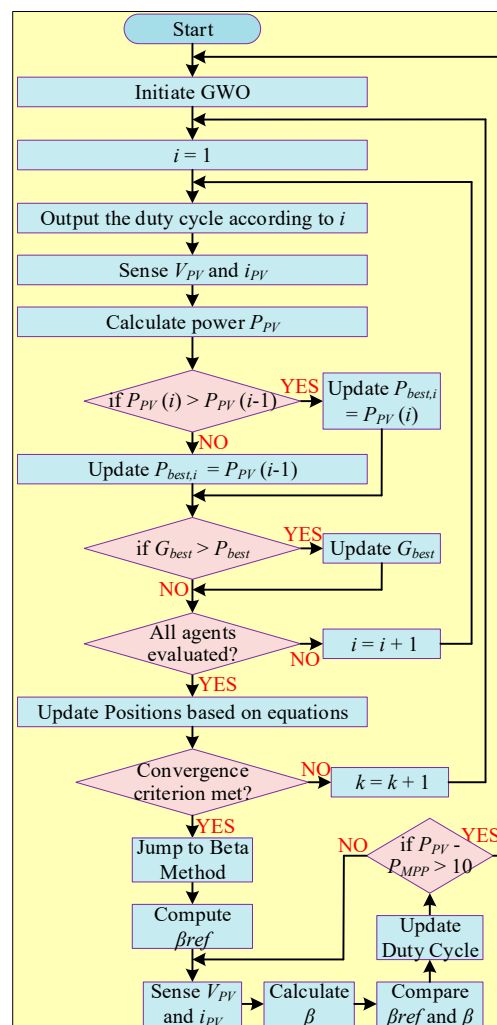

Figure 25. Flowchart of GWO-Beta hybrid MPPT technique [92].

2.2.36. GWO with FLC

As FLC has an advantage of very low steady-state oscillation around MPP but it may stick to one of the LMPPs. Therefore, the authors in [93] combined a GWO with FLC such that the resultant controller has low oscillations and fluctuations around MPP and tracks

the GMPP accurately with a fast dynamic response under PSC. In this hybrid technique, a GWO is initially applied to track the GMPP in an efficient and fast way. Then an FLC is applied to reduce the steady-state power oscillations around GMPP that were tracked by GWO. Hence, the advantageous features of GWO (the ability to track GMPP under PSC) and FLC (low oscillations around GMPP) were enhanced, which results in high conversion efficiency.

2.2.37. GWO with Crow Search Algorithm (CSA)

The operation of the FA is based on the behaviour of a firefly. The authors in [25] combine GWO with the CSA, referred to as GWO-CSA, for MPP tracking under PSC. In this technique, the advantages of both algorithms are combined, resulting in high convergence speed and accuracy, and particularly avoids getting trapped by LMPP. Initially, a GWO technique is used to solve the MPPT problem and determine the optimum duty cycle. The duty cycle determined by GWO is then used as an input to CSA. The performance of this technique is tested considering different irradiances, temperatures, and types of DC–DC converters. It is concluded that the GWO-CSA shows high performance and efficiency compared with the individual use of GWO and CSA.

2.2.38. GWO with Golden Section Optimization (GSO)

In [94], a GWO is integrated with GSO to track the MP. The operation of this MPPT technique can be divided into two stages, as presented in Figure 26. In the 1st stage, a modified GWO is applied for global search. In a modified GWO, the weights of the wolf leaders are adjusted automatically with hunting evaluations that contribute to accelerating the hunting. Furthermore, an idea of search density is also presented, which determines the wolf count and maximum number of iterations. In a 2nd stage, a GSO is applied for local search to reduce tracking time by avoiding unnecessary searches. Moreover, to increase the MPPT system reliability, a restart judgement based on the quasi-incline of the P-V curve is proposed in this technique.

2.2.39. ANFIS with Crowded Plant Height Optimization (CPHO)

The authors in [95] proposed a hybrid MPPT technique to cope with the problems of low tracking efficiency and speed, high steady-state oscillations, and low performance during PSCs of the conventional techniques. In this hybrid technique, an ANFIS is combined with the CPHO algorithm. Under UEC, a CPHO is used to determine the MPP.

However, in the case of PSCs, to accurately locate a real GMPP and generate an optimal duty cycle, a combined approach of ANFIS and CPHO algorithms is used. The performance of the ANFIS-CPHO is divided into two stages. In the 1st stage, an ANFIS estimates a GMPP among numerous LMPPs and tracks near a peak power point. In the 2nd stage, a CPHO algorithm is activated to locate an accurate GMPP. As a result, a proposed algorithm detects the GMPP with more precision and accuracy with low duty cycle oscillations. A proposed algorithm was compared with ANFIS, and it is found that the time required for ANFIS to reach the GMPP was 92 ms, while ANFIS-CPHO only takes 39 ms.
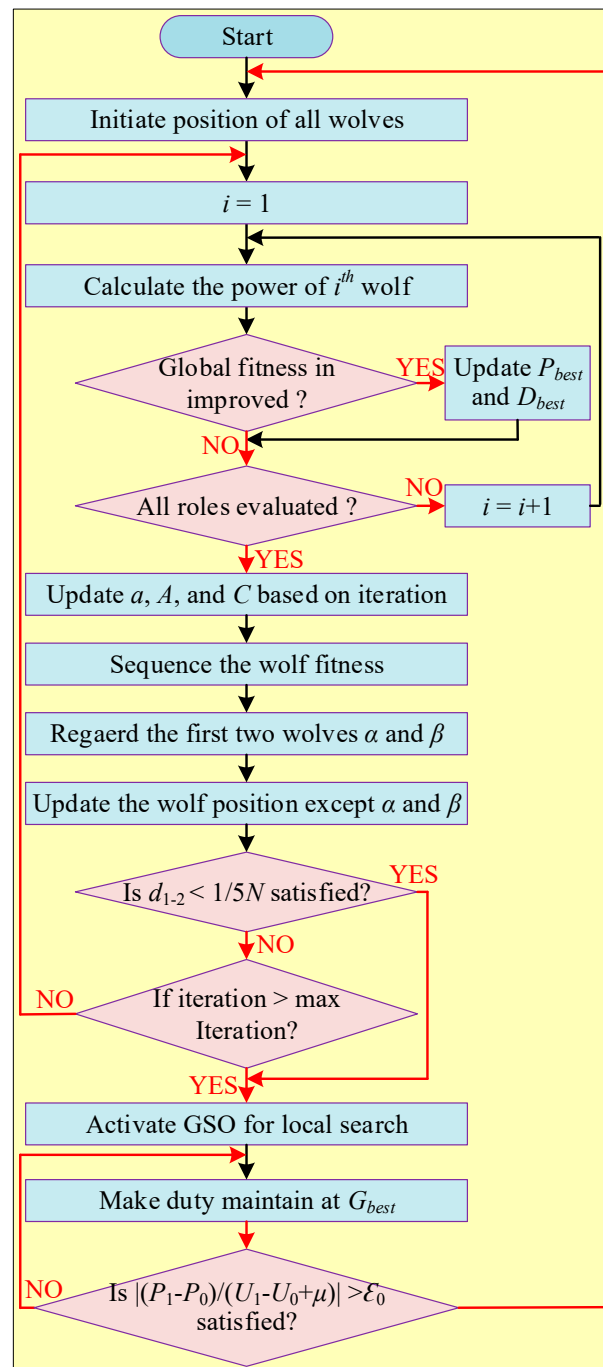
Figure 26. Flowchart of GWO-GSO hybrid MPPT technique [94].

2.2.40. FLC with MSFLA

FLC is very flexible in terms of input and output variables and shows significant performance to track the MPPT with low steady-state oscillations. Besides all these advantages, a major challenge in designing FLC-based techniques is that they are very dependent on the user's knowledge and may become stuck on one of the LMPP that affect the system's performance. Therefore, the authors in [96] proposed a hybrid MPPT technique that combines FLC with the Modified Shuffled Frog Leaping Algorithm (MSFLA) to overcome the disadvantageous features of FLC. In this method, a theoretical framework for efficiently tuning the controller's parameters is developed that accurately tracks the GMPP under different PSCs. Moreover, simulation and hardware results show that 99% efficiency is achieved by the FLC-MSFLA technique with fast convergence speed and low oscillations.

2.2.41. Beta Fuzzy Logic Controller

To enhance the tracking capability of conventional FLC, the authors in [97] introduced a beta (β) parameter as an input of the FLC. In this work, a β variable was introduced rather than the PV output power or varying terminal voltage as a 3rd input of FLC. Hence, the FLC with β parameter covers a wider range of operating conditions and simplifies the rule number, improving steady and dynamic performances as a result. Moreover, this method reduces the user knowledge dependency by measuring the current and voltage at every sampling time. It also enhances tracking accuracy and speed and offers zero oscillations.

2.2.42. FLC with GA

While designing FLC, two major steps were involved: structure and parameter identification. Structure identification involves the selection of a suitable control structure, such as the size of the rule base. In the parameter identification process, the values of parameters are determined, such as the contents of the rule base and the shape of the membership function. Therefore, GA is used to optimize the Fuzzy Rules (FRs) and Membership Functions (MFs) of FLC to overcome its disadvantageous feature, i.e., dependency on human knowledge [98]. In this method, both the FRs and MFs are optimized simultaneously, which results in high controller performance [99]. A GA is used to accurately calculate the peak locations and base lengths of the membership function in FLC, for which the FRs have already been generated. Thus, the proposed solution leads to improved performance of the MPPT tracker with a fast response time and reduced oscillations.

2.2.43. FLC with PI

A PI controller consists of proportional and integral gains, whose values are generally fixed constants. Hence, in case of system uncertainty or under PSC, a PI controller with fixed gain values is unable to perform satisfactorily. Therefore, to cope with this limitation of a PI controller, the authors in [100] proposed a technique in which the fixed gain parameters are updated at every sampling time by using FLC. The P-V characteristic curves of PV panels are used as the inputs of FLC. The FRs and MFs of FLC are designed on the fact that if a slop increases, it gets away from the MPP, and if a slop decreases, it moves towards the MPP. Moreover, the gains of PI controllers are adjusted in such a manner that the gains increase in the transient-state and decrease in the steady state. Hence, this approach increases the tracking speed of the algorithm and improves the steady-state error.

2.2.44. FLC with Teaching Learning-Based Optimization (TLBO)

The authors in [101] used a TLBO approach for optimizing the MFs of FLC and generating an appropriate duty cycle for MPPT. A schematic flowchart of this hybrid technique is presented in Figure 27. A TLBO has low dependency on system parameters; typical control factors like number of generations and population size [102]. This technique consists of two phases, i.e., Teacher Phase (TP) and Learner Phase (LP) and examines the effect of teachers on learners. In a TP, the learners attain knowledge from the teacher. Generally, a teacher is considered a competent knowledgeable person who shares their expertise with the learners. In an LP, the learners gain knowledge through interaction with each other. During the LP, learners also gain knowledge via engaging with one another; as a result, their performance is enhanced. A learner increases his or her knowledge through random interactions with other learners. If other learners have higher knowledge, then the peer learner picks up and learn new things. Additionally, simulation studies show that, compared with conventional FLC, TLBO-based MFs improve both MPPT convergence speed and tracking accuracy.
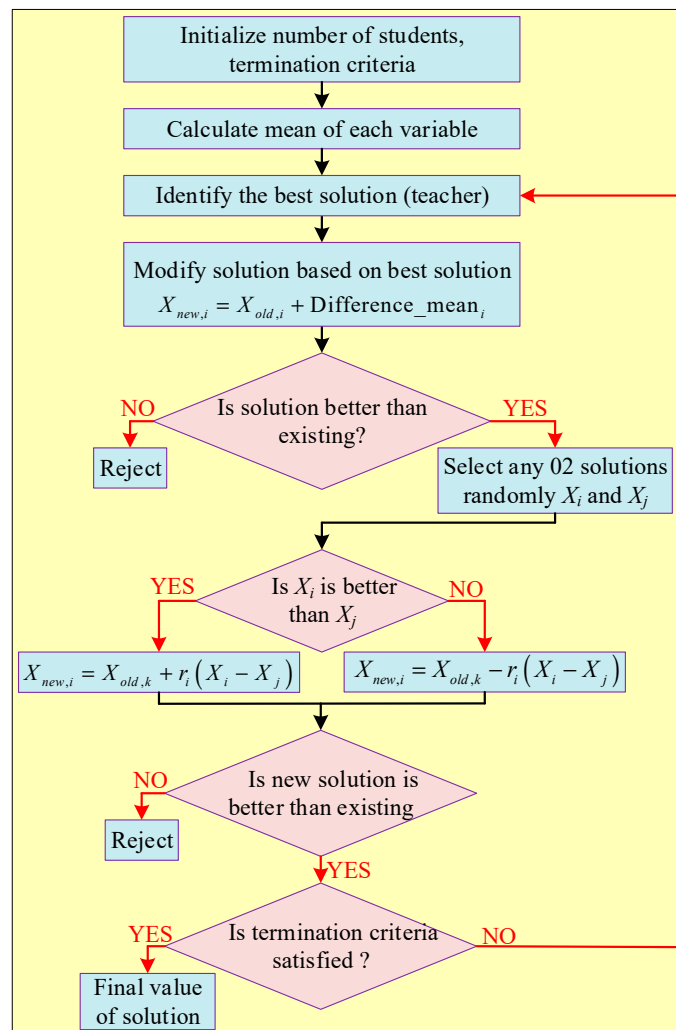
Figure 27. Flowchart of TLBO-FLC hybrid MPPT technique [101].

2.2.45. Hybrid Taguchi Genetic Algorithm (HTGA)

The usage of a GA for PV MPPT applications is not very favourable due to its complicated calculations, possibility to trap LMPP, and low tracking accuracy. Therefore, to overcome these limitations, it is combined with different other algorithms, and as a result, some new hybrid techniques have come into existence. One such example is a HTGA that is proposed in [103] for the extraction of MP from the PV system. Although, HTGA is more complex than GA, it enhances the calculation capability of variables, shows better performance under PSCs, and has better tracking accuracy. The operational methodology of HTGA consists of ten steps, as presented in Figure 28. These steps are: 1. start an algorithm; 2. initialize and set the parameters population N = 100, mutation rate y%, and crossover rate x%; 3. generate the position; 4. P = I × V × Ff represents the power of the PV system, where f is the fitness function and is provided as f = P^2; 5. when the algorithm meets the termination criteria, i.e., P_{max} = I × V × Ff, then the algorithm skips to step 9. On the contrary, if the termination criteria are not satisfied, then the algorithm moves on to step 6; in 6 step, crossover operation is performed, i.e., x% of the chromosomes doing two-point crossover; 7. the Taguchi method is applied to generate the new chromosomes; 8. the newly generated chromosomes generated by the Taguchi method are then passed through a mutation operation where the mutation nodes are selected randomly; 9. the fitness value and the output of the algorithm are achieved; 10. end of the algorithm.
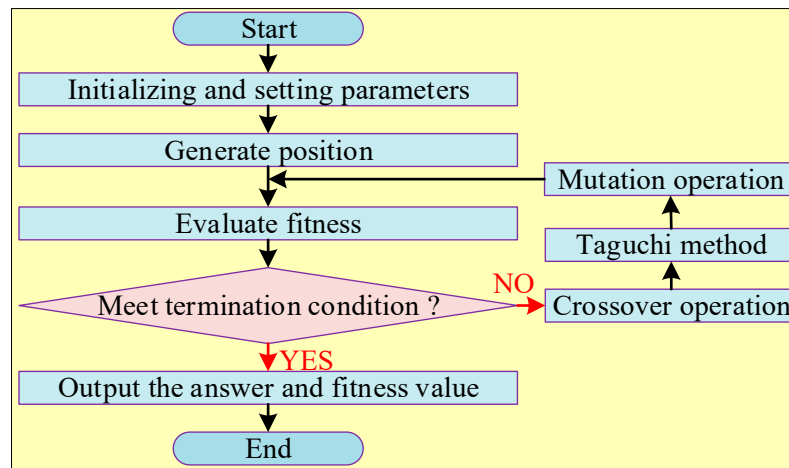
Figure 28. Flowchart of HTGA MPPT technique [103].

2.2.46. GA with FA and DE

In [104], a hybrid M PPT technique was designed where GA is combined with FA while DE is used to enhance the calculation process. In this method, the complex calculation of GA is simplified by integrating the attractive process of FA and the mutation process of DE. Due to this integration, the proposed method overcomes the disadvantages of GA, such as its low convergence speed and high execution time. Moreover, compared with GA, the proposed technique improves tracking accuracy by 4.16% and execution time by 69.4%. Similarly, compared with FA, the tracking accuracy and execution time are improved by 1.85% and 42.9%, respectively. Hence, it can be concluded that the high accuracy and fast dynamic response under PSCs are the main advantageous features of this method. A schematic flowchart of this technique is depicted in Figure 29.
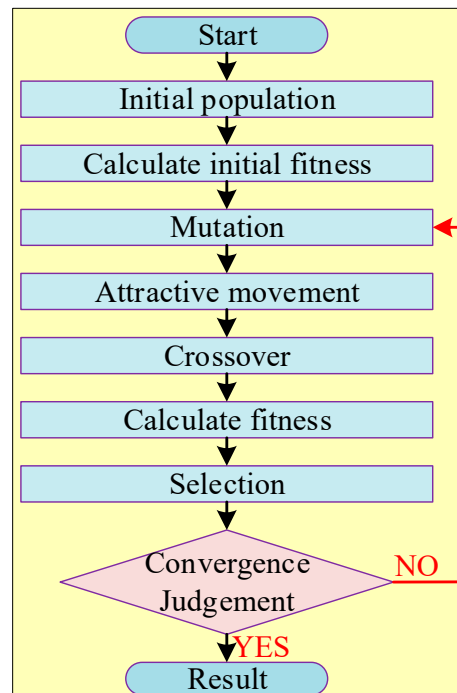
Figure 29. Flowchart of GA-FA MPPT technique [104].

2.2.47. GA with ACO

To enhance the speed and robustness of the GA MPPT technique, the authors in [105] proposed a hybrid technique where GA is combined with ACO. A flowchart of hybrid GA-ACO is presented in Figure 30. A GA is used to find a feasible solution and ensure fast convergence, while an ACO is used to search a subspace and avoid the LMPP traps. Due to these characteristics, a proposed technique converges very fast, and in some cases, GA-ACO accurately locates the GMPP in the 1st iteration. In the same environmental conditions, a GA-ACO is compared with P and O and ACO algorithms, and it can be concluded that both (P and O and ACO) algorithms take more than 20 iterations to reach a solution, while the GA-ACO technique takes only 10 iterations. Hence, it is stable, robust, and accurate, and can reach GMPP with rapid speed even in harsh temperature and irradiance conditions.
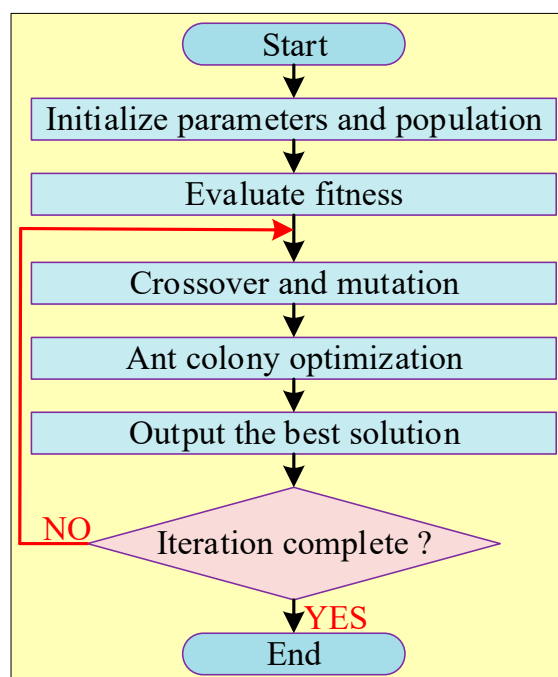
Figure 30. Flowchart of GA-ACO MPPT technique [105].

2.2.48. Deterministic Modified Jaya (DM-Jaya) Method

One of the major drawbacks of the Jaya technique is the stochastic process, where the movement of particles is based on irregular numbers. This unpredictable process may result in a high computational burden, which in turn affects the convergence speed and the tracking accuracy. Therefore, to cope with this drawback, the authors in [106] proposed a DM-Jaya method for GMPP tracking. In this method, the step size in the neighbourhood of GMPP and the method used to update the formula of the conventional Jaya method are greatly improved. With this approach, the random or irregular numbers in terms of update solutions are eliminated, making the particle solutions' movement toward the GMPP more deterministic. These improvements provide many pros, including the tuning of only one parameter, fast convergence speed, easy implementation, and zero steady-state oscillations. A flowchart of this proposed DM-Jaya is depicted in Figure 31.
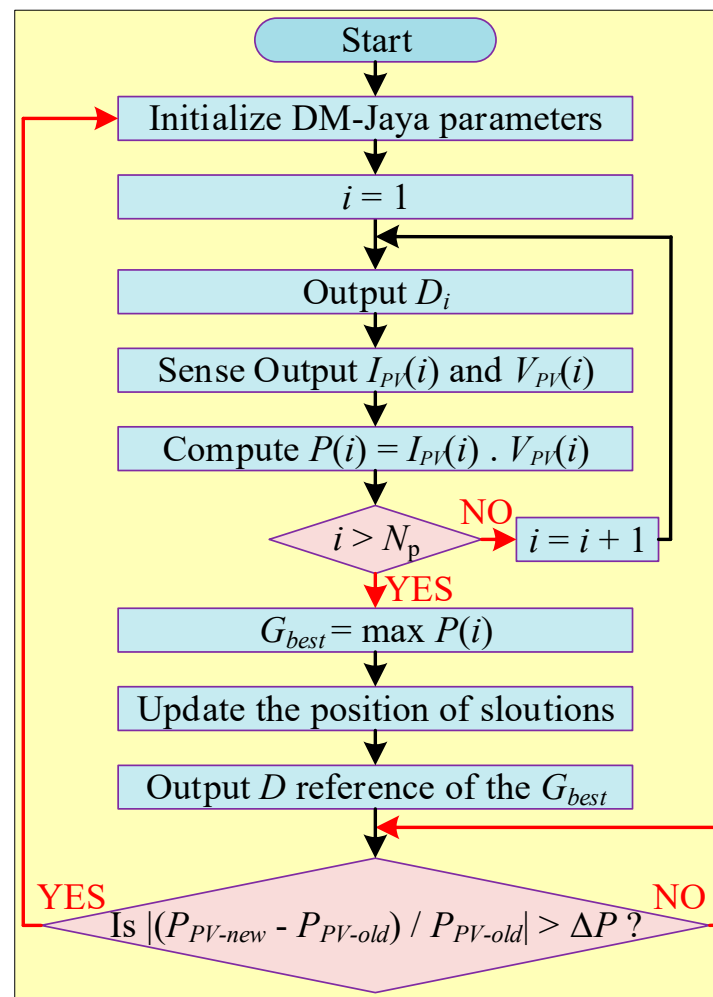
Figure 31. Flowchart of DM-Jaya MPPT technique [106].

2.2.49. Jaya Method with DE

A hybrid MPPT technique where the Jaya method is combined with the DE method was proposed in [107]. In this hybrid technique, all the solutions are pushed away from the MPP by the Jaya method, while all the solutions are pulled towards the MPP by the DE algorithm. Hence, by using this push-pull mechanism, the proposed MPPT method results in fast convergence. Moreover, a combined method like this can efficiently improve searching capability while reducing the number of search agents and iterations.

2.2.50. Estimation and Revision (E and R) Method

To track the MPP of the PV system under PSCs, the authors in [108] proposed a hybrid algorithm referred to as the E and R method, as presented in Figure 32. In this computational method, the mathematical model and equations of the PV are used to find the MPP. An E and R method consists of three stages: MPP estimation, revision, and steady state. In the MPP estimation stage, the temperature of the PV module is measured, and the V_{MPP} is estimated using (28), as provided:

$$I_{ph} - I_o \left(e^{\frac{V_{MPP}}{NV_t}} - 1 \right) - \frac{V_{MPP}}{NV_t} I_o e^{\frac{V_{MPP}}{NV_t}} = 0 \qquad (28)$$
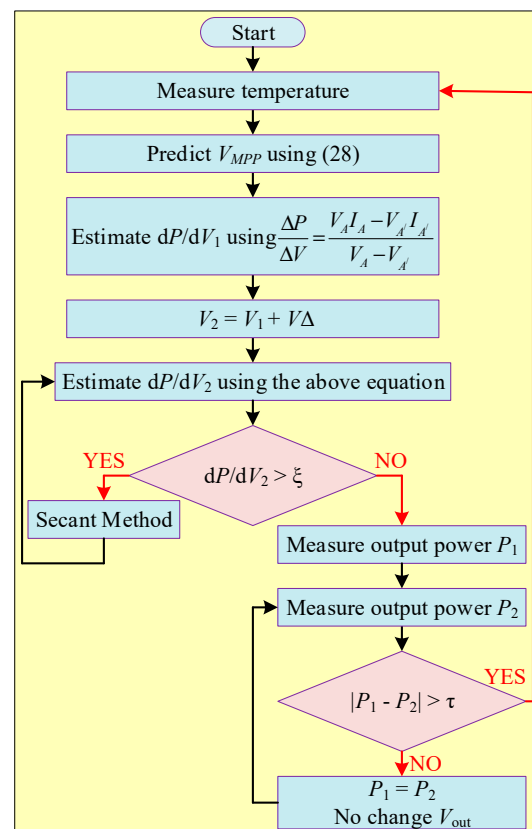
Figure 32. Flowchart of E and R MPPT method [108].

In the revision stage, a fixed step size P and O algorithm can be used. However, in this technique, the authors use a Secant Method (SM) [109] in the revision stage. An SM method has the advantage of variable step size and depends on the condition that dP/dV is equal to zero at MPP. In a revision stage, the MPP is tracked until the value of dP/dV comes below the predefined tolerance level. If the value of dP/dV becomes lower than the tolerance level, then the algorithm shifts towards the next stage, i.e., steady state. In this stage, the output power is monitored, if the variation in the power exceeds the tolerance level, then the algorithm moves back to the estimation stage and the process starts again.

2.2.51. Whale Optimization (WO) with DE

In this technique, two bio-inspired algorithms, i.e., WO and DE techniques, are combined to increase the accuracy and dynamic response of the system to track the MPP under PSC [12]. Due to the fast dynamic response and high searching capability of the DE algorithm, it is integrated in series with the WO. A DE algorithm pulls up the WO algorithm to jump out of the stagnation on LMPP to reduce the number of iterations or spiral paths. A DE algorithm in this technique chooses three favourable positions of the whale. All three positions go through a process of mutation, crossover, and selection in the WO algorithm to select the single best position of the whale. Therefore, in every spiral path, the WO algorithm obtains support from the DE algorithm, which reduces the iteration number and computation burden. Due to these features, this technique shows high convergence speed and tracks the MPP with high accuracy and reduced steady-state oscillations.

2.2.52. Dynamic Leader-Based Collective Intelligence (DLCI) Algorithm

The authors in [110] proposed a DLCI algorithm for PV MPPT applications. This method consists of five different sub-optimizers (GWO, WOA, MFO, ABC, and PSO) that autonomously search for an optimal solution and coordinate with the Dynamic Leader (DL) to improve the quality of the system. A sub-optimizer with the best solution is selected

as DL such that it guides the other sub-optimizers for efficient searching. A schematic flowchart of the DLCI optimization framework is presented in Figure 33. Although, this method results in high computational and implementation complexity, it enhances the search capability and offers fast convergence compared with the use of an individual sub-optimizer algorithm. Moreover, it offers low steady-state oscillations and high conversion efficiency compared with the single meta-heuristic-based MPPT method.
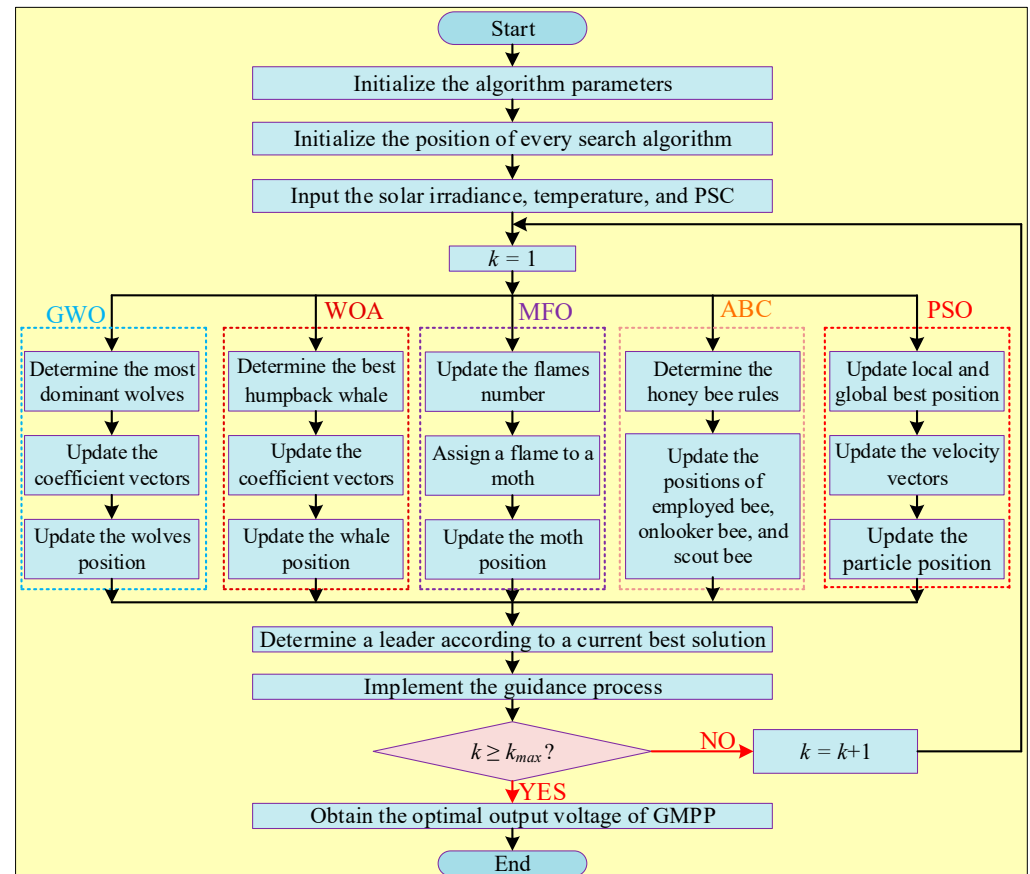
Figure 33. Flowchart of DLCI MPPT method [110].

2.2.53. Cauchy and Gaussian Sine Cosine Optimization (CGSCO)

In [111], a Cauchy density and Gaussian distribution function is integrated with the Sine Cosine Algorithm (SCA) to develop a hybrid technique referred to as CGSCO. In this technique, the main objective is to extract the MP from the PV system and efficiently charge the battery by maximizing the battery-charging current. To track the MPP, initially, an SCA is utilized to generate the initial population, then a Cauchy density is applied to improve the searching capability of the population and avoid getting trapped in LMPPs. Moreover, a Gaussian function is utilized to enhance the exploration part of the searching mechanism. The combined effect of these algorithms results in fast convergence of MPP (only in a few steps) with low computational burden. Moreover, this technique does not depend on the initial parameter values and uses only the current sensor for sensing, which results in a reduction in implementation cost.

2.3. Combination of Conventional with Soft Computing Algorithms

The techniques that are categorized in this type are a combination of conventional and soft computing algorithms. Numerous MPPT techniques that fall in this category are discussed in detail below and are presented in Figure 34.
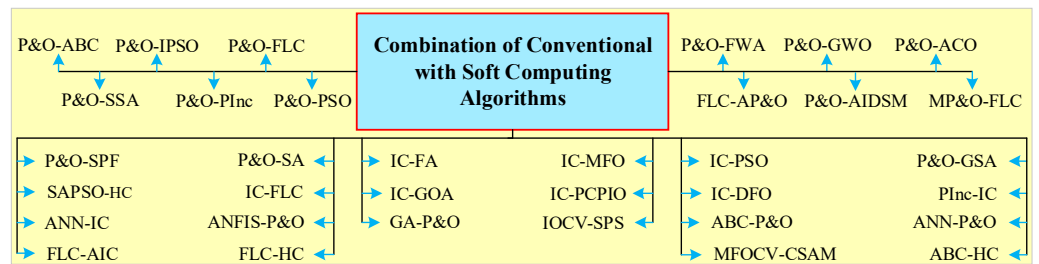
Figure 34. Types of combination of conventional with soft computing hybrid MPPT techniques.

2.3.1. P and O with Power Increment (PInc)

A traditional P and O method is unable to accurately locate the GMPP under VECs and gets trapped in LMPP. Therefore, to cope with this challenge, a hybrid algorithm is presented in [46], where a PInc method is integrated with the P and O technique to discover the GMPP under VEC. A schematic flowchart is presented in Figure 35. This technique is preferably endorsed for such sites that regularly face shading circumstances due to the capability of the PInc method to differentiate between global and local maxima. The operation of this algorithm can be divided into two stages. In the 1st stage, the PIN technique is applied to change the PV panel voltage among the two initially defined values to generate the converter duty cycle over a particular number of iterations. After the completion of every iteration, the output power is evaluated by multiplying the measured current with voltage. A new and old power are compared with each other; if the new power's value is larger than the previous one, then it is considered a new MPP. The PInc stage limits the MPP within a specified area, and the algorithm is then switched to P and O to accurately track the exact MPP. In this stage, the power calculation is evaluated again and compared with the preceding one. The algorithm chooses the next perturbation step in the same path if the power value is greater than the previous one, and vice versa.
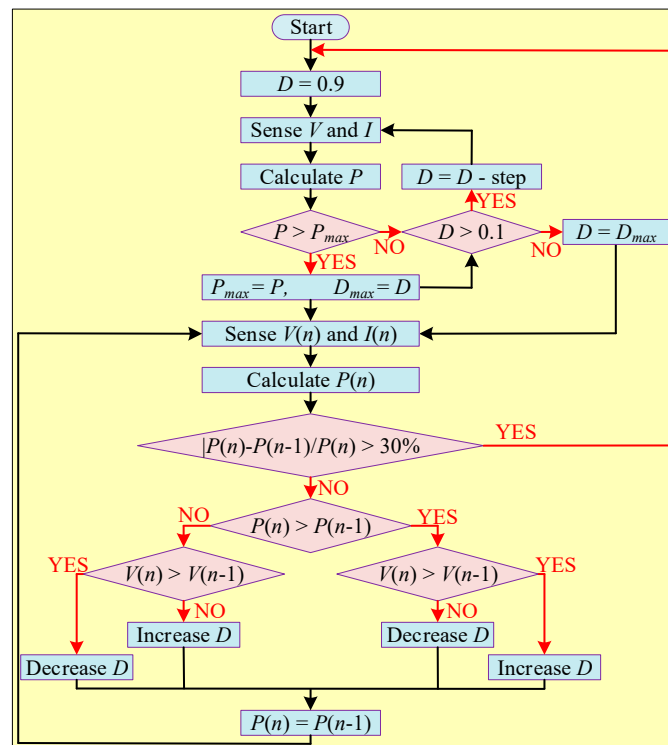
Figure 35. Flowchart of P and O-PInc MPPT [46].

2.3.2. P and O with PSO

In [112], both P and O and PSO are combined with PSO to track the GMPP with reduced oscillation under PSC. The operation of this technique is explained in 12 different steps, as presented in Figure 36. In the 1st step, the nominal values of voltage and current are set. Under UEC, a P and O is used to locate the MPP before the occurrence of any partial shading scenario (2nd and 3rd steps). If P and O accurately tracks the MPP, it saves all the information, i.e., power, voltage, etc. (4th step). The saved values of current and voltage are then compared with the user-defined current and voltage values to detect the PSC (5th step). Once the PSC is confirmed, the algorithm determines whether the 1st peak from the right side is the GMPPP or LMPP (6th step). If the defined inequality power constraint is satisfied, then the present GMPP is considered to be true. However, if it is not true, then the "Main Program" calls the "subroutine" to track the GMPP (7th step). In this procedure, an appropriate voltage window is defined where the PSO searches for GMPP (8th step) and proceeds to the 9th step, where the output power extracted by the PSO is stored. In the 10th step, it is determined whether there is a necessity to track the other MPP peak or not. If the power difference constraint is met, all the MPP values are compared to confirm the value of GMPP. If it is not true, then the procedure repeats itself, and all the peaks are once again taken into account in order to precisely locate the GMPP.
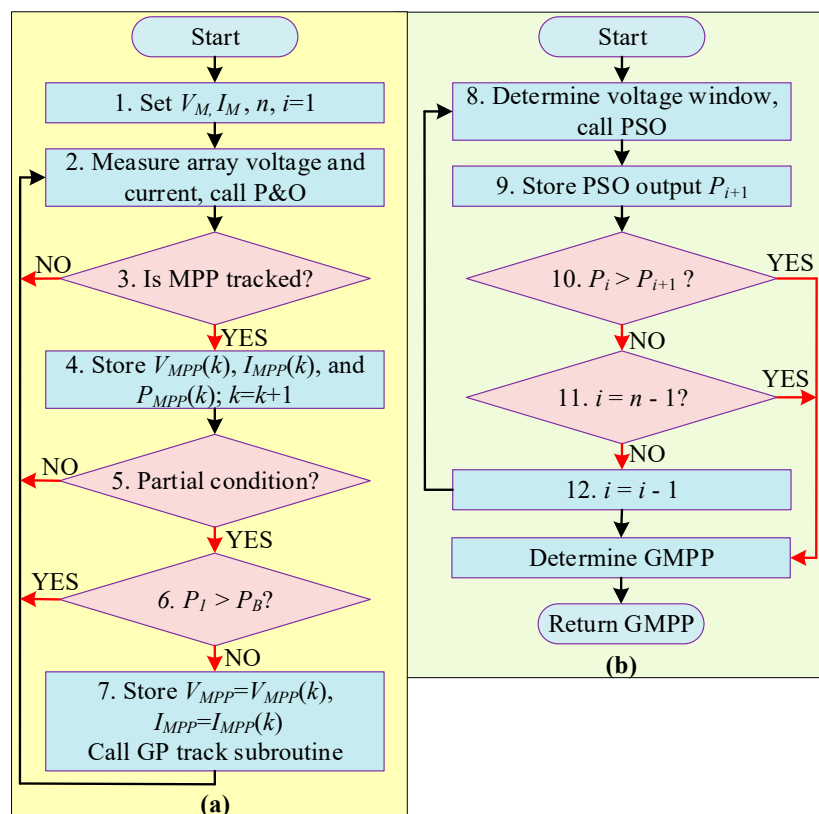
Figure 36. Flowcharts for the P and O-PSO method (**a**) main program (**b**) GP track subroutine [112].

2.3.3. P and O with Improved PSO

Another hybrid technique proposed in [113] combines an Improved PSO (IPSO) algorithm with a variable step P and O technique. A schematic of this hybrid structure is presented in Figure 37. In this hybrid technique, a traditional PSO method is modified 1st by incorporating the grouping concept of Shuffled Frog Leaping Algorithm (SFLA) into PSO, which guarantees the searching of GMPP and ensures the differences among the particles. In the next step, a variable step P and O is applied to efficiently and precisely track the GMPP under PSC. When the effectiveness of this hybrid algorithm is compared

with PSO, it is found that the proposed technique outperforms PSO in terms of convergence speed and accuracy.
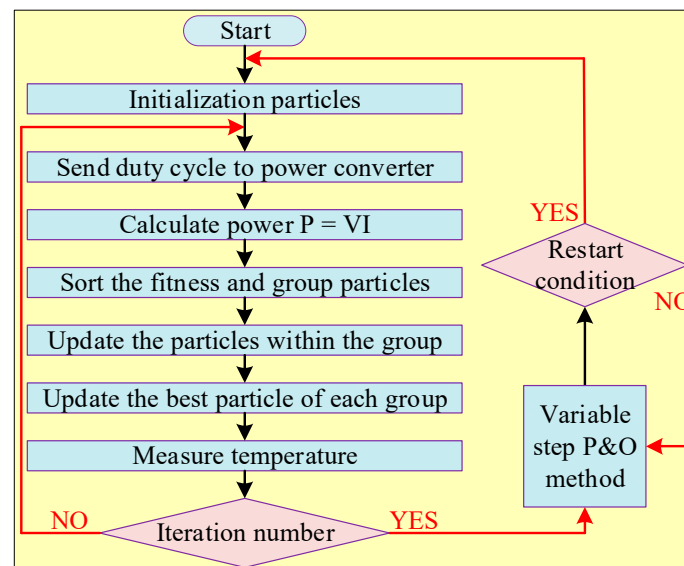
Figure 37. Flowchart of P and O-IPSO MPPT method [113].

2.3.4. P and O with FLC

In [114], P and O is combined with the FLC to overcome the disadvantageous features of slow tracking speed and large steady-state oscillations of P and O. In this hybrid technique, a FLC is implemented to locate the optimal operating point near the GMPP in the 1st stage. In the 2nd stage, a P and O is used to compare the two sequential points that continuously deliver the maximum output power while also changing the duty cycle of the converter based on the difference in sign among the two points on the P-V curve.

2.3.5. SSA with P and O

A conventional SSA has the advantage of simple upgrade functionality, but it creates large oscillations at the output and is unable to perform fast tracking [29]. Therefore, the authors in [115] proposed a hybrid technique in which an SSA is integrated with the P and O to track the MPP. To track the MPP under UEC, the P and O is executed. However, in the case of VEC or PSC, a combined approach of SSA and P and O is used for tracking the MPP. In VEC, SSA is executed first to find the preliminary global peak and is then followed by the P and O algorithm to achieve faster convergence. Hence, this results in high tracking accuracy.

2.3.6. GWO with P and O

In [116], GWO and P and O are combined to improve the convergence speed, tracking capability, and accuracy of the system. Unlike the other two-stage hybrid algorithms, a GWO operates in the 1st stage while P and O operates in the 2nd stage. In the 1st stage, a GWO is used in off-line mode to push the system operating point close to MPP. In the 2nd stage, the P and O technique is used in an online mode to achieve faster convergence and reduce the steady-state oscillations. Moreover, a GWO algorithm produces the controlled signals (actually the location of the wolf) for the boost converter, thus eliminating the use of the conventional controller (PI, etc.) loop. Besides all the advantages, this technique also reduces the controller adjustment burden and simplifies the overall control structure.

2.3.7. P and O with Artificial Bee Colony (ABC)

In [13] the P and O algorithm is combined with the ABC algorithm to enhance the advantageous features of both algorithms. In this hybrid method, in a 1st stage, an ABC algorithm is used for GMPP tracking while P and O in a 2nd stage is used to track a LMPP to obtain an efficient and fast MPPT. Thus, the global and local searching capabilities of ABC and P and O, respectively, are efficiently combined to provide an optimum duty cycle for switch of the converter. From the results it can be observed that this technique accurately and efficiently tracks the MPP under PSC with low oscillations and high convergence speed while attaining an efficiency of more than 99.5%. A complete schematic of this P and O-ABC technique is shown in Figure 38.
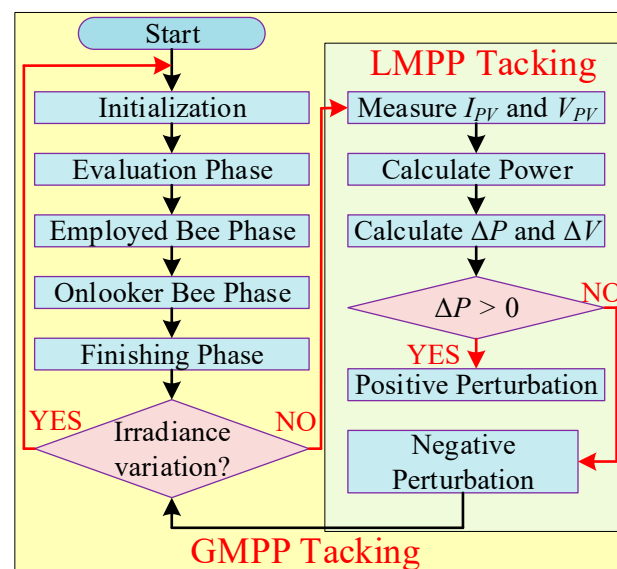
Figure 38. Flowchart of P and O-ABC algorithm [13].

2.3.8. P and O with Adaptive Integral Derivative Sliding Mode (AIDSM) Controller

The authors in [117] proposed a voltage-oriented hybrid MPPT technique in which a P and O is integrated with an AIDSM controller. In this method, initially, a P and O technique is used for generating the reference output voltage of the PV module and providing the control signal. Then an AIDSM is employed to regulate the measured PV voltage according to the reference generated by the P and O algorithm. Moreover, an AIDSM consists of two blocks. The 1st block is called an IDSM and is designed through a new sliding surface where the integral term is added for minimizing the steady-state error and the derivative term is added for eliminating the overshoot that occurs during fast variations in solar insolation level. In the 2nd block, an adaptive technique is applied to determine the gains of the IDSM controller at every irradiance level.

2.3.9. P and O with Fireworks Algorithm (FWA)

The author in [118] proposed a hybrid MPPT technique that can differentiate between the uniform and non-uniform irradiance levels by using the PV panel current and voltage. In this hybrid technique, P and O is combined with FWA. In this technique, P and O is employed for tracking MPP under UEC and FWA is used for VEC. During UEC, a P and O is employed because of its high potential to track the MPP with low steady-state oscillations compared with FWA. Alternatively, under PSC or VEC, FWA is used due to its high tracking capability of GMPP and fast convergence. Under PSC, when the proposed technique is initiated, FWA is called having no prior information about the shading pattern (step 1). P and O is applied for tracking of GMPP and check whether MPP is tracked or not (steps 2 and 3). Once the GMPP is tracked, the values of current and voltage at MPP (I_{MPP} and V_{MPP}, respectively) are stored and continuously monitored (step 4). When variations

in the irradiance level occur, the values of I_{MPP} and V_{MPP} also vary, and as a result, the power at MPP also changes. The variation in these values is compared and computed against the recently stored values (step 5). Based on the difference in values of I_{MPP} and V_{MPP} the current state of PSC is determined (step 6). When a PSC is not detected, the P and O algorithm is allowed to perform its operation near the present MPP. On the contrary, if PSC is detected, FWA is called to track the GMPP (step 1). A schematic flowchart of P and O-FWA is presented in Figure 39.
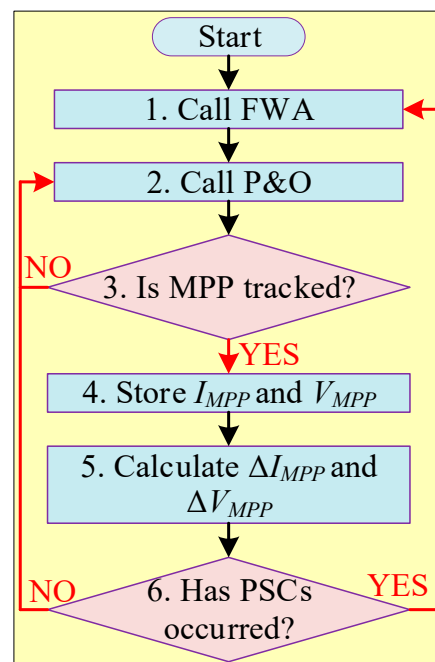
Figure 39. Flowchart of P and O-FWA MPPT technique [118].

2.3.10. P and O with ACO

The authors in [119] presented a hybrid technique in which P and O is combined with ACO to efficiently locate and extract the MPP under PSC. Initially, in the scanning stage, the ACO's foraging ants are used to carry out the global search, and after a predetermined number of ant movements, the most effective solution is determined. Once the most optimal solution is attained, in the next step, the P and O method is used to track the exact location of GMPP. This cascaded structure integrates the advantageous features of both P and O and ACO and leads towards efficient convergence with fast and smooth tracking characteristics.

2.3.11. FLC with Adaptive P and O

A hybrid technique presented in [120] combines FLC with Adaptive Perturb and Observe (AP and O) and is referred to as Artificial Intelligence-Based Adaptive Perturb and Observe (AIAP and O). A schematic flowchart of AIAP and O is depicted in Figure 40. The operation of this hybrid technique is based on the variation in the converter's duty cycle. As the converter's duty cycle varies, the system's output power changes accordingly. Therefore, the system's output power is examined to determine whether to decrease or increase the duty cycle in the upcoming cycle. If an increment in duty cycle results in high power, then the direction of perturbation is the same as the previous cycle. On the contrary, if a decrease in power is observed, then the direction of perturbation is in contrast with the previous cycle. Hence, the increment or decrement on the duty cycle is based on the perturbation (ΔD) that is generated by the AI system. Although this hybrid technique increases the mathematical computation, it provides fast and efficient accuracy with reduced oscillation around MPP.
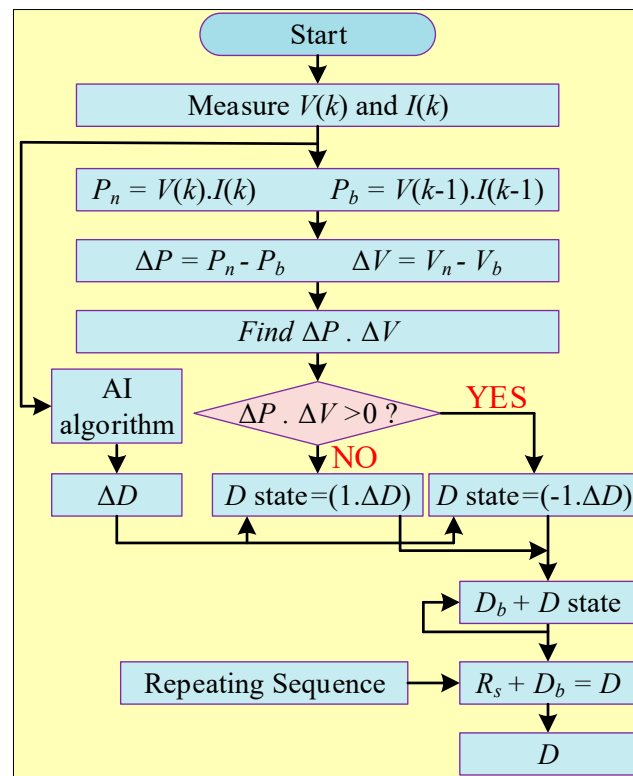
Figure 40. Flowchart of AIAP and O MPPT technique [120].

2.3.12. MP and O with FLC

In [121], an MP and O technique is combined with FLC for MPPT application. In this method, the step size of the duty cycle of the P and O algorithm is made adaptive using FLC. This method improves the steady as well as dynamic response effectively and simultaneously. The FLC computes the desired step size of duty cycle in every atmospheric condition from the P-V curve and change in sign of PV output power. Hence, if the operating point of the PV system is far from the MPP, then the duty cycle takes a large step. As soon as the PV operating point becomes close to the MPP, the step size becomes smaller. Lastly, when the MPP is achieved, the step size becomes very small until a change in the environmental conditions happens.

2.3.13. P and O with GSA

The authors in [122] combined P and O and GSA together to enhance the tracking speed and accuracy of an individual method for MPPT applications. This hybrid method operates in five steps. In the 1st step, the size of the population is assigned along with the upper and lower limits of the converter's duty cycle, which is generally set in the range of 10% to 90% in the 1st step. In the 2nd step, to attain an optimal convergence speed, the agents (solar voltages) are placed uniformly between the search space intervals. Based on the current and voltage, the output power is measured for every agent (the mass of the agent is considered as power) in the 3rd step. The fourth step involves calculating the force on each agent and the force between the agents. In the final step, the acceleration of each agent is computed. As the proposed hybrid technique operates in a cascaded manner, before triggering the P and O technique, the last three steps are frequently repeated until the convergence criteria are satisfied. When the P and O algorithm is activated, it continuously searches for the GMPP. For every two subsequent perturbations, a microcontroller measures the power variation. If the power variation exceeds the assigned threshold value, the MPPT is reinitiated.

2.3.14. P and O with Surface-Based Polynomial Fitting (SPF)

In [123], an SPF algorithm is combined with a P and O algorithm for PV MPPT applications. In this method, to extract the MP from the PV panel under UEC, the P and O technique is utilized. However, in the case of VEC, a combined approach of SPF-P and O is employed. In this combined approach, the P and O efficiency is improved by using a polynomial estimation that is optimized over the structure of the data. At last, in the MPPT stage, the resultant coefficients of the algorithm are used to achieve a more accurate estimation that fits the PV panel characteristic curves. The proficiency and efficacy of the SPF-P and O technique are verified under 133 different shading patterns, and it is concluded that this method tracks the GMPP accurately in all cases with fast convergence and low steady-state oscillations.

2.3.15. P and O with SA

The MPP locating technique proposed in [124] combines the SA algorithm with the P and O algorithm for GMPP searching. In this method, initially, an SA algorithm is employed, which is a random search technique inspired by the mechanism of annealing in metals. In SA, initially the duty cycle value is set high, and it is compared with the randomly generated value. In the next step, the power generated by these duty cycles is compared. If a random duty cycle generates more power, then it is assumed to be the current best solution, and this power is compared with the level of acceptable probability (the predetermined limit). The last duty cycle calculated is taken into consideration as the current solution if the acceptance probability is greater than the random value; however, if it is lower, the initial duty cycle computed is the current solution. Hence, a duty cycle that generates the worst power may be selected as the best optimal solution, thus enabling the system to escape the LMPP trap as the algorithm restarts and scans the whole search space after finding the best solution. After repeating the 3 or 4 iterations, a resultant duty cycle is then fed to P and O. The P and O then continuously searches for the GMPP. After every perturbation, the power difference between two adjacent perturbations is calculated and compared with the predefined threshold value to investigate; if the difference is large, then it means that irradiance variation occurs.

2.3.16. Simplified Accelerated Particle Swarm Optimization with Hill Climbing

The authors in [125] proposed a hybrid MPPT technique in which a Simplified Accelerated Particle Swarm Optimization (SAPSO) is combined with Hill Climbing (HC) algorithm. In this method, initially, the HC algorithm is used to explore the nearest MPP. It measures the actual PV current and voltage, then calculates the power and compares it with the previous measured value. Hence, the duty cycle of the power switch is adjusted either by decreasing or by increasing the perturbation size that automatically leads to a new operating point on P-V curve. If the perturbation size is small, then a deferred convergence might happen before switching to SAPSO method. On the contrary, if the perturbation size is large, then it can skip the nearest LMPP. In this method, a convergence is defined that allows the algorithm to switch towards SAPSO method. When a PV panel is subjected to PSC, the GMPP is located between 10 and 90% of V_{OC} on P-V curve. After tracking LMPP by the HC, the search space for SAPSO becomes smaller and ranges from voltage at LMPP to 90% of V_{OC}. This results in faster convergence compared with PSO and better performance compared with HC algorithm. A schematic flowchart of SAPSO-HC algorithm is shown in Figure 41.
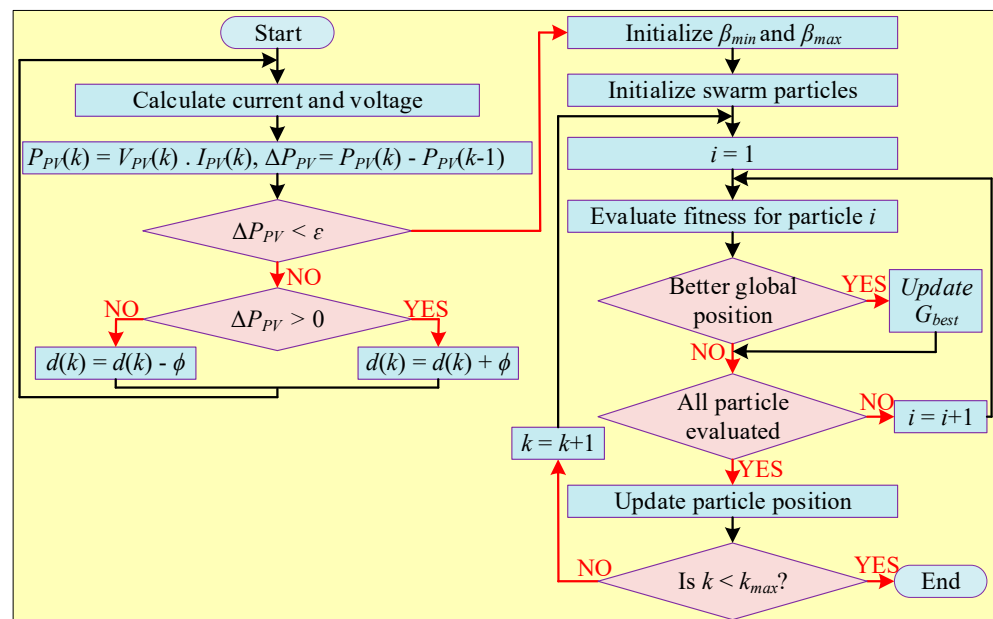
Figure 41. Flowchart of SAPSO-HC Hybrid MPPT technique [125].

2.3.17. Incremental Conductance with FLC

An Incremental Conductance (IC) algorithm is unable to accurately locate the GMPP in case of VECs due to its slow convergence speed, high steady-state oscillations, and possibly to trap in LMPP. Therefore, to overcome these disadvantages, the authors in [126] proposed a hybrid algorithm in which IC is combined with FLC. In this algorithm, an FLC is used to adopt the variable step size of an IC algorithm and adjust the duty cycle to drive the switch of the Cuk converter. Due to the adoptable feature of the FLC, this hybrid technique accurately locates the GMPP under PSCs with low steady-state oscillations and fast convergence speed compared with conventional IC. Similarly, the authors in [127] combined IC with FA to achieve faster convergence, and good tracking accuracy.

2.3.18. IC with GOA

A hybrid technique that combines IC with GOA was proposed in [128]. GOA displays well-defined supremacy in the event of convergence, power extraction, yields a good steady-state and dynamic responses, and accuracy to track the MPP under PSC, GOA has a high tracking time that needs to be enhanced [22]. Hence, to enhance the tracking time in this hybrid algorithm, the operation of this technique can be categorized into two stages. In the 1st stage, the GOA is used to locate a suitable tracking area where the GMPP lies. In the 2nd stage, an IC algorithm is used to accurately locate the GMPP within the area defined by the GOA in the 1st stage. This hybrid algorithm enhances the tracking speed of the GOA and locate the GMPP with high accuracy.

2.3.19. IC with Moth Flame Optimizer

In [129], an IC is combined with the Moth Flame Optimizer (MFO) to enhance the advantageous feature of individual algorithms and eliminate the disadvantageous feature. Hence, this combined approach results in a faster convergence in the case of uniform irradiance, and results in high accuracy and speed to track the GMPP in the case of non-uniform irradiance distribution. In a uniform irradiance distribution, there exists only a single peak in the P-V graph of the PV system. Therefore, to track the MPP under normal operation, an IC technique is used. However, in the case of non-uniform irradiance distribution, when there are multiple LMPP and one GMPP, an MFO algorithm is used to efficiently and accurately track the GMPP.

2.3.20. IC with Parallel and Compact Pigeon-Inspired Optimization

In [130], to overcome the disadvantages of IC algorithm, it was combined with Parallel and Compact Pigeon-Inspired Optimization (PCPIO) algorithm. In a proposed hybrid MPPT technique, a PCPIO is utilized to quickly locate the area where MPP lies and then a variable step size IC method is used to exactly locate the MPP. In this method, a local solution to the problem is avoided by introducing compound constraints, thus resulting in high accuracy and fast convergence speed. The simulations that are performed in a Simulink platform shows that the proposed method significantly reduced the power oscillation, achieve accurate and fast tracking, and enhance the stability of the system under complex VECs.

2.3.21. IC with PSO

The authors of [131] combined IC with PSO for PV MPPT application. The operation of this hybrid technique is divided into two stages. In the 1st stage, an IC is applied to track the 1st LMPP. In an IC stage, the PV voltage is either decremented or incremented with a small step in a right direction to track the GMPP. In the 2nd stage, PSO is employed to track the GMPP under intense VECs. An initial condition for the 1st particle of PSO is set to the converged value. The values of PSO particles in other cycles are set with $n-1$ and the values range from the previous converged value to the upper bound of the search space. As a result, the number of particles remain the same during the cycles. A flowchart of the proposed IC-PSO method is depicted in Figure 42.
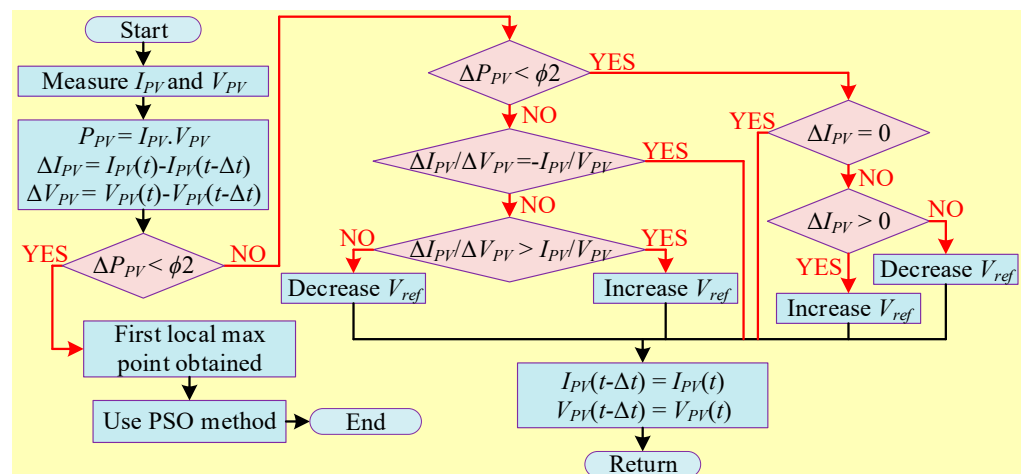
Figure 42. Schematic flowchart of IC-PSO MPPT technique [131].

2.3.22. IC with Dragonfly Optimization

In [132], a variable step IC was combined with Dragonfly Optimization (DFO) to accurately locate the GMPP among multiple LMPPs. In this method, the disadvantageous features of both algorithms are eliminated while enhancing the advantageous characteristics. These two algorithms are executed sequentially in such a manner that a variable step IC is applied initially due to its high performance under UEC. However, in the case of VEC, IC is particularly used to trap LMPP. Therefore, to avoid the local traps, a DFO is used in a 2nd stage to accurately locate the GMPP under VEC.

2.3.23. PInc with IC

To enhance the tracking performance of the IC MPPT technique, the authors of [133] proposed a hybrid technique where PInc is combined with the IC algorithm. The PInc-IC method uses either Constant Frequency Variable Duty Cycle (CFVD) or Variable Frequency Constant Duty Cycle (VFCD) method to perform its control actions [134,135]. In PInc-IC technique, a two phased method, i.e., Conductance Threshold Zone (CTZ) and Power

Threshold Zone (PTZ) are used to identify the threshold zones on the I_{PV}-V_{PV} and P_{PV}-V_{PV} curves, respectively. A CTZ is established along the I_{PV}-V_{PV} curve and around the MPP, whereas, a PTZ is established along the P_{PV}-V_{PV} curve. Both CTZ and PTZ are equal, referring to boundaries, and are mutually called the Threshold Tracking Zone (TTZ). Considerably, the variation in power along the P_{PV}-V_{PV} curve has a noticeable variation in the slope, whereas the variation in conductance along the I_{PV}-V_{PV} curve is less sensitive to PV voltage; however, both of these are ideal for the tracking control. In the proposed technique, before entering the TTZ, the PInc performs a coarse tracking along the P_{PV}-V_{PV} curve while in TTZ an IC performs a fine tracking along P_{PV}-V_{PV} curve. A detailed schematic flowchart of PInc-IC technique is presented in Figure 43.
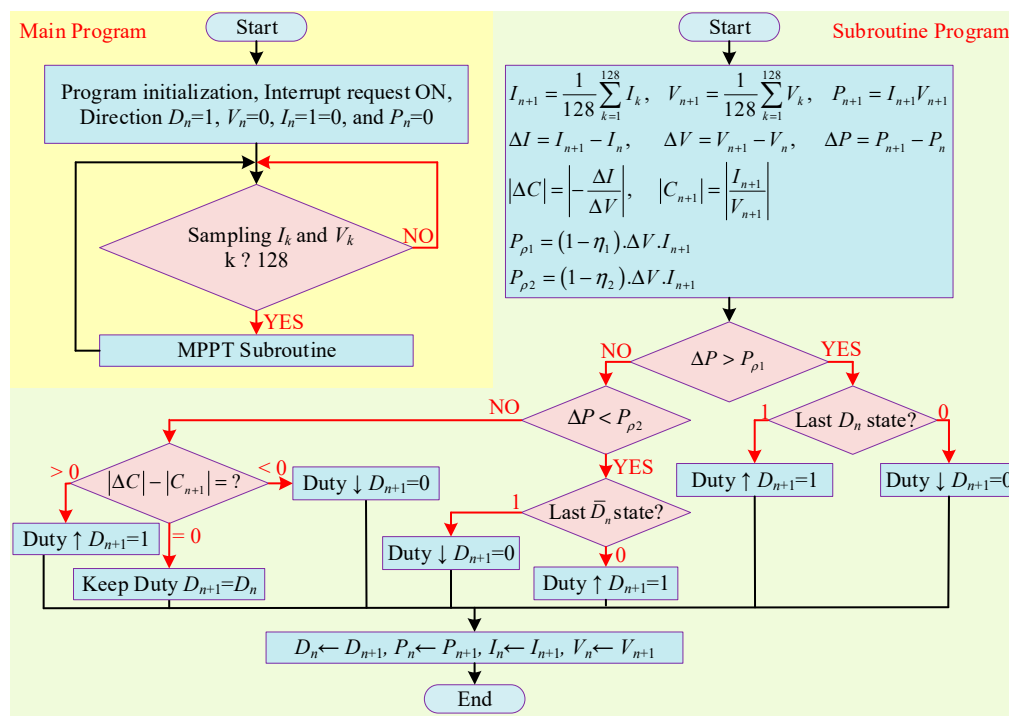
Figure 43. Flowchart of PInc-IC hybrid MPPT technique [133].

2.3.24. ANN with P and O

An ANN is very flexible in terms of input and output variables; therefore, when it is used to extract the MP from the PV panel, the input variables can be non-electrical (irradiance and temperature) or electrical (power, current, and voltage). Similarly, the output can be current or voltage at MPP or the duty cycle of the converter. Moreover, ANN shows significant performance with low steady-state oscillations and fast dynamic response. Besides all these advantages, a major challenge in designing an ANN-based MPPT technique is that it requires large and accurate training data sets to train ANN for efficient tracking. To accurately train the ANN that efficiently and precisely track the MPP under PSC, it is combined with the P and O technique in [136]. The operation of this method is performed in two stages. In the 1st stage, an ANN algorithm is activated when PSCs are identified. An ANN samples the data from different operating points on the I-V curve and use these values to predict the GMPP region. Once the GMPP region is predicated, in a 2nd stage, a P and O algorithm is applied to the local search area to exactly locate the GMPP. This method predicts the MPP region directly and does not require any irradiance sensor; therefore, the cost is relatively reduced. The other major advantages of this method include simple structure, high tracking accuracy, and tracking speed. A schematic flowchart of this technique is presented in Figure 44.
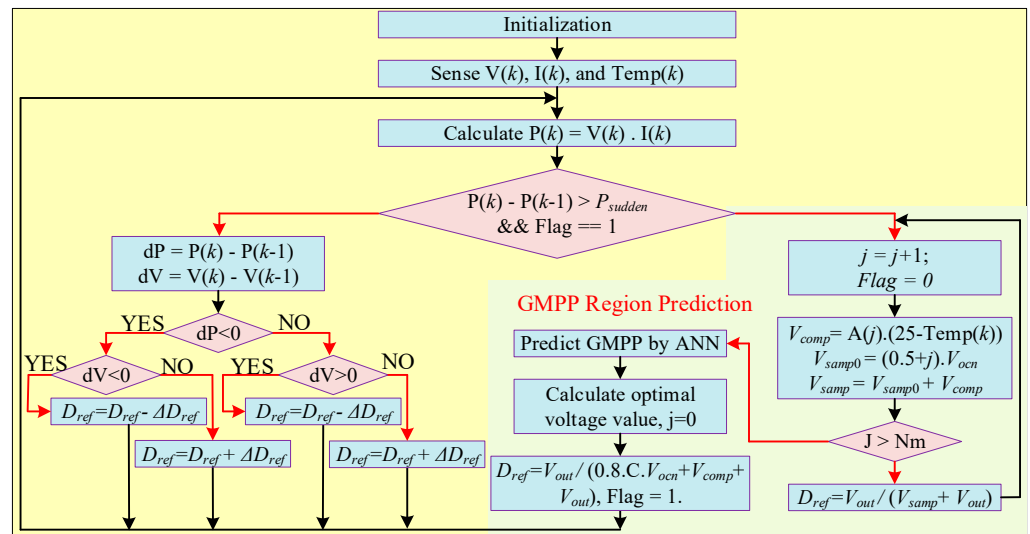
Figure 44. Flowchart of ANN-P and O MPPT technique [136].

2.3.25. ANN with IC

In [137], the authors combined an ANN algorithm with the IC method for PV MPPT application. The operation of this method is divided into two stages. In the 1st stage, an ANN algorithm is trained with respect to I-V characteristics of a PV panel operating close to MPP corresponding to different T and G levels. The I-V characteristics are considered as the input data of ANN while the MPP is recorded as the output. In the 2nd stage, an IC technique is used to find the exact MPP. Moreover, in the case of PSCs, when the characteristics of the PV changes, then a trained ANN algorithm changes its output characteristics close to MPP according to the new G and T level and is then accurately tracked by IC in the 2nd stage. The schematic of ANN-IC is presented in Figure 45.
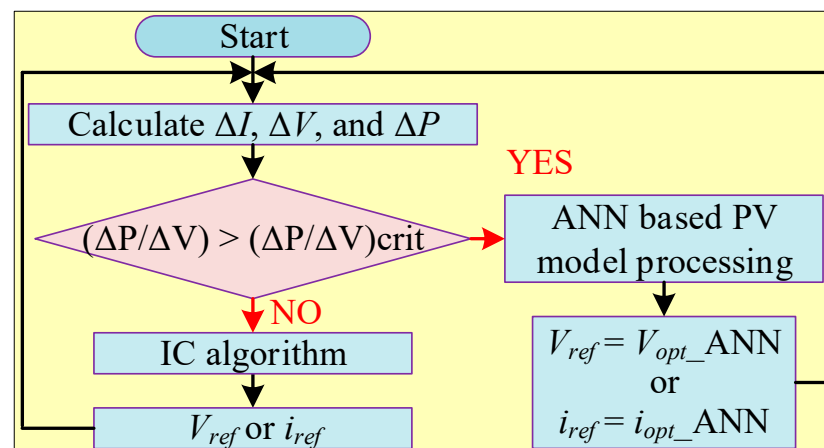
Figure 45. Flowchart of ANN-IC MPPT technique [137].

2.3.26. ANFIS with P and O

To efficiently track the MPP, the authors in [138] proposed an FA-trained ANFIS technique that is combined with the P and O technique. This method identifies and tracks the MPP in two stages. In the 1st stage, an FA is used to generate the optimal operating point based on different P-V curves that are used to train the membership function of ANFIS. In the 2nd stage, the combination of ANFIS and P and O is applied for MPPT tracking. In the 2nd stage, the trained ANFIS is applied 1st to approximate the MPP

based on the irradiance level or pattern. Then the P and O algorithm starts to operate in a tracking cycle and starts the MPP tracking from that point. An ANFIS is unable to accurately locate the GMPP (P and O cover the deficiency); therefore, compared with the individual usage of the ANFIS technique, in a proposed method, less samples are required for ANFIS training.

2.3.27. FLC with Angle of Incremental Conductance

FLC is very flexible in terms of input and output variables and shows significant performance to track the MPPT with low steady-state oscillations. Besides all these advantages, a major challenge in designing an FLC-based technique is that it is dependent on the user's knowledge and may stick to one of the LMPPs that affect the system performance. Therefore, to extract the MP from the PV system and minimize power fluctuations in transient and steady states, a hybrid MPPT method is proposed where Angle of Incremental Conductance (AIC) method is combined with Interval Type-2 Takagi Sugeno Kang FLC (IT2-TSK-FLC) [139]. In this technique, an AIC method is used due its well-defined finite range of input variable and MPP operation in steady state. Moreover, an AIC also produces an error function and is then used as an input for IT2-TSK-FLC. Moreover, IT2-TSK-FLC is used to handle the temperature and irradiance uncertainties and generate a suitable duty cycle to drive the converter's power switch. A proposed method shows high capability to adapt new operating point at any moment and handle the harsh VECs efficiently.

2.3.28. FLC with HC

A hybrid MPPT method that combines a Modified Hill Climb (MHC) with FLC is proposed in [140]. In this work, both the MHC and FLC are integrated in such a manner that the resultant algorithm enhances the advantageous features and eliminate the disadvantageous features (slow convergence, steady-state oscillations, low tracking accuracy in case of HC and user dependency, and lack of capability to track the GMPP in case of FLC). In the MHC-FLC method, the inputs and outputs of FLC are divided into 4 variable subsets, i.e., positive big, positive small, negative big, and negative small. As there are 4 subsets, therefore 16 fuzzy rules are set that are based on the regulation of MHC.

2.3.29. GA with P and O

In [141], a GA is combined with the P and O algorithm where GA is applied in the 1st stage followed by the P and O algorithm in the 2nd stage. The aim of this technique is to track the GMPP under VECs with fast tracking speed, low oscillations, and a reduced number of iterations. Initially, an average of 6 chromosomes are taken in the range of 10% to 90% as 6 duty cycle ratios that are distributed uniformly. A GA then activated to execute the 1st 3 chromosomes and the duty cycle ratios to determine the MP generated by the PV system, which is assumed to be an initial point of P and O algorithm. Hence, in the 2nd stage, to ensure fast and accurate convergence to GMPP, the P and O algorithm is applied where the length of step size decreases as the search proceeds. To update the step size length for next move, the following equation is used:

$$d_k = d_{k-1} + \Delta d_k \tag{29}$$

where, $\Delta d_k = \alpha \Delta d_{k-1}$ is a step size with $\alpha = 0.9$. For better and further understanding, the flowchart of GA-P and O is presented in Figure 46.
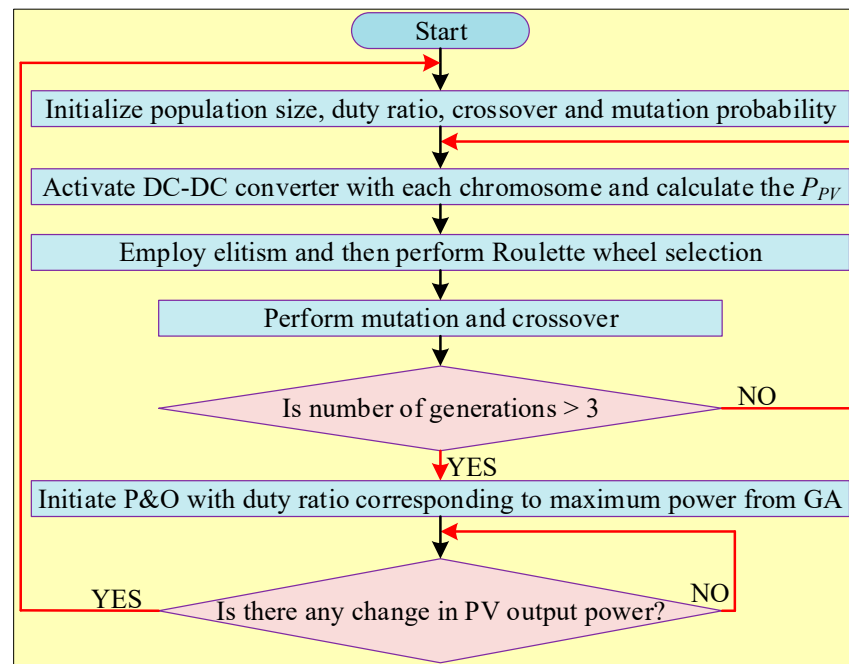
Figure 46. Flowchart of GA-P and O MPPT technique [141].

2.3.30. Modified FOCV with Current Sensor-Less Auto Modulation

The authors in [142] proposed a hybrid MPPT technique in which a Modified FOCV (MFOCV) is combined with Current Sensor-Less Auto Modulation (CSAM) to determine MPP. In this method, MFOCV is applied 1st, where initially, the PV array voltage (V_{PV}) is compared with the predefined lower (V_{MPPL}) and upper (V_{MMPH}) voltage values. In the next step, a variation in duty cycle (D) is estimated in reference with the variation in V_{MPPL} and V_{MMPH} to determine the operating point. In the 2nd stage, the CSAM algorithm is activated for fine-tuning of MPP under VECs and to ensure fast convergence that followed the provided equations as:

$$
\begin{aligned}
\frac{dV_{PV}}{dD} &< -V_{PV}\frac{1}{1-D}, \; D = D + \Delta D \\
\frac{dV_{PV}}{dD} &= -V_{PV}\frac{1}{1-D}, \; D = D \\
\frac{dV_{PV}}{dD} &> -V_{PV}\frac{1}{1-D}, \; D = D - \Delta D
\end{aligned}
\tag{30}
$$

Based on (30), the step size of the duty cycle is determined, i.e., when the system operating point is far from MPP, then MFOCV takes the large steps to ensure fast convergence. On the contrary, if the operating point is close to MPP then MFOCV take the small duty cycle steps to prevent the tracking oscillations.

2.3.31. Improved Open Circuit Voltage with Smart Power Scanning

In [143], an Improved Open Circuit Voltage (IOCV) method is combined with the Smart Power Scanning (SPS) method to accurately locate the MPP. In this method, a 0.8 V_{OC} model-based SPS procedure that is based on the change in sign of PV power is used. During this procedure, the scanning of voltage range is extended where GMPP is searched. Moreover, the tracking efficiency is significantly improved due to prevention of blind searching; as a result, the tracking speed is also enhanced. A schematic flowchart of IOCV-SPS is presented in Figure 47.
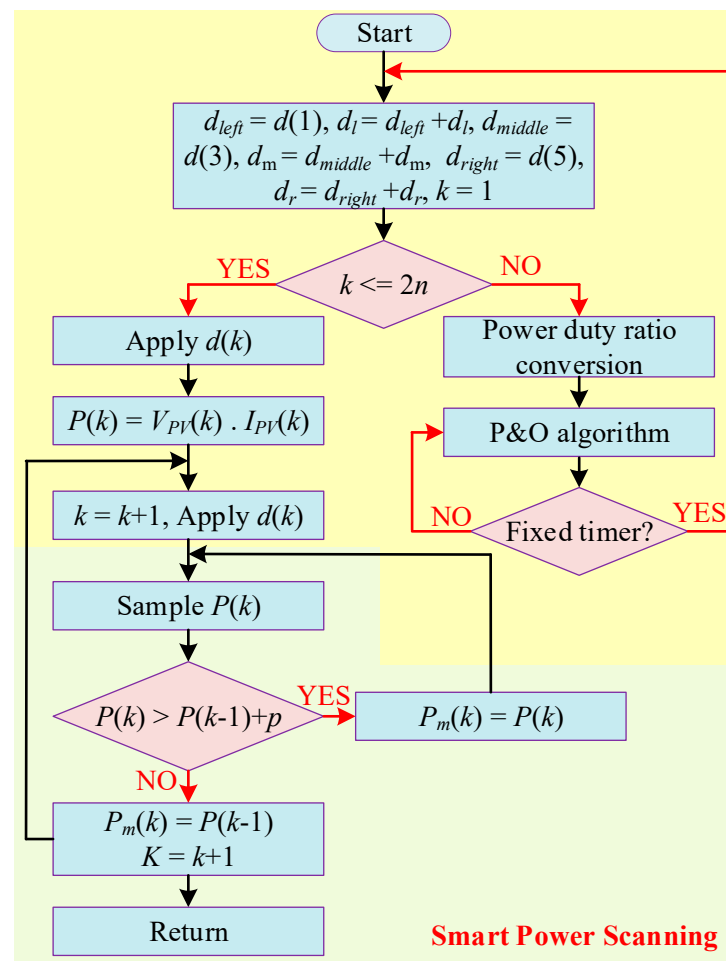
Figure 47. Flowchart of IOCV-SPS algorithm [143].

2.3.32. ABC with HC

An ABC algorithm is independent of initial parameters settings and is easy to develop with less regulated constraints. It can easily resolve problems involving multi-modal and multi-dimensional optimization [144]. ABC algorithm has only two control parameters in MPPT application that results in simplicity. Although it can track GMPP under PSCs, due to its slow convergence speed and performance degradation in terms of exploitation, a precise and accurate GMPP cannot be guaranteed [145]. Therefore, to cope with these issues, the ABC algorithm is combined with HC in [146]. This combined approach enhances the searching capability and convergence speed of the ABC algorithm. This battery-charging current (I_{charge}) versus D characteristics of the circuitry are scanned to identify the type of shading pattern. Once a shading pattern is recognized, the proposed algorithm uses either HC or ABC to track the GMPP. A proposed solution reduces the search space of ABC algorithm that results in improved convergence speed. Moreover, due to usage of a single current sensor, the overall cost of the system is considerably reduced.

2.3.33. ABC with P and O

ABC and P and O algorithms are combined to create a new hybrid MPPT technique, which is referred to as ABC-P and O [147]. Under uniform irradiation, the MPP is tracked using the P and O approach while an ABC algorithm is applied where irradiance varies rapidly. Additionally, two-layered control loops are designed that optimally regulate the duty cycle of the converter's switch to remove the oscillations from the output current and voltage waveforms. These control loops (i.e., inner current control and outer voltage control loops) together with the proposed MPPT technique allow one to control a PV system's

output voltage even in adverse climatic conditions. Moreover, reference output of this method responds with a voltage rather than the duty cycle, as a result the steady-state oscillations in the output waveforms are almost negligible. This approach guarantees quick convergence at a low computing cost and great efficacy.

3. Performance Evaluation Parameters and Comparative Analysis

The hybrid MPPT algorithms show very efficient performance and accurately track the MPP under PSC. However, every MPPT technique has different features and characteristics that make its selection a function of numerous parameters such as accuracy, convergence speed, implementation cost, etc. Besides the MPPT technique, there are many other factors that should be considered while installing a PV system, such as location, season, PV panel tilts, and orientations, etc. All these parameters are discussed in detail below. Moreover, a comprehensive comparison of the aforementioned MPPT techniques is presented in Table 2.

3.1. Tracking Accuracy

In conventional algorithms like P and O, high oscillations occur near the MPP under UEC; however, in the case of VEC or PSC, this algorithm cannot track the MPP accurately [148]. Similarly, the main disadvantages of the INC technique are its high computational time, high steady-state oscillations, and lack of tracking accuracy. Therefore, a variable step size IC algorithm is proposed in [149] that enhances the tracking efficiency, but at the same time it limits the tracking speed, and high oscillations are observed around the MPP. Hence, different hybrid techniques are proposed that achieve high tracking speed in the under fast VEC, such as MFA, which attained higher tracking precision and accuracy than conventional FA and PSO techniques [150]. In an ANN-based FLC hybrid algorithm, a higher tracking accuracy is attained than conventional ANN and FLC techniques [151].

3.2. Implementation Complexity

To select an appropriate MPPT technique for a PV system on the basis of implementation complexity is one of the most important factors to consider. The number of optimization parameters, the size of a PV system, the input and output variables of the MPPT algorithm, the number of steps in the algorithm, and other systematic parameters should be considered while analysing the complexity of the MPPT technique. Hence, some MPPT techniques have simple implementations that do not require any prior calibration or training, some techniques require system knowledge and proper training, and some techniques require extra hardware for their implementation [30]. The IC technique has a simple implementation, but due to recent advancements in technologies to extract the MP, its implementation has become complex [9]. Similarly, in the case of an intelligent algorithms, if the initial points are selected incorrectly, then it significantly increases its implantation complexity [152]. In the case of hybrid MPPT algorithms such as CSA-GSS [153], ABC-HC [146], etc., a high accuracy in locating the GMPP is achieved at the expense of increased implementation complexity. As most of the hybrid algorithms are implemented in digital platform, that requires software experts and computer programmers.

3.3. Tracking Speed

An efficient MPPT algorithm must be able to converge to its desired rating with good accuracy and speed, irrespective of any environmental variation. The level of complexity and accuracy of the MPPT technique are typically the two key elements that influence the tracking speed. Generally, a single individual MPPT algorithm requires more time to converge to GMPP compared with the hybrid algorithms. The hybrid algorithms have high convergence speed and reach the GMPP with minimal oscillations. The main barrier while designing a fast and accurate convergent MPPT technique is the cost; therefore, the designer should keep the cost in mind while designing [154].

3.4. Steady-State Oscillation

Another important factor that should be considered when selecting MPPT is its stability around the MPP. In most of the online MPPT techniques, the power losses are usually due to oscillations around the MPP [155]. These oscillations become extreme if a traditional MPPT technique like P and O is used. In this case, the P and O algorithm continuously searches for the operating point on the I-V or P-V curve even if the MPP is already tracked [156]. These large oscillations cause power loss, and thus the efficiency of the overall system decreases. In modified algorithms, such as those with variable step size, the steady-state oscillations are considerably reduced compared with traditional ones [157]. Moreover, all intelligent, meta-heuristic, and hybrid algorithms significantly control the oscillations around the MPP.

3.5. Power Conversion Efficiency

The quality of the MPPT algorithm is determined by its power efficiency and is said to be efficient when it accurately tracks the GMPP with fast convergence speed and low steady-state oscillations under any environmental conditions. The traditional MPPT techniques did not accurately track the GMPP and often became stuck in the LMPP under PSC; therefore, their efficiency is low. On the contrary, the novel soft computing and hybrid algorithms can accurately track the GMPP under VEC, showing high efficiency. For example, the PSO technique has high tracking accuracy and shows fast convergence with zero steady-state oscillations; therefore, it exhibits high conversion efficiency [158]. The efficiency of different hybrid algorithms is presented in Table 2. Besides the MPPT technique, a DC–DC converter that integrated the PV generation with the load also affected the efficiency of the system.

3.6. Sensors

Sensors are necessary to sense the input and output variables that are needed to track the MPP. To extract the MP from the PV panel, there are four different types of sensors used: irradiance, voltage, temperature, and current sensors. The usage of these sensors totally depends on the MPPT technique that is under consideration. For example, a traditional offline OCV technique utilizes only a voltage sensor [149]. The power angle-based technique does not require a current sensor when operating in a grid connected mode [159]. In hybrid techniques, such as FSCC-P and O, it is not necessary to use an irradiance sensor [156]. Hence, the MPPT techniques that utilize fewer sensors are more desirable, as a smaller number of sensors reduces implementation complexity and cost.

3.7. DC–DC Converter Selection

DC–DC converters play a prominent role in the integration of PV panels output with load. They are used to regulate and maintain the PV panel output voltage at a constant value irrespective of any variation in PV generation or load [160]. Usually, conventional converters such as boost, buck, Cuk, SEPIC, etc., are used for integration purposes. However, when these converters are operated at a high duty cycle to meet the application demands, they possess some drawbacks, such as (a) the parasitic losses associated with the resistances of capacitors, diodes, and inductors increase, causing low efficiency; (b) the stress across the switch increases; and (c) the conduction and switching losses increase [161]. Hence, to overcome these disadvantages, the authors have proposed numerous boosting techniques that accomplish a high voltage conversion ratio with a low duty cycle, for example, voltage multiplier cells [162], coupled inductors [163], switched inductors [164], etc. Based on these boosting techniques, numerous topologies are reported in the literature, such as single switch quadratic buck–boost [165], modified SEPIC [166], high gain boost [167], and modified Cuk [168] converters. These newly developed modified converter topologies significantly overcome the drawbacks of conventional converters and widen the applications of the PV system.

3.8. Cost

The cost dependency of the MPPT technique mainly relies on the type of control method (analogue or digital), the computational process, the required sensors, power components, and circuitry [148]. It also involves the operator's training cost and the MPPT maintenance cost. A digitally designed system is more expensive than analogue controllers as it requires more difficult programming. In general, the traditional techniques such as INC and P and O that are implemented on analogue platforms are cheaper compared with soft computing or hybrid techniques. However, the traditional MPPT techniques are also not very cheap, as they require high computational steps and at least two sensors for operation [154]. On the contrary, the techniques that involve AI, such as FA with FLC [75] and ANFIS with ABC [169], are very expensive due to their high hardware implementation complexity and require high-performance processors and software [148].

3.9. PSCs Handling

A PV system can be partially or completely shaded by flying objects, large trees, tall buildings, etc., thus resulting in numerous LMPPs and one GMPP. Hence, during shaded conditions, sometimes the applied MPPT technique tracks the LMPPs rather than the GMPP that causes huge power losses. Generally, techniques such as P and O, IC, etc., cannot accurately locate the GMPP under PSCs. Hence, to overcome this problem, numerous soft computing and hybrid algorithms are developed. The detailed description of the hybrid algorithms is already discussed in the above sections. Moreover, to handle PSC, voltage equalizers, DC–DC converters, micro-inverters, etc., are employed along with MPPT algorithms. A voltage equalizer is used in a series of connected panels to avoid an unwanted LMPP. A micro-inverter is usually interconnected in every module to accurately track the GMPP under PSCs [170].

3.10. PV Module Connections

An individual PV cell generates very little voltage and current; therefore, they are interconnected to form an array or module. There are numerous cell configurations present in the literature, in which usually 36 cells are connected in Series (SC), Bridge-Linked (BL), Total Cross-Tied (TCT), Series Parallel (SP), and Honey Comb (HCB). BL, HCB, and TCT are categorized based on their power extraction ability. When a PV array having these cell configurations is exposed to PSC, a power mismatch occurs. If a short circuit occurs at the array terminals due to a power mismatch, then different voltages are created that are negatively biased in some cells. Therefore, the Newton Raphson method and Piece-wise linear parallel branches model are developed to solve the mismatch problem [171]. In the SC module, cells are connected in series, while in the SP module, every array is treated as an individual unit that tracks the MPP individually for every array. Additionally, each cell in an SP module has independent but identical irradiance; as a result, the output power is affected by minor variations in MPP voltages [172].

3.11. Location and Seasons

A primary factor that influences the PV system's performance is the geographical position and climate of the site where it is installed. Therefore, for a location that is subjected to frequent climatic variation, a MPPT technique that has the ability to track the GMPP accurately and precisely with a fast convergence speed should be selected. Besides MPPT technique, a selection of suitable solar cells greatly affects the efficiency of the system [173]. An investigative study was performed by the authors in [148] about the performance of the crystalline silicon solar cells in different locations. In this study, it is found that the energy production is 8% in Aswan, Egypt; 30% in Turkey; 39% in Berlin, Germany; and nearly 16.8% in Stuttgart, Germany.

Table 2. Comparative assessment of different hybrid MPPT techniques.

Ref.	Year	Algorithm	C	S.U.	T.A.	T.S.	O.L.	PV.M.D.	E.V.	C.T.	Cost	η
Combination of Conventional Algorithms
[42]	2017	P and O-FSCC	L	V, I, T	M	L	H	No	No	Buck Boost	H	M
[44]	2016	FSCC-IC	L	I, V	M	L	L	Yes	No	N.G.	L	M
[46]	2016	FOCV-P and O	L	I, V	M	L	M	Yes	Yes	Buck	L	M
[47]	2016	FOCV-IC	L	I, V	M	L	L	Yes	No	Boost	L	M
[48]	2017	P and O-IC	M	V, I	M	M	M	No	Yes	Boost	H	M
[49]	2008	MP and O-MP and O	M	V, I	M	M	M	No	Yes	Boost	H	M
[51]	2014	EPP-IC	M	V, I	M	M	L	No	No	Boost	M	M
Combination of Soft Computing Algorithms
[12]	2017	WO-DE	H	I, V	H	H	M	Yes	No	N.G.	H	H
[25]	2020	GWO-CSA	H	I, V	H	H	L	No	No	Buck-Boost	H	VH
[52]	2021	PSO-DE	H	I, V	VH	VH	L	No	No	SEPIC	H	VH
[54]	2013	PSO-PI	H	V, I	H	H	L	No	Yes	NG	H	H
[55]	2018	PSO-OD	H	V, I	H	VH	L	No	Yes	Boost	H	VH
[56]	2019	PSO-ANFIS	H	V, I	V.H	V.H	L	No	Yes	Zeta	H	VH
[57]	2018	PSO-OCC	H	I	H	H	L	Yes	No	Boost	H	H
[60]	2017	PSO-EL	H	V, I	VH	VH	L	No	No	Boost	H	VH
[61]	2017	PSO-SA	H	V, I	H	V.H	L	No	No	NG	H	VH
[62]	2021	PSO-LFO	H	V, I	V.H	V.H	L	No	Yes	Boost	H	VH
[63]	2015	PSO-FLC	H	V, I	VH	H	L	No	Yes	Boost	H	VH
[64]	2020	PSO-TSMC	H	V, I	VH	VH	L	No	No	NG	H	VH
[65]	2013	PSO-GSA	H	I, V	H	L	H	No	No	Boost	H	H
[66]	2011	ANN-PSO	VH	V, I	V.H	H	VL	No	No	Boost	VH	H
[67]	2017	PSO-SFLA	H	I, V, P	H	H	L	No	No	Boost	H	H
[68]	2018	MPV-PSO	H	V, I	H	H	L	No	Yes	Boost	VH	H
[69]	2019	ISSA-PSO	H	V, I	VH	V.H.	VL	No	No	NG	VH	VH
[70]	2019	SSA-GWO	H	V, I	VH	V.H.	VL	No	No	Buck Boost	H	VH
[71]	2022	TSA-PSO	VH	V, I	VH	H	VL	No	Yes	Boost	VH	H
[72]	2017	PSOEM-FSA	VH	V, I	H	VH	L	No	Yes	Interleaved Boost	VH	VH
[74]	2020	FFA	H	I, V	V.H.	V.H.	L	No	Yes	Interleaved Boost	H	VH
[75]	2016	FA-FLC	H	I, V	H	H	L	Yes	No	Boost	H	H
[76]	2019	ACSA	M	I, V	M	H	L	Yes	No	Boost	M	H
[77]	2019	CSA-GSS	V.H.	V, I	V.H.	V.H.	L	No	Yes	N.G.	H	VH
[79]	2018	RQGPR trained ANN	VH	V, I	VH	VH	L	No	No	Cuk	H	VH
[79]	2018	CGSVM trained ANN	VH	V, I	VH	VH	L	No	Yes	Cuk	H	VH
[80]	2018	FPSOGSA-trained ANN	VH	V, I	VH	VH	VL	No	Yes	Boost	VH	VH
[81]	2022	GS-PS trained ANN	VH	V, I, G, T	VH	VH	VL	No	No	Buck	VH	VH
[82]	2016	ANN-GA	VH	V, I	VH	H	VL	No	No	NG	VH	H
[83]	2018	ANFIS	H	V, I, P	H	H	L	No	Yes	Buck	H	VH
[84]	2017	ANN-SP	H	I, V, G	H	M	L	Yes	No	Boost	H	H
[85]	2022	ANN-ACO	VH	V, I	VH	V.H.	L	No	Yes	Boost	H	VH
[86]	2019	ANN-MC	VH	I, V	H	H	L	No	No	NG	VH	H
[87]	2018	ANN vision-BS	VH	V, I	VH	VH	VL	No	Yes	Buck Boost	VH	VH
[88]	2020	IANN-PSO	H	I, V	VH	VH	L	No	No	NG	H	VH
[89]	2019	RBFNN-PSO	VH	I, V	VH	VH	L	No	Yes	Boost	H	VH
[90]	2021	RBFNN-BTSMC	VH	G, T	VH	V.H.	VL	No	No	Buck Boost	VH	VH
[92]	2018	GWO-Beta	VH	V, I	VH	VH	VL	No	Yes	Boost	H	VH
[93]	2019	GWO-FLC	H	I, V	VH	VH	L	No	No	Boost	H	VH
[94]	2018	GWO-GSO	VH	V, I	H	V.H.	L	No	Yes	Boost	H	VH

Table 2. *Cont.*

Ref.	Year	Algorithm	C	S.U.	T.A.	T.S.	O.L.	PV.M.D.	E.V.	C.T.	Cost	η
[95]	2021	ANFIS-CPHO	VH	V, I	VH	VH	VL	No	No	Boost	H	VH
[96]	2020	MSFLA-FLC	VH	V, I, P	VH	VH	L	No	No	NG	VH	VH
[97]	2019	Beta-FLC	H	I, V	H	H	VL	No	Yes	Boost	H	H
[99]	2011	FLC-GA	VH	I, V	VH	VH	L	No	Yes	Boost	H	VH
[100]	2019	PI-FLC	H	I, V	H	VH	L	No	No	Boost	H	H
[101]	2019	TLBO-FLC	H	V, I	H	H	L	No	Yes	Boost	H	H
[103]	2018	HTGA	VH	V, I, P	VH	H	M	Yes	No	Buck	H	VH
[104]	2018	GA + FA and DE	M	I, V	M	H	L	Yes	Yes	Buck	H	VH
[105]	2021	GA + ACO	H	V, I	H	H	L	No	No	Boost	VH	VH
[106]	2020	DM-Jaya	H	V, I	H	H	L	No	Yes	Boost	H	VH
[107]	2017	Jaya-DE	H	I, V, D	VH	VH	L	No	Yes	Boost	H	VH
[108]	2013	E and R	M	V, I	H	M	L	Yes	No	NG	M	M
[110]	2018	DLCI	VH	V, I	V.H.	V.H.	L	No	Yes	N.G.	VH	VH
[111]	2017	CGSCO	VH	I	VH	VH	L	No	Yes	Boost	VH	VH
Combination of Conventional with Soft Computing Algorithms												
[13]	2019	IP and O-ABC	M	I, V	VH	H	L	No	Yes	Boost	H	VH
[46]	2016	P and O-PInc	M	V, I	M	L	M	No	Yes	Buck	M	M
[112]	2016	P and O-PSO	H	I, V	V.H.	V.H.	L	No	Yes	Boost	H	H
[113]	2017	P and O-IPSO	H	V, I	H	V.H.	L	No	Yes	Buck Boost	H	VH
[114]	2018	P and O-FLC	M	I, V	H	M	L	No	No	Boost	M	H
[115]	2021	P and O-SSA	H	V, I	H	H	L	No	Yes	Boost	H	VH
[116]	2016	P and O-GWO	H	I, V	V.H.	V.H.	L	No	Yes	Boost	M	VH
[117]	2019	P and O-AIDSM	VH	I, V	H	VH	L	No	Yes	Boost	VH	VH
[118]	2016	P and O-FWA	H	I, V	H	H	M	Yes	Yes	Boost	H	H
[119]	2015	P and O-ACO	H	I, V	VH	VH	L	No	Yes	Boost	H	VH
[120]	2021	AIAPO	H	V, I	H	H	L	No	No	Boost	VH	VH
[121]	2015	AP and O-FLC	M	I, V	M	M	L	Yes	Yes	Cuk	M	M
[122]	2016	GSA-P and O	H	V, I	H	H	L	No	Yes	Boost	H	H
[123]	2021	SPF-P and O	H	V, I	H	H	VL	No	Yes	Boost	VH	H
[124]	2015	SA-P and O	H	V, I	H	H	L	No	No	NG	H	VH
[125]	2018	SAPSO-HC	H	I, V	VH	H	L	No	Yes	Buck	H	H
[126]	2014	IC-FLC	M	V, I	M	M	M	No	No	Cuk	M	M
[127]	2016	IC-FA	H	I, V	H	H	M	Yes	No	Boost	H	H
[128]	2020	IC-GOA	H	V, I	V.H.	V.H.	L	Yes	Yes	Interleaved Boost	H	VH
[129]	2019	IC-MFO	M	V, I	H	M	M	Yes	No	Boost	M	M
[130]	2020	PCPIO-IC	H	V, I	VH	H	VL	No	No	Boost	VH	VH
[131]	2014	IC-PSO	H	I, V	VH	H	L	No	No	NG	H	H
[132]	2022	IC-DFO	H	V, I	H	H	L	No	No	Boost	H	VH
[133]	2012	Pinc-IC	M	V, I	M	M	L	Yes	Yes	Fly back	L	M
[136]	2014	ANN-P and O	H	V, I	VH	H	L	No	Yes	Buck Boost	VH	H
[137]	2010	ANN-IC	H	I	M	H	L	No	No	Boost	H	H
[138]	2020	FA-ANFIS-P and O	VH	V, I, G	VH	VH	VL	No	No	Buck Boost	VH	VH
[139]	2020	AIC-FLC	H	I, V	M	H	L	Yes	Yes	Boost	H	VH
[140]	2010	HC-FLC	M	I, V	M	H	L	No	No	Boost	M	M
[141]	2015	P and O-GA	H	I, V	H	H	L	No	Yes	Boost	VH	H
[142]	2016	MFOCV-CSAM	H	V, I	H	VH	L	No	Yes	Boost	M	H
[143]	2018	IOCV-SPS	M	I, V	M	H	L	No	Yes	SEPIC	M	H
[146]	2018	ABC-HC	VH	I, V	H	H	L	No	Yes	Boost	H	H
[147]	2021	ABC-P and O	M	V, I	V.H	V.H	L	Yes	Yes	Boost	VH	VH

Abbreviations: C: complexity; S.U.: sensors used; T.A.: tracking accuracy; T.S.: tracking speed; O.L.: oscillation level; PV.M.D.: PV module dependency; E.V.: experimental validation; C.T.: converter topology; S.A.: stand alone; G.C.: grid connected; L: low; M: medium; H: high; V.H.: very high; N.P.: not provided.

4. Conclusions and Future Work

To extract the MP from the PV system under UEC or VEC, different MPPT techniques are developed. However, an optimum individual MPPT technique, i.e., conventional, meta-

heuristic, artificial intelligence, etc., or even hybrid MPPT technique does not exist, as these vary with cost, complexity, efficiency, convergence speed, etc. However, compared with the usage of an individual technique, the usage of a hybrid technique is a better solution to track the MPP under PSC, as it results in better speed, accuracy, and efficiency. Therefore, in this research work, numerous MPPT techniques are reviewed, and their working principle and schematic diagram, along with their prominent features, are described. A total of 93 different hybrid MPPT techniques are discussed and classified into three categories: combinations of conventional algorithms, combinations of soft computing algorithms, and combinations of conventional and soft computing algorithms. From the above discussed hybrid techniques, it can be concluded that the techniques that are developed by combining two or more soft computing methods show high tracking accuracy and efficiency with fast convergence speed and low steady-state oscillations as compared with the other two types. Moreover, different factors such as algorithm complexity, cost, DC–DC converter, etc., are discussed that enable the researchers and engineers to select the most suitable and appropriate MPPT technique based on the requirements. Finally, a reasonable evaluation criteria based on cost, complexity, accuracy, etc., is employed to make a complete and detailed comparative analysis of different MPPT techniques as listed in Table 2.

In the future, the following aspects regarding PV MPPT techniques can be considered: (a) the hybrid techniques provide optimal performance but at the expense of simplicity and computational burden. Hence, a hybrid technique can be developed that results in high accuracy and convergence speed with a low computational burden and ease of implementation; (b) the performance of the techniques to detect the occurrence of PSC can be further improved; (c) the combination of AI-based algorithms is gaining popularity; therefore, attention should be provided to optimizing the weighting parameters of these algorithms; (d) currently, most of the hybrid algorithms are evaluated through simulation tests only, and consideration should be provided to test the MPPT performance through hardware experiments; (e) to reduce the measurement errors, hardware implantation complexity, and cost, more attention should be provided to develop sensor-less hybrid techniques; (f) due to the increase in the development of different MPPT techniques, more guidelines should be provided in the selection of specific MPPT techniques for specific operation scenarios.

Author Contributions: Conceptualization, supervision, project administration, writing—original draft, H.L.; writing—review and editing, writing—original draft, methodology, M.Y.A.K.; software, formal analysis, investigation, resources, and visualization, X.Y. All authors have read and agreed to the published version of the manuscript.

Data Availability Statement: Data are contained within the article.

References

1. Khan, M.Y.A.; Liu, H.; Alhani, E.; Karim, H. Design of a phase disposition PWM technique for reduced switch asymmetric 31-level inverter. In Proceedings of the 2021 International Conference on Computing, Electronic and Electrical Engineering (ICE Cube), Quetta, Pakistan, 26–27 October A2021; pp. 1–10.
2. Gibb, D.; Ledanois, N.; Ranalder, L.; Yaqoob, H.; Murdock, H.E.; Achury, N.; Andre, T.; Benachir, I.; Dhar, A.; Gicquel, S. Renewables 2022 global status report+ Renewable energy data in perspective+ Press releases+ Regional fact sheets+ Country fact sheets. In *Energy Planning, Policy and Economy*; IEAE: Paris, France, 2022.
3. Ali Khan, M.Y.; Liu, H.; Yang, Z.; Yuan, X. A comprehensive review on grid connected photovoltaic inverters, their modulation techniques, and control strategies. *Energies* **2020**, *13*, 4185. [CrossRef]
4. Priyadarshi, N.; Bhaskar, M.; Sanjeevikumar, P.; Azam, F.; Khan, B. High-power DC-DC converter with proposed HSFNA MPPT for photovoltaic based ultra-fast charging system of electric vehicles. *IET Renew. Power Gener.* **2022**, 1–13. [CrossRef]
5. Alik, R.; Jusoh, A. An enhanced P&O checking algorithm MPPT for high tracking efficiency of partially shaded PV module. *Sol. Energy* **2018**, *163*, 570–580.

6. Xiao, W.; Dunford, W.G. A modified adaptive hill climbing MPPT method for photovoltaic power systems. In Proceedings of the 2004 IEEE 35th Annual Power Electronics Specialists Conference, (IEEE Cat. No. 04CH37551), Aachen, Germany, 20–25 June 2004; pp. 1957–1963.

7. Belhachat, F.; Larbes, C. Global maximum power point tracking based on ANFIS approach for PV array configurations under partial shading conditions. *Renew. Sustain. Energy Rev.* **2017**, *77*, 875–889. [CrossRef]

8. Khan, M.Y.A.; Liu, H.; Hashemzadeh, S.M.; Yuan, X. A novel high step-up DC–DC converter with improved P&O MPPT for photovoltaic applications. *Electr. Power Compon. Syst.* **2021**, *49*, 884–900.

9. Loukriz, A.; Haddadi, M.; Messalti, S. Simulation and experimental design of a new advanced variable step size Incremental Conductance MPPT algorithm for PV systems. *ISA Trans.* **2016**, *62*, 30–38. [CrossRef] [PubMed]

10. Yunliang, W.; Nan, B. Research of MPPT control method based on PSO algorithm. In Proceedings of the 2015 4th International Conference on Computer Science and Network Technology (ICCSNT), Harbin, China, 19–20 December 2015; pp. 698–701.

11. Pervez, I.; Sarwar, A.; Tayyab, M.; Sarfraz, M. Gravitational search algorithm (GSA) based maximum power point tracking in a solar PV based generation system. In Proceedings of the 2019 Innovations in Power and Advanced Computing Technologies (i-PACT), Vellore, India, 22–23 March 2019; pp. 1–6.

12. Kumar, N.; Hussain, I.; Singh, B.; Panigrahi, B.K. MPPT in dynamic condition of partially shaded PV system by using WODE technique. *IEEE Trans. Sustain. Energy* **2017**, *8*, 1204–1214. [CrossRef]

13. Pilakkat, D.; Kanthalakshmi, S. An improved P&O algorithm integrated with artificial bee colony for photovoltaic systems under partial shading conditions. *Sol. Energy* **2019**, *178*, 37–47.

14. Fitriyah, F.; Efendi, M.Z.; Murdianto, F.D. Modeling and simulation of MPPT zeta converter using human psychology optimization algorithm under partial shading condition. In Proceedings of the 2020 International Electronics Symposium (IES), Cagliari, Italy, 20–22 April 2020; pp. 14–20.

15. Rao, R. Jaya: A simple and new optimization algorithm for solving constrained and unconstrained optimization problems. *Int. J. Ind. Eng. Comput.* **2016**, *7*, 19–34.

16. Baimel, D.; Tapuchi, S.; Bronshtein, S.; Horen, Y.; Baimel, N. Novel segmentation algorithm for maximum power point tracking in pv systems under partial shading conditions. In Proceedings of the 2018 IEEE 18th International Power Electronics and Motion Control Conference (PEMC), Budapest, Hungary, 26–30 August 2018; pp. 406–410.

17. Li, X.; Wen, H.; Hu, Y.; Jiang, L.; Xiao, W. Modified beta algorithm for GMPPT and partial shading detection in photovoltaic systems. *IEEE Trans. Power Electron.* **2017**, *33*, 2172–2186. [CrossRef]

18. Guruambeth, R.; Ramabadran, R. Fuzzy logic controller for partial shaded photovoltaic array fed modular multilevel converter. *IET Power Electron.* **2016**, *9*, 1694–1702. [CrossRef]

19. Elobaid, L.M.; Abdelsalam, A.K.; Zakzouk, E.E. Artificial neural network-based photovoltaic maximum power point tracking techniques: A survey. *IET Renew. Power Gener.* **2015**, *9*, 1043–1063. [CrossRef]

20. Dhivya, P.; Kumar, K.R. MPPT based control of sepic converter using firefly algorithm for solar PV system under partial shaded conditions. In Proceedings of the 2017 International Conference on Innovations in Green Energy and Healthcare Technologies (IGEHT), Coimbatore, India, 16–18 March 2017; pp. 1–8.

21. Eltamaly, A.M. An improved cuckoo search algorithm for maximum power point tracking of photovoltaic systems under partial shading conditions. *Energies* **2021**, *14*, 953. [CrossRef]

22. Sridhar, R.; Subramani, C.; Pathy, S. A grasshopper optimization algorithm aided maximum power point tracking for partially shaded photovoltaic systems. *Comput. Electr. Eng.* **2021**, *92*, 107124. [CrossRef]

23. Kishore, D.K.; Mohamed, M.; Sudhakar, K.; Peddakapu, K. Swarm intelligence-based MPPT design for PV systems under diverse partial shading conditions. *Energy* **2023**, *265*, 126366. [CrossRef]

24. Zhou, L.; Chen, Y.; Guo, K.; Jia, F. New approach for MPPT control of photovoltaic system with mutative-scale dual-carrier chaotic search. *IEEE Trans. Power Electron.* **2010**, *26*, 1038–1048. [CrossRef]

25. Davoodkhani, F.; Arabi Nowdeh, S.; Abdelaziz, A.Y.; Mansoori, S.; Nasri, S.; Alijani, M. A new hybrid method based on gray wolf optimizer-crow search algorithm for maximum power point tracking of photovoltaic energy system. In *Modern Maximum Power Point Tracking Techniques for Photovoltaic Energy Systems*; Springer: Berlin/Heidelberg, Germany, 2020; pp. 421–438.

26. Batarseh, M.G.; Za'ter, M.E. Hybrid maximum power point tracking techniques: A comparative survey, suggested classification and uninvestigated combinations. *Sol. Energy* **2018**, *169*, 535–555. [CrossRef]

27. Yang, B.; Zhu, T.; Wang, J.; Shu, H.; Yu, T.; Zhang, X.; Yao, W.; Sun, L. Comprehensive overview of maximum power point tracking algorithms of PV systems under partial shading condition. *J. Clean. Prod.* **2020**, *268*, 121983. [CrossRef]

28. Ali, A.; Almutairi, K.; Padmanaban, S.; Tirth, V.; Algarni, S.; Irshad, K.; Islam, S.; Zahir, M.H.; Shafiullah, M.; Malik, M.Z. Investigation of MPPT techniques under uniform and non-uniform solar irradiation condition–a retrospection. *IEEE Access* **2020**, *8*, 127368–127392. [CrossRef]

29. Wasim, M.S.; Amjad, M.; Habib, S.; Abbasi, M.A.; Bhatti, A.R.; Muyeen, S. A critical review and performance comparisons of swarm-based optimization algorithms in maximum power point tracking of photovoltaic systems under partial shading conditions. *Energy Rep.* **2022**, *8*, 4871–4898. [CrossRef]

30. Ali, A.; Almutairi, K.; Malik, M.Z.; Irshad, K.; Tirth, V.; Algarni, S.; Zahir, M.H.; Islam, S.; Shafiullah, M.; Shukla, N.K. Review of online and soft computing maximum power point tracking techniques under non-uniform solar irradiation conditions. *Energies* **2020**, *13*, 3256. [CrossRef]

31. Jalil, M.F.; Khatoon, S.; Nasiruddin, I.; Bansal, R. Review of PV array modelling, configuration and MPPT techniques. *Int. J. Model. Simul.* **2022**, *42*, 533–550. [CrossRef]

32. Sarvi, M.; Azadian, A. A comprehensive review and classified comparison of MPPT algorithms in PV systems. *Energy Syst.* **2022**, *13*, 281–320. [CrossRef]

33. Hanzaei, S.H.; Gorji, S.A.; Ektesabi, M. A scheme-based review of MPPT techniques with respect to input variables including solar irradiance and PV arrays' temperature. *IEEE Access* **2020**, *8*, 182229–182239. [CrossRef]

34. Omar, F.A.; Pamuk, N.; KULAKSIZ, A.A. A critical evaluation of maximum power point tracking techniques for PV systems working under partial shading conditions. *Turk. J. Eng.* **2023**, *7*, 73–81. [CrossRef]

35. Verma, P.; Alam, A.; Sarwar, A.; Tariq, M.; Vahedi, H.; Gupta, D.; Ahmad, S.; Shah Noor Mohamed, A. Meta-heuristic optimization techniques used for maximum power point tracking in solar pv system. *Electronics* **2021**, *10*, 2419. [CrossRef]

36. Bollipo, R.B.; Mikkili, S.; Bonthagorla, P.K. Critical review on PV MPPT techniques: Classical, intelligent and optimisation. *IET Renew. Power Gener.* **2020**, *14*, 1433–1452. [CrossRef]

37. Baba, A.O.; Liu, G.; Chen, X. Classification and evaluation review of maximum power point tracking methods. *Sustain. Futures* **2020**, *2*, 100020. [CrossRef]

38. Naseem, M.; Husain, M.A.; Minai, A.F.; Khan, A.N.; Amir, M.; Dinesh Kumar, J.; Iqbal, A. Assessment of meta-heuristic and classical methods for GMPPT of PV system. *Trans. Electr. Electron. Mater.* **2021**, *22*, 217–234. [CrossRef]

39. Alrubaie, A.J.; Al-Khaykan, A.; Malik, R.; Talib, S.H.; Mousa, M.I.; Kadhim, A.M. Review on MPPT techniques in solar system. In Proceedings of the 2022 8th International Engineering Conference on Sustainable Technology and Development (IEC), Erbil, Iraq, 23–24 February 2022; pp. 123–128.

40. Raj, S.A.; Samuel, G.G. Survey of AI based MPPT algorithms in PV systems. In Proceedings of the 2022 4th International Conference on Smart Systems and Inventive Technology (ICSSIT), Tirunelveli, India, 20–22 January 2022; pp. 597–604.

41. Sandali, A.; Oukhoya, T.; Cheriti, A. Modeling and design of PV grid connected system using a modified fractional short-circuit current MPPT. In Proceedings of the 2014 International Renewable and Sustainable Energy Conference (IRSEC), Ouarzazate, Morocco, 17–19 October 2014; pp. 224–229.

42. Sher, H.A.; Murtaza, A.F.; Al-Haddad, K. In A hybrid maximum power point tracking method for photovoltaic applications with reduced offline measurements. In Proceedings of the 2017 IEEE International Conference on Industrial Technology (ICIT), Toronto, ON, Canada, 22–25 March 2017; pp. 1482–1485.

43. Penella, M.T.; Gasulla, M. A simple and efficient MPPT method for low-power PV cells. *Int. J. Photoenergy* **2014**, *2014*, 153428. [CrossRef]

44. Labeeb, K.; Shankar, S.; Ramprabhakar, J. Hybrid MPPT controller for accurate and quick tracking. In Proceedings of the 2016 IEEE International Conference on Recent Trends in Electronics, Information & Communication Technology (RTEICT), Bangalore, India, 20–21 May 2016; pp. 1533–1537.

45. Soualmia, A.; Chenni, R. A survey of maximum peak power tracking techniques used in photovoltaic power systems. In Proceedings of the 2016 Future Technologies Conference (FTC), San Francisco, CA, USA, 6–7 December 2016; pp. 430–443.

46. Al-Soeidat, M.R.; Cembrano, A.; Lu, D.D. Comparing effectiveness of hybrid mppt algorithms under partial shading conditions. In Proceedings of the 2016 IEEE International Conference on Power System Technology (POWERCON), Wollongong, NSW, Australia, 28 September–1 October 2016; pp. 1–6.

47. Javed, M.Y.; Gulzar, M.M.; Rizvi, S.T.H.; Arif, A. A hybrid technique to harvest maximum power from PV systems under partial shading conditions. In Proceedings of the 2016 International Conference on Emerging Technologies (ICET), Islamabad, Pakistan, 18–19 October 2016; pp. 1–5.

48. Yüksek, G.; Mete, A.N. A hybrid variable step size MPPT method based on P&O and INC methods. In Proceedings of the 2017 10th International Conference on Electrical and Electronics Engineering (ELECO), Bursa, Turkey, 30 November–2 December 2017; pp. 949–953.

49. Patel, H.; Agarwal, V. Maximum power point tracking scheme for PV systems operating under partially shaded conditions. *IEEE Trans. Ind. Electron.* **2008**, *55*, 1689–1698. [CrossRef]

50. Ansari, F.; Chatterji, S.; Iqbal, A.; Afzal, A. Control of MPPT for photovoltaic systems using advanced algorithm EPP. In Proceedings of the 2009 International Conference on Power Systems, Kharagpur, India, 27–29 December 2009; pp. 1–6.

51. Rout, A.; Samantara, S.; Dash, G.; Choudhury, S.; Sharma, R.; Dash, B. Modeling and simulation of hybrid MPPT based standalone PV system with upgraded multilevel inverter. In Proceedings of the 2014 Annual IEEE India Conference (INDICON), Pune, India, 11–13 December 2014; pp. 1–6.

52. Ahmad, M.S.; Ahmad, A. Hybrid pso-de technique to optimize energy resource for pv system. *Int. J. Electr. Eng. Technol. IJEET* **2021**, *12*, 128–139.

53. Seyedmahmoudian, M.; Rahmani, R.; Mekhilef, S.; Oo, A.M.T.; Stojcevski, A.; Soon, T.K.; Ghandhari, A.S. Simulation and hardware implementation of new maximum power point tracking technique for partially shaded PV system using hybrid DEPSO method. *IEEE Trans. Sustain. Energy* **2015**, *6*, 850–862. [CrossRef]

54. Phimmasone, V.; Kondo, Y.; Shiota, N.; Miyatake, M. The effectiveness evaluation of the newly improved pso-based mppt controlling multiple PV arrays. In Proceedings of the 2013 1st International Future Energy Electronics Conference (IFEEC), Tainan, Taiwan, 3–6 November 2013; pp. 81–86.

55. Li, H.; Yang, D.; Su, W.; Lü, J.; Yu, X. An overall distribution particle swarm optimization MPPT algorithm for photovoltaic system under partial shading. *IEEE Trans. Ind. Electron.* **2018**, *66*, 265–275. [CrossRef]

56. Priyadarshi, N.; Padmanaban, S.; Holm-Nielsen, J.B.; Blaabjerg, F.; Bhaskar, M.S. An experimental estimation of hybrid ANFIS–PSO-based MPPT for PV grid integration under fluctuating sun irradiance. *IEEE Syst. J.* **2019**, *14*, 1218–1229. [CrossRef]

57. Anoop, K.; Nandakumar, M. A novel maximum power point tracking method based on particle swarm optimization combined with one cycle control. In Proceedings of the 2018 International Conference on Power, Instrumentation, Control and Computing (PICC), Thrissur, India, 18–20 January 2018; pp. 1–6.

58. Anoop, K.; Nandakumar, M. A Novel control strategy for power extraction from Photo Voltaic panels based on One Cycle Control. In Proceedings of the 2014 IEEE 6th India International Conference on Power Electronics (IICPE), Kurukshetra, India, 8–10 December 2014; pp. 1–6.

59. Ram, J.P.; Rajasekar, N.; Miyatake, M. Design and overview of maximum power point tracking techniques in wind and solar photovoltaic systems: A review. *Renew. Sustain. Energy Rev.* **2017**, *73*, 1138–1159. [CrossRef]

60. Gavhane, P.S.; Krishnamurthy, S.; Dixit, R.; Ram, J.P.; Rajasekar, N. EL-PSO based MPPT for solar PV under partial shaded condition. *Energy Procedia* **2017**, *117*, 1047–1053. [CrossRef]

61. Guan, T.; Zhuo, F. An improved SA-PSO global maximum power point tracking method of photovoltaic system under partial shading conditions. In Proceedings of the 2017 IEEE International Conference on Environment and Electrical Engineering and 2017 IEEE Industrial and Commercial Power Systems Europe (EEEIC/I&CPS Europe), Milan, Italy, 6–9 June 2017; pp. 1–5.

62. Charin, C.; Ishak, D.; Zainuri, M.A.A.M.; Ismail, B.; Jamil, M.K.M. A hybrid of bio-inspired algorithm based on Levy flight and particle swarm optimizations for photovoltaic system under partial shading conditions. *Sol. Energy* **2021**, *217*, 1–14. [CrossRef]

63. Cheng, P.-C.; Peng, B.-R.; Liu, Y.-H.; Cheng, Y.-S.; Huang, J.-W. Optimization of a fuzzy-logic-control-based MPPT algorithm using the particle swarm optimization technique. *Energies* **2015**, *8*, 5338–5360. [CrossRef]

64. Lamzouri, F.E.-z.; Boufounas, E.; Brahmi, A.; El Amrani, A. Optimized TSMC control based MPPT for PV system under variable atmospheric conditions using PSO algorithm. *Procedia Comput. Sci.* **2020**, *170*, 887–892. [CrossRef]

65. Dhas, B.G.S.; Deepa, S. A hybrid PSO and GSA-based maximum power point tracking algorithm for PV systems. In Proceedings of the 2013 IEEE International Conference on Computational Intelligence and Computing Research, Enathi, India, 26–28 December 2013; pp. 1–4.

66. Ngan, M.S.; Tan, C.W. Multiple peaks tracking algorithm using particle swarm optimization incorporated with artificial neural network. *Int. J. Electron. Commun. Eng.* **2011**, *5*, 1325–1331.

67. Mao, M.; Zhang, L.; Duan, Q.; Oghorada, O.; Duan, P.; Hu, B. A two-stage particle swarm optimization algorithm for MPPT of partially shaded PV arrays. *Int. J. Green Energy* **2017**, *14*, 694–702. [CrossRef]

68. Sen, T.; Pragallapati, N.; Agarwal, V.; Kumar, R. Global maximum power point tracking of PV arrays under partial shading conditions using a modified particle velocity-based PSO technique. *IET Renew. Power Gener.* **2018**, *12*, 555–564. [CrossRef]

69. Ibrahim, R.A.; Ewees, A.A.; Oliva, D.; Abd Elaziz, M.; Lu, S. Improved salp swarm algorithm based on particle swarm optimization for feature selection. *J. Ambient Intell. Humaniz. Comput.* **2019**, *10*, 3155–3169. [CrossRef]

70. Wan, Y.; Mao, M.; Zhou, L.; Zhang, Q.; Xi, X.; Zheng, C. A novel nature-inspired maximum power point tracking (MPPT) controller based on SSA-GWO algorithm for partially shaded photovoltaic systems. *Electronics* **2019**, *8*, 680. [CrossRef]

71. Sharma, A.; Sharma, A.; Jately, V.; Averbukh, M.; Rajput, S.; Azzopardi, B. A novel TSA-PSO based hybrid algorithm for GMPP tracking under partial shading conditions. *Energies* **2022**, *15*, 3164. [CrossRef]

72. Mao, M.; Duan, Q.; Duan, P.; Hu, B. Comprehensive improvement of artificial fish swarm algorithm for global MPPT in PV system under partial shading conditions. *Trans. Inst. Meas. Control* **2018**, *40*, 2178–2199. [CrossRef]

73. Nugraha, S.D.; Wahjono, E.; Sunarno, E.; Anggriawan, D.O.; Prasetyono, E.; Tjahjono, A. Maximum power point tracking of photovoltaic module for battery charging based on modified firefly algorithm. In Proceedings of the 2016 International Electronics Symposium (IES), Denpasar, Indonesia, 29–30 September 2016; pp. 238–243.

74. Huang, Y.-P.; Huang, M.-Y.; Ye, C.-E. A fusion firefly algorithm with simplified propagation for photovoltaic MPPT under partial shading conditions. *IEEE Trans. Sustain. Energy* **2020**, *11*, 2641–2652. [CrossRef]

75. Ajiatmo, D.; Robandi, I. A hybrid Fuzzy Logic Controller-Firefly Algorithm (FLC-FA) based for MPPT Photovoltaic (PV) system in solar car. In Proceedings of the 2016 IEEE International Conference on Power and Renewable Energy (ICPRE), Shanghai, China, 21–23 October 2016; pp. 606–610.

76. Mirza, A.F.; Ling, Q.; Javed, M.Y.; Mansoor, M. Novel MPPT techniques for photovoltaic systems under uniform irradiance and Partial shading. *Sol. Energy* **2019**, *184*, 628–648. [CrossRef]

77. Nugraha, D.A.; Lian, K.-L. A novel MPPT method based on cuckoo search algorithm and golden section search algorithm for partially shaded PV system. *Can. J. Electr. Comput. Eng.* **2019**, *42*, 173–182. [CrossRef]

78. Kiran, S.R.; Basha, C.H.; Singh, V.P.; Dhanamjayulu, C.; Prusty, B.R.; Khan, B. Reduced simulative performance analysis of variable step size ANN based MPPT techniques for partially shaded solar PV systems. *IEEE Access* **2022**, *10*, 48875–48889. [CrossRef]

79. Farayola, A.M.; Hasan, A.N.; Ali, A. Optimization of PV systems using data mining and regression learner MPPT techniques. *Indones. J. Electr. Eng. Comput. Sci.* **2018**, *10*, 1080–1089. [CrossRef]

80. Duman, S.; Yorukeren, N.; Altas, I.H. A novel MPPT algorithm based on optimized artificial neural network by using FPSOGSA for standalone photovoltaic energy systems. *Neural Comput. Appl.* **2018**, *29*, 257–278. [CrossRef]

81. Alkhalaf, S.; Ali, Z.M.; Oikawa, H. A novel hybrid gravitational and pattern search algorithm based MPPT controller with ANN and perturb and observe for photovoltaic system. *Soft Comput.* **2022**, *26*, 7293–7315. [CrossRef]

82. Prasad, L.B.; Sahu, S.; Gupta, M.; Srivastava, R.; Mozhui, L.; Asthana, D.N. An improved method for MPPT using ANN and GA with maximum power comparison through Perturb & Observe technique. In Proceedings of the 2016 IEEE Uttar Pradesh Section International Conference on Electrical, Computer and Electronics Engineering (UPCON), Varanasi, India, 9–11 December 2016; pp. 206–211.

83. Nikolovski, S.; Reza Baghaee, H.; Mlakić, D. ANFIS-based peak power shaving/curtailment in microgrids including PV units and BESSs. *Energies* **2018**, *11*, 2953. [CrossRef]

84. Bouselham, L.; Hajji, M.; Hajji, B.; Bouali, H. A new MPPT-based ANN for photovoltaic system under partial shading conditions. *Energy Procedia* **2017**, *111*, 924–933. [CrossRef]

85. Babes, B.; Boutaghane, A.; Hamouda, N. A novel nature-inspired maximum power point tracking (MPPT) controller based on ACO-ANN algorithm for photovoltaic (PV) system fed arc welding machines. *Neural Comput. Appl.* **2022**, *34*, 299–317. [CrossRef]

86. Chen, L.; Wang, X. Enhanced MPPT method based on ANN-assisted sequential Monte–Carlo and quickest change detection. *IET Smart Grid* **2019**, *2*, 635–644. [CrossRef]

87. Martin, A.D.; Vazquez, J.R.; Cano, J. MPPT in PV systems under partial shading conditions using artificial vision. *Electr. Power Syst. Res.* **2018**, *162*, 89–98. [CrossRef]

88. Chouksey, A.; Awasthi, S.; Singh, S.K. Fuzzy cognitive network-based maximum power point tracking using a self-tuned adaptive gain scheduled fuzzy proportional integral derivative controller and improved artificial neural network-based particle swarm optimization. *Fuzzy Sets Syst.* **2020**, *381*, 26–50. [CrossRef]

89. Hamdi, H.; Regaya, C.B.; Zaafouri, A. Real-time study of a photovoltaic system with boost converter using the PSO-RBF neural network algorithms in a MyRio controller. *Sol. Energy* **2019**, *183*, 1–16. [CrossRef]

90. Khan, Z.A.; Khan, L.; Ahmad, S.; Mumtaz, S.; Jafar, M.; Khan, Q. RBF neural network based backstepping terminal sliding mode MPPT control technique for PV system. *PLoS ONE* **2021**, *16*, e0249705. [CrossRef]

91. Tjahjono, A.; Anggriawan, D.O.; Habibi, M.N.; Prasetyono, E. Modified grey wolf optimization for maximum power point tracking in photovoltaic system under partial shading conditions. *Int. J. Electr. Eng. Inform.* **2020**, *12*, 94–104. [CrossRef]

92. Rocha, M.; Sampaio, L.; da Silva, S.O. Maximum power point extraction in PV array under partial shading conditions using GWO-assisted beta method. In Proceedings of the International Conference on Renewable Energies and Power Quality, Madrid, Spain, 24–26 May 2018; pp. 450–455.

93. Eltamaly, A.M.; Farh, H.M. Dynamic global maximum power point tracking of the PV systems under variant partial shading using hybrid GWO-FLC. *Sol. Energy* **2019**, *177*, 306–316. [CrossRef]

94. Shi, J.-Y.; Zhang, D.-Y.; Ling, L.-T.; Xue, F.; Li, Y.-J.; Qin, Z.-J.; Yang, T. Dual-algorithm maximum power point tracking control method for photovoltaic systems based on grey wolf optimization and golden-section optimization. *J. Power Electron.* **2018**, *18*, 841–852.

95. Pachaivannan, N.; Subburam, R.; Padmanaban, M.; Subramanian, A. Certain investigations of ANFIS assisted CPHO algorithm tuned MPPT controller for PV arrays under partial shading conditions. *J. Ambient Intell. Humaniz. Comput.* **2021**, *12*, 9923–9938. [CrossRef]

96. Li, Y.; Samad, S.; Ahmed, F.W.; Abdulkareem, S.S.; Hao, S.; Rezvani, A. Analysis and enhancement of PV efficiency with hybrid MSFLA–FLC MPPT method under different environmental conditions. *J. Clean. Prod.* **2020**, *271*, 122195. [CrossRef]

97. Li, X.; Wen, H.; Hu, Y.; Jiang, L. A novel beta parameter based fuzzy-logic controller for photovoltaic MPPT application. *Renew. Energy* **2019**, *130*, 416–427. [CrossRef]

98. Messai, A.; Mellit, A.; Guessoum, A.; Kalogirou, S.A. Maximum power point tracking using a GA optimized fuzzy logic controller and its FPGA implementation. *Sol. Energy* **2011**, *85*, 265–277. [CrossRef]

99. Shill, P.C.; Akhand, M.; Murase, K. Simultaneous design of membership functions and rule sets for type-2 fuzzy controllers using genetic algorithms. In Proceedings of the 14th International Conference on Computer and Information Technology (ICCIT 2011), Dhaka, Bangladesh, 22–24 December 2011; pp. 554–559.

100. Kim, J.-C.; Huh, J.-H.; Ko, J.-S. Improvement of MPPT control performance using fuzzy control and VGPI in the PV system for micro grid. *Sustainability* **2019**, *11*, 5891. [CrossRef]

101. Farajdadian, S.; Hosseini, S.H. Optimization of fuzzy-based MPPT controller via metaheuristic techniques for stand-alone PV systems. *Int. J. Hydrogen Energy* **2019**, *44*, 25457–25472. [CrossRef]

102. Rao, R.V.; Savsani, V.J.; Vakharia, D. Teaching–learning-based optimization: A novel method for constrained mechanical design optimization problems. *Comput.-Aided Des.* **2011**, *43*, 303–315. [CrossRef]

103. Lee, C.-T.; Tsou, H.-I.; Chou, T.-H.; Weng, K.-W. Application of the hybrid Taguchi genetic algorithm to maximum power point tracking of photovoltaic system. In Proceedings of the 2018 IEEE International Conference on Applied System Invention (ICASI), Tokyo, Japan, 13–17 April 2018; pp. 231–234.

104. Huang, Y.-P.; Chen, X.; Ye, C.-E. A hybrid maximum power point tracking approach for photovoltaic systems under partial shading conditions using a modified genetic algorithm and the firefly algorithm. *Int. J. Photoenergy* **2018**, *2018*, 7598653. [CrossRef]

105. Chao, K.-H.; Rizal, M.N. A hybrid MPPT controller based on the genetic algorithm and ant colony optimization for photovoltaic systems under partially shaded conditions. *Energies* **2021**, *14*, 2902. [CrossRef]

106. Deboucha, H.; Mekhilef, S.; Belaid, S.; Guichi, A. Modified deterministic Jaya (DM-Jaya)-based MPPT algorithm under partially shaded conditions for PV system. *IET Power Electron.* **2020**, *13*, 4625–4632. [CrossRef]

107. Kumar, N.; Hussain, I.; Singh, B.; Panigrahi, B.K. Rapid MPPT for uniformly and partial shaded PV system by using JayaDE algorithm in highly fluctuating atmospheric conditions. *IEEE Trans. Ind. Inform.* **2017**, *13*, 2406–2416. [CrossRef]

108. Ma, J.; Man, K.L.; Ting, T.; Zhang, N.; Lei, C.-U.; Wong, N. A hybrid MPPT method for photovoltaic systems via estimation and revision method. In Proceedings of the 2013 IEEE International Symposium on Circuits and Systems (ISCAS), Beijing, China, 19–23 May 2013; pp. 241–244.

109. Polak, E. Survey of secant methods for optimization. In Proceedings of the 1973 IEEE Conference on Decision and Control Including the 12th Symposium on Adaptive Processes, San Diego, CA, USA, 5–7 December 1973; p. 416.

110. Yang, B.; Yu, T.; Zhang, X.; Li, H.; Shu, H.; Sang, Y.; Jiang, L. Dynamic leader based collective intelligence for maximum power point tracking of PV systems affected by partial shading condition. *Energy Convers. Manag.* **2019**, *179*, 286–303. [CrossRef]

111. Kumar, N.; Hussain, I.; Singh, B.; Panigrahi, B.K. Single sensor-based MPPT of partially shaded PV system for battery charging by using cauchy and gaussian sine cosine optimization. *IEEE Trans. Energy Convers.* **2017**, *32*, 983–992. [CrossRef]

112. Manickam, C.; Raman, G.R.; Raman, G.P.; Ganesan, S.I.; Nagamani, C. A hybrid algorithm for tracking of GMPP based on P&O and PSO with reduced power oscillation in string inverters. *IEEE Trans. Ind. Electron.* **2016**, *63*, 6097–6106.

113. Yang, Z.; Duan, Q.; Zhong, J.; Mao, M.; Xun, Z. Analysis of improved PSO and perturb & observe global MPPT algorithm for PV array under partial shading condition. In Proceedings of the 2017 29th Chinese Control And Decision Conference (CCDC), Chongqing, China, 28–30 May 2017; pp. 549–553.

114. Bataineh, K.; Eid, N. A hybrid maximum power point tracking method for photovoltaic systems for dynamic weather conditions. *Resources* **2018**, *7*, 68. [CrossRef]

115. Premkumar, M.; Kumar, C.; Sowmya, R.; Pradeep, J. A novel salp swarm assisted hybrid maximum power point tracking algorithm for the solar photovoltaic power generation systems. *Autom. Časopis Autom. Mjer. Elektron. Računarstvo Komun.* **2021**, *62*, 1–20. [CrossRef]

116. Mohanty, S.; Subudhi, B.; Ray, P.K. A grey wolf-assisted perturb & observe MPPT algorithm for a PV system. *IEEE Trans. Energy Convers.* **2016**, *32*, 340–347.

117. Kihal, A.; Krim, F.; Laib, A.; Talbi, B.; Afghoul, H. An improved MPPT scheme employing adaptive integral derivative sliding mode control for photovoltaic systems under fast irradiation changes. *ISA Trans.* **2019**, *87*, 297–306. [CrossRef]

118. Manickam, C.; Raman, G.P.; Raman, G.R.; Ganesan, S.I.; Chilakapati, N. Fireworks enriched P&O algorithm for GMPPT and detection of partial shading in PV systems. *IEEE Trans. Power Electron.* **2016**, *32*, 4432–4443.

119. Sundareswaran, K.; Vigneshkumar, V.; Sankar, P.; Simon, S.P.; Nayak, P.S.R.; Palani, S. Development of an improved P&O algorithm assisted through a colony of foraging ants for MPPT in PV system. *IEEE Trans. Ind. Inform.* **2015**, *12*, 187–200.

120. Khan, M.J.; Pushparaj. A novel hybrid maximum power point tracking controller based on artificial intelligence for solar photovoltaic system under variable environmental conditions. *J. Electr. Eng. Technol.* **2021**, *16*, 1879–1889. [CrossRef]

121. Radjai, T.; Gaubert, J.P.; Rahmani, L.; Mekhilef, S. Experimental verification of P&O MPPT algorithm with direct control based on Fuzzy logic control using CUK converter. *Int. Trans. Electr. Energy Syst.* **2015**, *25*, 3492–3508.

122. Sundareswaran, K.; Vigneshkumar, V.; Simon, S.P.; Nayak, P.S.R. Gravitational search algorithm combined with P&O method for MPPT in PV systems. In Proceedings of the 2016 IEEE Annual India Conference (INDICON), Bangalore, India, 16–18 December 2016; pp. 1–5.

123. González-Castaño, C.; Restrepo, C.; Revelo-Fuelagán, J.; Lorente-Leyva, L.L.; Peluffo-Ordóñez, D.H. A fast-tracking hybrid mppt based on surface-based polynomial fitting and p&o methods for solar pv under partial shaded conditions. *Mathematics* **2021**, *9*, 2732.

124. Lyden, S.; Haque, M. A hybrid simulated annealing and perturb and observe method for maximum power point tracking in PV systems under partial shading conditions. In Proceedings of the 2015 Australasian Universities Power Engineering Conference (AUPEC), Wollongong, Australia, 27–30 September 2015; pp. 1–6.

125. Chaieb, H.; Sakly, A. A novel MPPT method for photovoltaic application under partial shaded conditions. *Sol. Energy* **2018**, *159*, 291–299. [CrossRef]

126. Radjai, T.; Gaubert, J.P.; Rahmani, L. The new FLC-variable incremental conductance MPPT with direct control method using Cuk converter. In Proceedings of the 2014 IEEE 23rd International Symposium on Industrial Electronics (ISIE), Istanbul, Turkey, 1–4 June 2014; pp. 2508–2513.

127. Yetayew, T.T.; Jyothsna, T.; Kusuma, G. Evaluation of Incremental conductance and Firefly algorithm for PV MPPT application under partial shade condition. In Proceedings of the 2016 IEEE 6th International Conference on Power Systems (ICPS), New Delhi, India, 4–6 March 2016; pp. 1–6.

128. Wijaya, B.H.; Subroto, R.K.; Lian, K.L.; Hariyanto, N. A maximum power point tracking method based on a modified grasshopper algorithm combined with incremental conductance. *Energies* **2020**, *13*, 4329. [CrossRef]

129. Rezk, H.; Ali, Z.M.; Abdalla, O.; Younis, O.; Gomaa, M.R.; Hashim, M. Hybrid moth-flame optimization algorithm and incremental conductance for tracking maximum power of solar PV/thermoelectric system under different conditions. *Mathematics* **2019**, *7*, 875. [CrossRef]

130. Tian, A.-Q.; Chu, S.-C.; Pan, J.-S.; Liang, Y. A novel pigeon-inspired optimization based MPPT technique for PV systems. *Processes* **2020**, *8*, 356. [CrossRef]

131. Abdulkadir, M.; Yatim, A.H.M. Hybrid maximum power point tracking technique based on PSO and incremental conductance. In Proceedings of the 2014 IEEE Conference on Energy Conversion (CENCON), Johor Bahru, Malaysia, 13–14 October 2014; pp. 271–276.

132. Sarwar, S.; Javed, M.Y.; Jaffery, M.H.; Arshad, J.; Ur Rehman, A.; Shafiq, M.; Choi, J.-G. A novel hybrid MPPT technique to maximize power harvesting from pv system under partial and complex partial shading. *Appl. Sci.* **2022**, *12*, 587. [CrossRef]

133. Hsieh, G.-C.; Hsieh, H.-I.; Tsai, C.-Y.; Wang, C.-H. Photovoltaic power-increment-aided incremental-conductance MPPT with two-phased tracking. *IEEE Trans. Power Electron.* **2012**, *28*, 2895–2911. [CrossRef]

134. Hsieh, G.-C.; Chen, H.-L.; Chen, Y.; Tsai, C.-M.; Shyu, S.-S. Variable frequency controlled incremental conductance derived MPPT photovoltaic stand-along DC bus system. In Proceedings of the 2008 Twenty-Third Annual IEEE Applied Power Electronics Conference and Exposition, Austin, TX, USA, 24–28 February 2008; pp. 1849–1854.

135. Chen, Z.; Yang, P.; Zhou, G.; Xu, J.; Chen, Z. Variable duty cycle control for quadratic boost PFC converter. *IEEE Trans. Ind. Electron.* **2016**, *63*, 4222–4232. [CrossRef]

136. Jiang, L.; Maskell, D.L. A simple hybrid MPPT technique for photovoltaic systems under rapidly changing partial shading conditions. In Proceedings of the 2014 IEEE 40th Photovoltaic Specialist Conference (PVSC), Denver, CO, USA, 8–13 June 2014; pp. 782–787.

137. Dzung, P.Q.; Lee, H.H.; Vu, N.T.D. The new MPPT algorithm using ANN-based PV. In Proceedings of the International Forum on Strategic Technology 2010, Ulsan, Republic of Korea, 13–15 October 2010; pp. 402–407.

138. Farzaneh, J. A hybrid modified FA-ANFIS-P&O approach for MPPT in photovoltaic systems under PSCs. *Int. J. Electron.* **2020**, *107*, 703–718.

139. Kececioglu, O.F.; Gani, A.; Sekkeli, M. Design and hardware implementation based on hybrid structure for MPPT of PV system using an interval type-2 TSK fuzzy logic controller. *Energies* **2020**, *13*, 1842. [CrossRef]

140. Alajmi, B.N.; Ahmed, K.H.; Finney, S.J.; Williams, B.W. Fuzzy-logic-control approach of a modified hill-climbing method for maximum power point in microgrid standalone photovoltaic system. *IEEE Trans. Power Electron.* **2010**, *26*, 1022–1030. [CrossRef]

141. Sundareswaran, K.; Vigneshkumar, V.; Palani, S. Development of a hybrid genetic algorithm/perturb and observe algorithm for maximum power point tracking in photovoltaic systems under non-uniform insolation. *IET Renew. Power Gener.* **2015**, *9*, 757–765. [CrossRef]

142. Hua, C.C.; Fang, Y.H.; Chen, W.T. Hybrid maximum power point tracking method with variable step size for photovoltaic systems. *IET Renew. Power Gener.* **2016**, *10*, 127–132. [CrossRef]

143. Başoğlu, M.E.; Çakır, B. Hybrid global maximum power point tracking approach for photovoltaic power optimisers. *IET Renew. Power Gener.* **2018**, *12*, 875–882. [CrossRef]

144. Soufyane Benyoucef, A.; Chouder, A.; Kara, K.; Silvestre, S. Artificial bee colony based algorithm for maximum power point tracking (MPPT) for PV systems operating under partial shaded conditions. *Appl. Soft Comput.* **2015**, *32*, 38–48. [CrossRef]

145. Li, N.; Mingxuan, M.; Yihao, W.; Lichuang, C.; Lin, Z.; Qianjin, Z. Maximum power point tracking control based on modified ABC algorithm for shaded PV system. In Proceedings of the 2019 AEIT International Conference of Electrical and Electronic Technologies for Automotive (AEIT AUTOMOTIVE), Turin, Italy, 2–4 July 2019; pp. 1–5.

146. Goud, J.S.; Singh, B.; Kumar, S. Maximum power point tracking technique using artificial bee colony and hill climbing algorithms during mismatch insolation conditions on PV array. *IET Renew. Power Gener.* **2018**, *12*, 1915–1922. [CrossRef]

147. Restrepo, C.; Yanẽz-Monsalvez, N.; González-Castaño, C.; Kouro, S.; Rodriguez, J. A fast converging hybrid mppt algorithm based on abc and p&o techniques for a partially shaded pv system. *Mathematics* **2021**, *9*, 2228.

148. Verma, D.; Nema, S.; Shandilya, A.; Dash, S.K. Maximum power point tracking (MPPT) techniques: Recapitulation in solar photovoltaic systems. *Renew. Sustain. Energy Rev.* **2016**, *54*, 1018–1034. [CrossRef]

149. Karami, N.; Moubayed, N.; Outbib, R. General review and classification of different MPPT Techniques. *Renew. Sustain. Energy Rev.* **2017**, *68*, 1–18. [CrossRef]

150. Seyedmahmoudian, M.; Horan, B.; Soon, T.K.; Rahmani, R.; Oo, A.M.T.; Mekhilef, S.; Stojcevski, A. State of the art artificial intelligence-based MPPT techniques for mitigating partial shading effects on PV systems–A review. *Renew. Sustain. Energy Rev.* **2016**, *64*, 435–455. [CrossRef]

151. Messalti, S.; Harrag, A.; Loukriz, A. A new variable step size neural networks MPPT controller: Review, simulation and hardware implementation. *Renew. Sustain. Energy Rev.* **2017**, *68*, 221–233. [CrossRef]

152. Wang, Y.; Li, Y.; Ruan, X. High-accuracy and fast-speed MPPT methods for PV string under partially shaded conditions. *IEEE Trans. Ind. Electron.* **2015**, *63*, 235–245. [CrossRef]

153. Anand, R.; Swaroop, D.; Kumar, B. Global maximum power point tracking for PV array under partial shading using cuckoo search. In Proceedings of the 2020 IEEE 9th Power India International Conference (PIICON), Sonepat, India, 28 February–1 March 2020; pp. 1–6.

154. Ezinwanne, O.; Zhongwen, F.; Zhijun, L. Energy performance and cost comparison of MPPT techniques for photovoltaics and other applications. *Energy Procedia* **2017**, *107*, 297–303. [CrossRef]

155. Babu, T.S.; Rajasekar, N.; Sangeetha, K. Modified particle swarm optimization technique based maximum power point tracking for uniform and under partial shading condition. *Appl. Soft Comput.* **2015**, *34*, 613–624. [CrossRef]

156. Sher, H.A.; Murtaza, A.F.; Noman, A.; Addoweesh, K.E.; Al-Haddad, K.; Chiaberge, M. A new sensorless hybrid MPPT algorithm based on fractional short-circuit current measurement and P&O MPPT. *IEEE Trans. Sustain. Energy* **2015**, *6*, 1426–1434.

157. Tousi, S.R.; Moradi, M.H.; Basir, N.S.; Nemati, M. A function-based maximum power point tracking method for photovoltaic systems. *IEEE Trans. Power Electron.* **2015**, *31*, 2120–2128. [CrossRef]

158. Husain, M.A.; Tariq, A.; Hameed, S.; Arif, M.S.B.; Jain, A. Comparative assessment of maximum power point tracking procedures for photovoltaic systems. *Green Energy Environ.* **2017**, *2*, 5–17. [CrossRef]

159. Dousoky, G.M.; Shoyama, M. New parameter for current-sensorless MPPT in grid-connected photovoltaic VSIs. *Sol. Energy* **2017**, *143*, 113–119. [CrossRef]

160. Khan, M.Y.A.; Liu, H.; Rehman, N.U. Design of a multiport bidirectional DC-DC converter for low power PV applications. In Proceedings of the 2021 International Conference on Emerging Power Technologies (ICEPT), Topi, Pakistan, 10–11 April 2021; pp. 1–6.

161. Khan, M.Y.A.; Liu, H.; Habib, S.; Khan, D.; Yuan, X. Design and performance evaluation of a step-up DC–DC converter with dual loop controllers for two stages grid connected PV inverter. *Sustainability* **2022**, *14*, 811.

162. Andrade, A.M.S.S.; Mattos, E.; Schuch, L.; Hey, H.L.; da Silva Martins, M.L. Synthesis and comparative analysis of very high step-up DC–DC converters adopting coupled-inductor and voltage multiplier cells. *IEEE Trans. Power Electron.* **2017**, *33*, 5880–5897.

163. Kumar, A.; Sensarma, P. Ripple-free input current high voltage gain DC–DC converters with coupled inductors. *IEEE Trans. Power Electron.* **2018**, *34*, 3418–3428. [CrossRef]

164. Bao, D.; Kumar, A.; Pan, X.; Xiong, X.; Beig, A.R.; Singh, S.K. Switched inductor double switch high gain DC-DC converter for renewable applications. *IEEE Access* **2021**, *9*, 14259–14270. [CrossRef]

165. Zhang, N.; Zhang, G.; See, K.W.; Zhang, B. A single-switch quadratic buck–boost converter with continuous input port current and continuous output port current. *IEEE Trans. Power Electron.* **2017**, *33*, 4157–4166. [CrossRef]

166. Banaei, M.R.; Sani, S.G. Analysis and implementation of a new SEPIC-based single-switch buck–boost DC–DC converter with continuous input current. *IEEE Trans. Power Electron.* **2018**, *33*, 10317–10325. [CrossRef]

167. Khan, M.Y.A.; Azhar, M.; Saeed, L.; Khan, S.A.; Soomro, J. A High Gain Multiport Non-Isolated DC-DC Converter for PV Applications. In Proceedings of the 2019 2nd International Conference on Computing, Mathematics and Engineering Technologies (iCoMET), Sukkur, Pakistan, 30–31 January 2019; pp. 1–6.

168. Oluwafemi, A.W.; Ozsoy, E.; Padmanaban, S.; Bhaskar, M.S.; Ramachandaramurthy, V.K.; Fedák, V. A modified high output-gain cuk converter circuit configuration for renewable applications—A comprehensive investigation. In Proceedings of the 2017 IEEE Conference on Energy Conversion (CENCON), Kuala Lumpur, Malaysia, 30–31 October 2017; pp. 117–122.

169. Padmanaban, S.; Priyadarshi, N.; Bhaskar, M.S.; Holm-Nielsen, J.B.; Ramachandaramurthy, V.K.; Hossain, E. A hybrid ANFIS-ABC based MPPT controller for PV system with anti-islanding grid protection: Experimental realization. *IEEE Access* **2019**, *7*, 103377–103389. [CrossRef]

170. Uno, M.; Kukita, A. Two-switch voltage equalizer using an LLC resonant inverter and voltage multiplier for partially shaded series-connected photovoltaic modules. *IEEE Trans. Ind. Appl.* **2014**, *51*, 1587–1601. [CrossRef]

171. Wang, Y.-J.; Hsu, P.-C. An investigation on partial shading of PV modules with different connection configurations of PV cells. *Energy* **2011**, *36*, 3069–3078. [CrossRef]

172. Gao, L.; Dougal, R.A.; Liu, S.; Iotova, A.P. Parallel-connected solar PV system to address partial and rapidly fluctuating shadow conditions. *IEEE Trans. Ind. Electron.* **2009**, *56*, 1548–1556.

173. Eldin, S.S.; Abd-Elhady, M.; Kandil, H. Feasibility of solar tracking systems for PV panels in hot and cold regions. *Renew. Energy* **2016**, *85*, 228–233. [CrossRef]